The Role of Aluminate in the Activation of Catalytic Systems for Ethylene Oligomerization

Ahmed Hoyshel Alzamly

Thesis submitted to the
Faculty of Graduate and Postdoctoral Studies
in Partial fulfillment of the requirements
for the Doctorate in Philosophy degree in Chemistry

Department of Chemistry
Faculty of Science
University of Ottawa

A special feeling of gratitude to my loving wife, Rania Tejani, for her continuous support, encouragement and sacrifices throughout my entire doctorate program, to my two wonderful daughters Nada and Raneen and my adored son Khalid – without their patience and understanding; I would not have achieved the success I have today.

Contents

Acknowledgments

First and foremost, I would like to express my sincere gratitude to my supervisor, Professor Sandro Gambarotta for his continuous guidance and motivation throughout my doctoral research. This thesis would not have been possible without Sandro's support, insight and patience.

I am very grateful to the members of my thesis committee; prof. Darrin Richeson (University of Ottawa), Professor Jaclyn Brusso (University of Ottawa), Professor Sean Barry (Carleton University) and Professor Davit Zargarian (Université de Montréal) for their time and valuable comments.

The Gambarotta group has been a great environment for research, creativity and advancement. I feel fortunate to have been able to work with such a talented, well-rounded and supportive lab mates. Nick, Indira, Camilo, Joanna, Jac and Saba were a great source of friendship, advice and encouragement.

I am very grateful to Professor Muralee Murugesu (University of Ottawa) for his help with the magnetic susceptibility measurement using SQUID analysis. Also, I would like to thank professor Serge Gorelski (University of Ottawa) for the DFT calculations performed on mixed valent Cr(II)-Cr(I) complex. I would like to extend my appreciation to Professor Peter Budzelaar (University of Manitoba) for the DFT calculations performed on the Hexanuclear Chromium Cluster.

Special thanks to Dr. Ilia Korobkov (University of Ottawa) who assisted me with X-ray crystallography, starting with tips on crystallization to solving X-ray structures for many compounds presented in this thesis. I would like also to thank the University of Ottawa mass spectrometry team for their assistance analyzing my samples.

Finally, I would like to express my deepest gratitude to my wife, two daughters and son, for their unwavering love, support and encourgment. My wife has been my best friend and great companion; without her sacrifices and dedication I would not have achieved the success I have today.

Abstract

The reaction mechanisms followed by ethylene polymerization and selective oligomerization (tri- and tetramerization) are conceptually very different, being a non-redox chain growth and a redox metallacycle ring expansion pathway respectively. With chromium being the metal of choice, metal oxidation states and the variation of ancillary ligand able to support specific metal oxidation states responsible for selective trimerization, tetramerization or nonselective oligomerization/polymerization were varied.

In this research project we have explored a broad range of novel pyridine containing modified PN ligand scaffolds with the aim of probing the role of the pyridine donor substituent in stabilizing lower oxidation states and ultimately affecting the selectivity of the ethylene in the catalytic cycle.

In this study, pyridine PNP pincer ligands in conjunction with chromium salts and alkylaluminium activators have been explored. Their catalytic activities toward ethylene oligomerization were rationalized through the isolation of different chromium-aluminate intermediates in different oxidation states during the catalytic reaction.

Moreover, we explored other pyridine modification of NNP type ligand. Its anionic ligand shows a rare example of a Cr(II) hydride cluster which shows a high activity as a nonselective ethylene oligomerization catalyst.

Finally, a cyclic PNPN type ligand was explored. The ligand enabled the isolation of a mix-valent Cr(I)/Cr(II) species which was found to be inactive toward ethylene oligomerization due to its geometric constraint.

Publications Generated from this Research Work

[1] Alzamly, A.; Gambarotta, S.; Korobkov, I. *Organometallics* **2013**, *32*, 7107.

[2] Alzamly, A.; Gambarotta, S.; Korobkov, I. *Organometallics* **2013**, *32*, 7204.

[3] Alzamly, A.; Gambarotta, S.; Korobkov, I. *Organometallics* **2014**, *33*, 1602.

[4] Alzamly, A.; Gambarotta, S.; Korobkov, I.; Murugesu, M.; LeRoy, J. J.; Budzelaar, P. *Inorg. Chem.* Submitted.

[5] Alzamly, A.; Gambarotta, S.; Korobkov, I.; Gorelski, S. Manuscript in preparation.

List of Figures

List of Tables

List of Abbreviations

AF	Anti-Ferromagnetically
BP	British Petroleum
CCD	Charge Coupled Device
CHN	Carbon, Hydrogen, Nitrogen
DEAC	Diethylaluminum chloride
DMAP	4-Dimethylaminopyridine
DFT	Density Functional Theory
DMAO	Depleted methylaluminoxane
F	Ferromagnetically
GC-MS	Gas Chromatography-Mass Spectrometry
HDPE	High density polyethylene
ICI	Imperial Chemical Industries
i-Bu	iso-butyl
i-Pr	iso-propyl
IR	Infrared
LAO	Linear Alpha Olefins
LDPE	Linear density polyethylene
LLDPE	Linear low density polyethylene
MAO	Methylaluminoxane
Me	Methyl
MeCy	Methy Cyclohexane
Mw	Weight-average molecular weight

NMR	Nuclear Magnetic Resonance
PDI	Polydispersity
PE	Polyethylene
Py	Pyridine
R	Alkyl group
S-F	Schulz-Flory -Flory distribution (random statistical distribution)
SHOP	Shell Higher Olefin Process
SQUID	Superconducting Quantum Interference Device
TC	Thermal Conductivity
TEAL	Triethylaluminum
THF	Tetrahydrofuran
TIBA	Tri-isobutylaluminum
TMA	Trimethylaluminum
ULDPE	Ultra Low Density Polyethylene
VLDPE	Very Low Density Polyethylene
Z-N	Ziegler-Natta

CHAPTER 1

Introduction

Preamble

The carbon-carbon bond forming reaction from α-olefins is a thermodynamically highly favourable process evolving a considerable amount of energy (19 kcal/mole). This can be easily explained with the favourable balance between the cleavage of the olefin's π-bond (+64 kcal/mole) and the formation of a new C-C σ-bond (-83 kcal). Nonetheless, forming chains or higher molecular weight molecules occurs only if a suitable catalyst is provided. In fact the discovery of such catalysts has been a true landmark in the evolution of chemistry, having enabled entry into the world of polymers and plastic materials. The impact of such chemicals on societal development has been enormous on positive but also negative sides. On the positive side, there is an array of commodity chemicals made available and which significantly contributed to a more comfortable lifestyle. On the negative side, there has been a negative impact on environment due to the very high stability of these polymers.

Controlling the rheology of the polymers is central to their value, range of applications and stability. Co-polymerization of ethylene with other α-olefins is the factor enabling a perfect control of polymer rheology. However, these comonomers are not largely available. Hence, there is a need for developing selective catalytic systems to improve their availability.

In this thesis work we have focused on the problem of catalyst selectivity. In this introductory chapter, I will provide a brief highlight of the ethylene polymerization process to better understand the role of the comonomers, and then on the selective processes for the production of such additives.

1.1 Ethylene Polymerization

1.1.1 Overview

Polyethylenes (PE) provide by far the largest volume of synthetic polymers[1] since their broad range of applications makes them integral part of our modern life style. The reason for such tremendous popularity, also in sharp contrast to the growing concern about their negative environmental impact, has to be found in the convenient physical properties of these polymers rendering them particularly versatile in terms of applications. As a result of a large body of research, the polymer rheology is today completely tunable. Toughness, hardness, clarity, and other physical characteristics can be controlled by varying the molecular weight and co-monomer type and content. The most common types of polyethylene are depicted in Figure 1.1: high density polyethylene (HDPE), low density polyethylene (LDPE) and linear low density polyethylene (LLDPE).

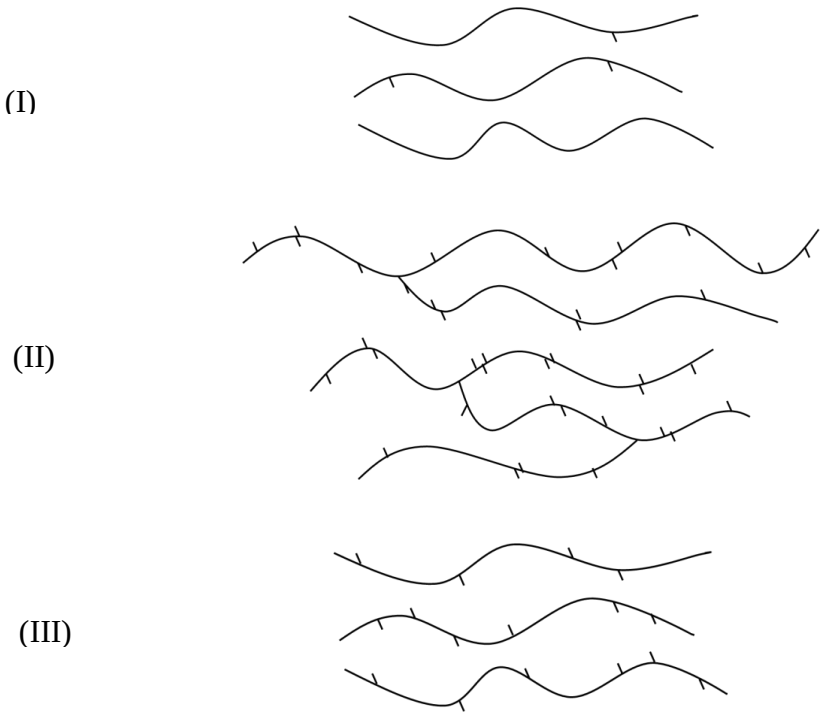

Figure 1.1. Schematic representations of different types of polyethylene. (I) HDPE; (II) LDPE; and (III) LLDPE.[2]

The linearity associated with HDPE with an extremely low level of branching determines a high degree of crystallinity, which in turn is responsible for the highest stiffness and lowest permeability of all types of polyethylene. This combination makes HDPE highly desirable for a broad range of household and industrial applications such as bottles and containers for a variety of products. To fine tune its crystallinity level, HDPE can be produced by copolymerization with variable amounts of α-olefins.[2]

The introduction of numerous short-chain branches is the primary characteristic of LDPE. The branching reduces the polymer crystallinity and lowers its density. Such characteristic enhances polymer flexibility and lowers its melting point. Longer chain branches cause high melt strength and low viscosity, a desirable property during processing. These rheological characteristics make LDPE unsurpassable so far for the film-casting process and which is mainly used in retail packaging applications. Other minor uses include wire and cable insulation, squeeze bottle and food containers.[2]

Linear Low Density Polyethylene (LLDPE) consists of a polyethylene backbone attached to a large number of randomly distributed short alkyl groups. LLDPE are produced by the copolymerization of ethylene with linear alpha olefins. Depending on the content of the comonomer used, LLDPE can form resins with a broad range of different properties ranging from transparent non-crystalline to rigid and opaque elastomer that share many characteristics of HDPE. Such resins are used in many applications, including grocery sacks and stretch-wrap. LLDPE can also be extruded as cable insulation and pipes, where the stiffness of high density polyethylene is not required. Injection moulding is used to convert linear low-density polyethylene into materials of convenient flexibility and toughness. Such materials are used as food container lids and toys.[2]

The incorporation of very large amount of comonomer typically 1-butene, 1-hexene, and 1-octene tend to suppress crystallization, and consequently polymer density, to levels below that of low-density polyethylene. The ultralow density (ULDPE) or very low density (VLDPE) provides only limited crystallinity to these polymers causing low stiffness and high clarity. These properties are suitable for applications such as medical tubing, meat packaging, and diaper backing. Moreover, they can blend into other polymers as impact strength and clarity modifiers.[2]

1.1.2 Brief historical background

The existence of polyethylene was first recognized in 1898 by a German scientist, Hans von Pechmann[3], with the discovery of a waxy residue in the thermal decomposition of diazomethane. He had completely by accident made polyethylene, the world's most widely used material. Two years later Eugen Bamberger and Friedrich Tschirner called this waxy material polymethylene.[4]

In 1930 Friedrich and Marvel, reported the unexpected polymerization of ethylene to what they described as "non-gaseous" product.[5] However, there was no follow-up on this observation nor investigation of the polymerization reaction.

It was not until 1933, when Eric Fawecett and Reginald Gibson from Imperial Chemical Industries (ICI) were investigating the high pressure chemistry of some organic compounds including ethylene that the white waxy material produced in the high pressure reaction vessel was recognized as a polymer of ethylene. Two years later, Michael Perrin found a set of condition that could be used to polymerize ethylene consistently.[6] The polyethylene made was a ductile solid with melting temperature of about 115 ^{o}C. This material is what we know today as low density polyethylene.

By the outbreak of World War II, ICI established pilot plants for producing polyethylene commercially. The first polyethylene produced was used as an insulator for submarine communication cables. The use of polyethylene as an insulator enabled smaller components fabrication, which facilitated the mounting of such equipment on airplanes and other confined location.

In the early 1950s, Karl Ziegler and Giulio Natta independently developed the first catalyst that enabled polymerization of α-olefins at room temperature and atmospheric pressure. The Ziegler-Natta catalysts include many mixtures of halides of transition metals, especially titanium, chromium, vanadium, and zirconium, with organic derivatives of non-transition metals, namely alkyl aluminum compounds.[7]

The significance of Ziegler's discovery was acknowledged by the awarding of the Nobel Prize in chemistry in 1963 jointly to G. Natta for their work in the field of ethylene and propylene polymerization.[8-10] Nowadays, Ziegler-Natta catalysis is one of two methods used to produce HDPE, the other being metal oxide catalysis.[11,12]

A classic example of a Ziegler-Natta catalyst capable of polymerizing ethylene into HDPE is the complex of triethyl aluminum with titanium tetrachloride.[13-15]The proposed reaction mechanism is shown in Scheme 1.1. For many years, the heterogeneous nature of this catalytic system posed a challenge for understanding its mechanistic details.

Cossee and Arlman were among the first to propose a comprehensive mechanism for Ziegler-Natta type polymerization.[16-18] The proposal involves a catalytically active center consisting of a titanium atom coordinated to four bridging chlorine atoms and an alkyl group and one empty site in an overall octahedral arrangement. The polymerization starts with the coordination of one ethylene molecule at the vacant site, followed by alkyl insertion. A new

vacancy is thus generated at the apical position and repetitive additions of ethylene may generate a polyethylene chain. The growth of the polyethylene chain terminates with β-hydride elimination or alkyl transfer to the aluminum cocatalyst.

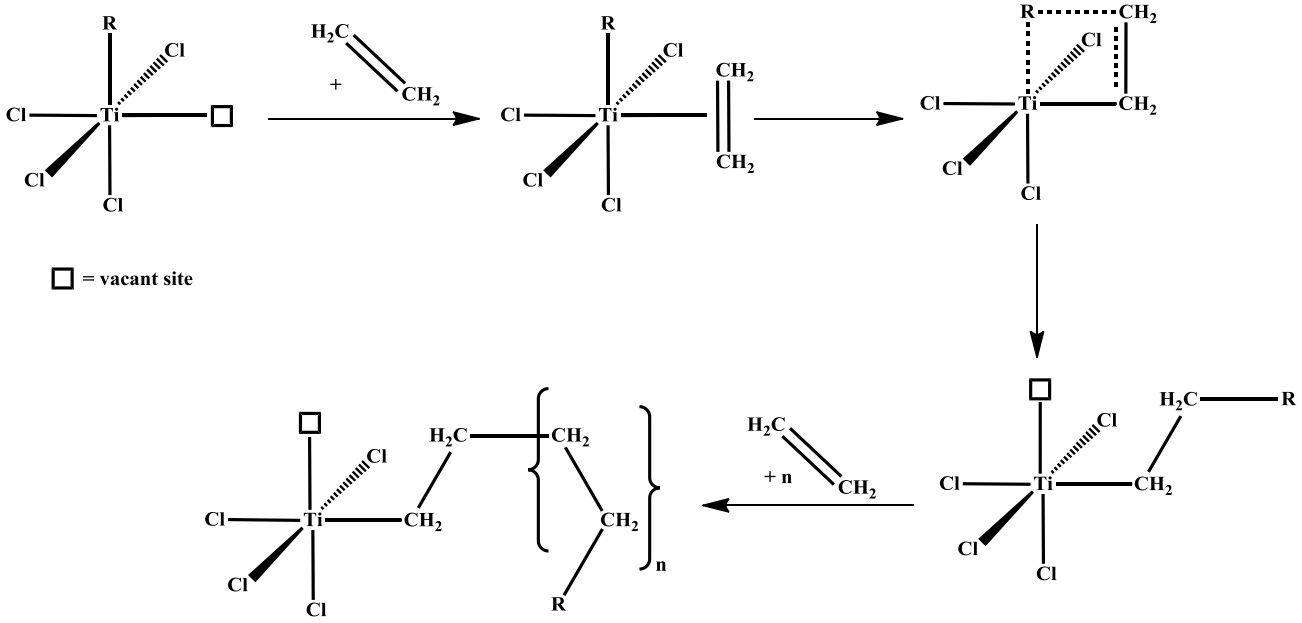

Scheme 1.1. Cossee-Arlman mechanism for Ziegler-Natta catalyzed ethylene polymerization.

At about the same time of the landmark discovery of Ziegler, P. Hogan and R. Banks at Phillips Petroleum were investigating a similar reaction catalyzed by various supported transition metal oxides. The ethylene polymerization promoted by chromium oxide supported over silica yielded a high molecular weight polymer. This product proved to be similar to the high-density polyethylene produced by Ziegler's low pressure, low temperature polymerization process.[19]

Since 1950 onwards, research had been directed toward the copolymerization of various monomers with ethylene. The commercialization of the Ziegler and Phillips processes provided an avenue whereby the properties of polyethylene could be modified by polymerizing ethylene with 1-alkenes comonomers. The Phillips process is the most extensively used process for the

production of high density polyethylene, accounting for approximately a quarter of the worldwide production.[20]

Ziegler-Natta catalysts have multiple active sites that polymerize ethylene, thus resulting in polyethylene with typical polydispersities of 4-6. Single-site catalysts have typically one type of active center "single site", consequently producing polyethylene with very narrow molecular weight distribution (polydispersities of 2-3).[21]

Today, there are two types of single site catalysts, metallocenes and non-metallocenes type catalysts. Metallocenes catalysts are π-bonded organometallic complexes[22,23] where the metal is "sandwiched" between two substituted aromatic ligands, such as dicyclopentadienyl or indenyl groups. In the so called "*ansa*" variation, the cyclopentadienyl rings maybe linked by a silicon or carbon atom, alkyl or other substituents. (Scheme 1.2)

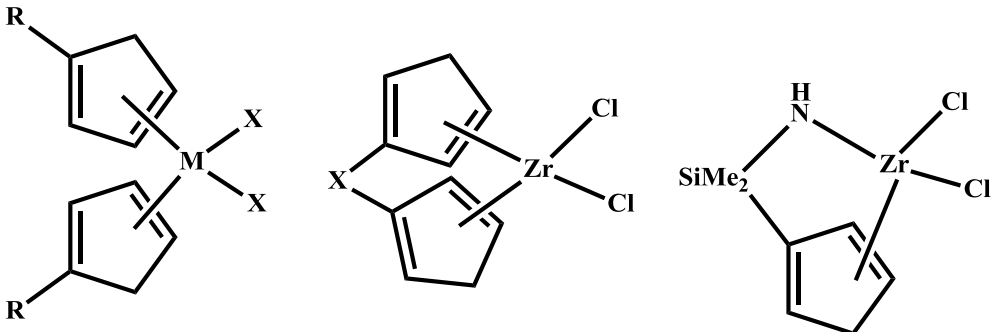

Scheme 1.2. Examples of single site metallocene catalysts for olefin polymerization.[2]

These versatile systems have been discovered as a development of the early work by Natta, Newburg and Breslow who first showed that ethylene could be polymerized, albeit with low activity using Cp_2TiCl_2 and alkyl aluminum.[24-27] The breakthrough in metallocene-catalyzed polymerization came in the late 1970s, with Kaminsky and Sinn[28,29] discovering that extremely

high ethylene polymerization activity could be achieved using Cp_2ZrMe_2 or Cp_2ZrCl_2 in combination with partly hydrolyzed $AlMe_3$ recognized as methyaluminoxane (MAO), one the most formidable activators.

Non-metallocenes single site or post metallocene catalysts were discovered in the 1990s. These catalysts are based on chelated late transition metals, namely Pd, Ni and Fe (Scheme 1.3).[30,31] These species offer the same advantages of metallocenes with the bonus of being less costly and oxophilic and allowing copolymerization of ethylene with polar monomer. Non-metallocene single site catalysts may also perform well with a broader range of co-catalysts. In turn, it is possible to eliminate expensive co-catalysts.

In 1995, Brookhart and coworkers discovered that complexes of Ni(II) and Pd(II) bearing chelating nitrogen-based α-diimine ligands afforded high molecular weight polymer with high catalytic activity (Scheme 1.3).[32]

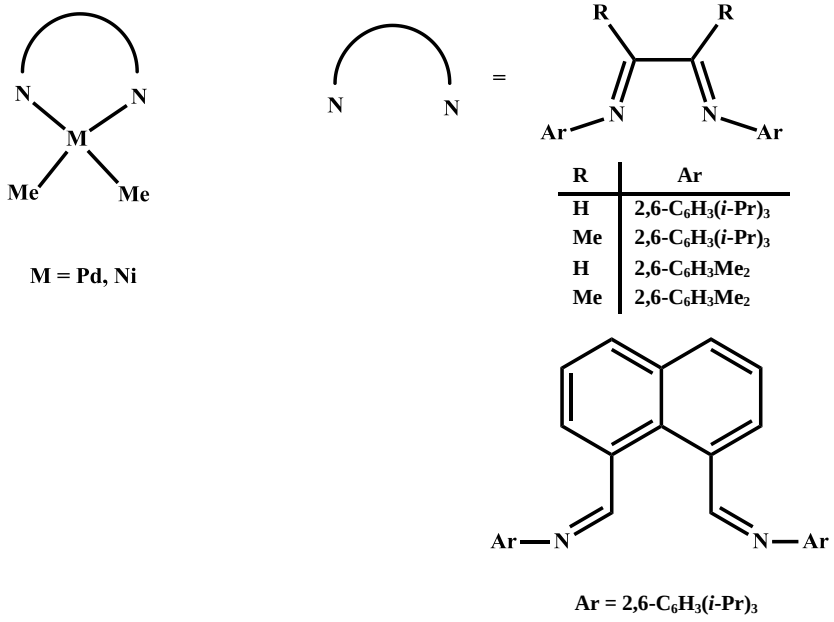

Scheme 1.3. Ni(II) and Pd(II) bearing chelating nitrogen-based α-diimine ligands.[32]

Following the advent of the nickel α-diimine complexes, a second major advance in the area of the late transition metal catalysts for ethylene polymerization took place in 1998, when highly active bis(imino)pyridyl iron catalysts (Scheme 1.4) were discovered independently by the Brookhart and Gibson groups.[33,34] In contrast to the nickel and palladium complexes, these catalysts produce highly linear, high density polyethylene, the molecular weight of which is dependent on the substituents present at the imino-aryl rings. A critical role was recognized to the *ortho*-substituents of the aryl rings, which block the axial approach of olefins and delay the rate of chain transfer by associative displacement.

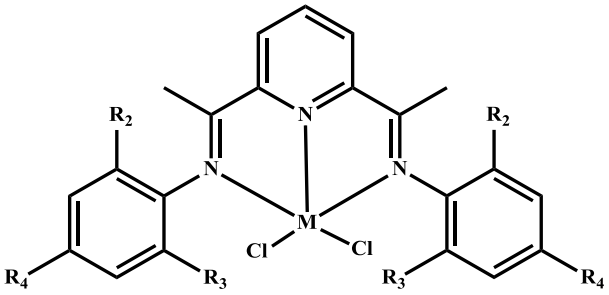

M	R_2	R_3	R_4
Fe	*i*-Pr	*i*-Pr	H
Fe	Me	Me	H
Fe	Me	Me	Me
Fe	Me	*i*-pr	Me
Co	*i*-Pr	Me	H

Scheme 1.4. Bis(imino)pyridyl iron single site catalyst.[34]

1.2 Ethylene Oligomerization

Linear Alpha Olefins (LAOs) or 1-Alkenes, featuring an accessible terminal double bond are widely used in a variety of industrial applications.[35-37] In particular; 1-butene, 1-hexene and 1-octene are utilized as co-monomer for the copolymerization with ethylene to produce Linear Low Density Polyethylene (LLDPE). Heavier LAOs have a range of useful applications in plasticizer alcohols (C_{10}-C_{12}), detergent alcohols (C_{10}-C_{18}), and additives for synthetic lubricant, and wide range of specialty applications (C_{10}-C_{18}).[38]

Ethylene oligomerization may be either selective or statistical. The first is a process where individual LAOs are selectively formed. The second yields mixtures of LAO distributed

over a range from C_4 to C_{40}. Commercial applications of different alpha-olefins are summarized in Figure 1.2.

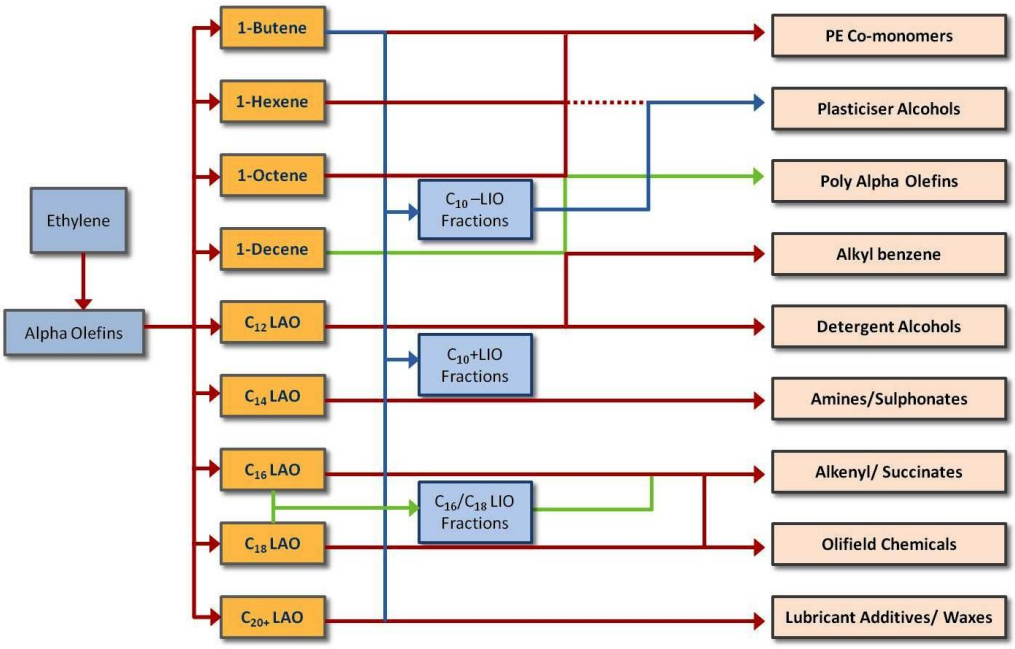

Figure 1.2. Industrial applications of different LAOs.[39]

The Dutch company Shell operates the proprietary Shell Higher Olefins Process (SHOP), one of the best known non-selective oligomerization processes, characterized by high productivity and no need for activators.[40-48] This process uses Ni(II) catalysts developed by Keim and coworkers such as in Scheme 1.5 bearing O-P chelating ligands to oligomerize ethylene into alpha olefins.[49-58] Late transition metals are notorious for their high tendency to undergo β-hydride elimination, a property that is in fact at the basis of the success of this technology. The active catalyst is nickel hydride complex,[59] formed by insertion of ethylene into a Ni-phenyl group followed by elimination of styrene. (Scheme 1.5)

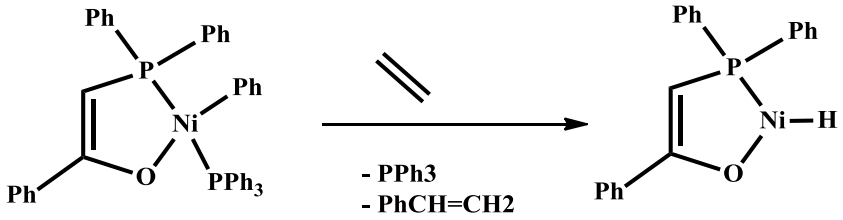

Scheme 1.5. Shell Higher Olefins (SHOP), nonselective ethylene oligomerization process.

Ethylene oligomerization takes place via coordination and migratory insertion of ethylene to generate Ni-alkyl species. As the alkyl group chain is assumed to be more strongly coordinated in the position *trans* to the oxygen atom, an isomerisation step prior to the following insertion will lead to the catalytic cycle illustrated in Scheme 1.6. When, as in this particular case, the rate of the migratory insertion versus that of the elimination is independent on the chain length, the concentration of lighter oligomers will be higher with respect to the heavier congener because of entropic reasons. The resulting distribution has a constant value of the $[C_{n+2}]/[C_n]$ ratio [the so-called α-factor] and it is called Schulz-Flory distribution. In the opposite scenario, where the elimination step has variable velocity a Gaussian sort of distribution centered on a certain oligomer is instead obtained (Poisson distribution).

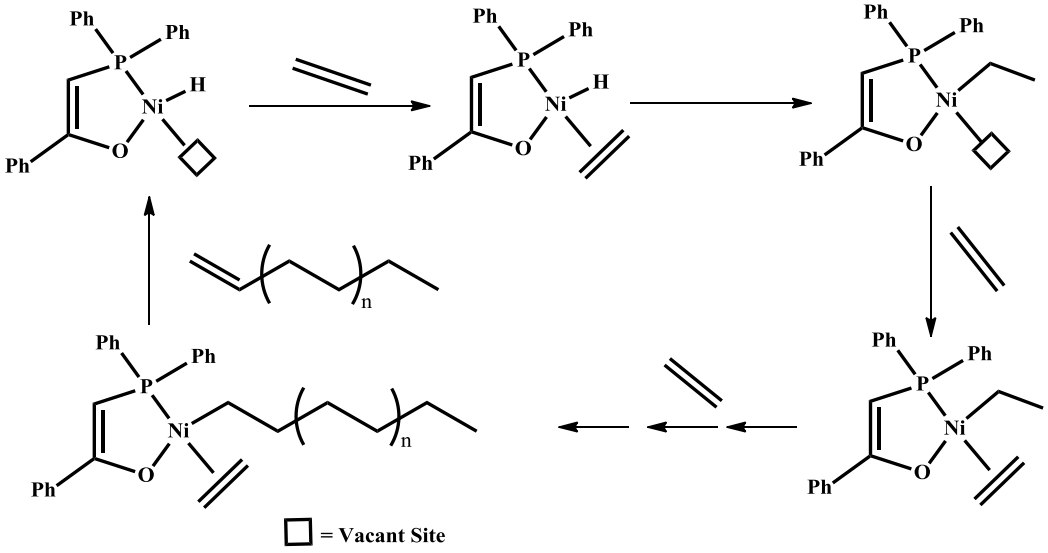

Scheme 1.6. Shell Higher Olefins Process (SHOP), mechanistic pathway.

Selective trimerization has steadily gained significance due to the increased demand for 1-hexene and 1-octene as comonomers for the polymerization of ethylene into LLDPE. Currently, selective trimerization, even though not very common, is well established.[60-68] The most efficient process is that owned by Phillips Petroleum as implemented on industrial scale in Qatar in 2003 producing 47 thousand tons of 1-hexene per year.[69] There are also several other processes operating on industrial scale and based on variations of the Phillips process. Some might display even better performance but the catalytic system requires more complex and expensive synthetic procedure.

In contrast, the tetramerization process is more rare and limited to only two examples. The most promising is the chromium catalyst based on $R_2PNR_1PR_2$ type diphosphinamine ligands. Some of these complexes are also used to produce 1-hexene. The selectivity for 1-octene is, however, substantially lower than in the trimerization, only being in the 70% range. The Sasol company has built the first ethylene tetramerization plant capable of producing over 100,000 metric tons per year of combined 1-octene and 1-hexene.[70]

1.3 Mechanistic Considerations

1.3.1 Chain Growth Mechanism (Non-Redox)

Non-selective oligomerization is proposed to occur via a Cossee-Arlman type of mechanism, involving formation of linear alkyl chains intermediates which, upon β-hydrogen elimination, produce a statistical distribution of linear alpha olefins referred to as Shultz-Flory distribution. (Scheme 1.7)

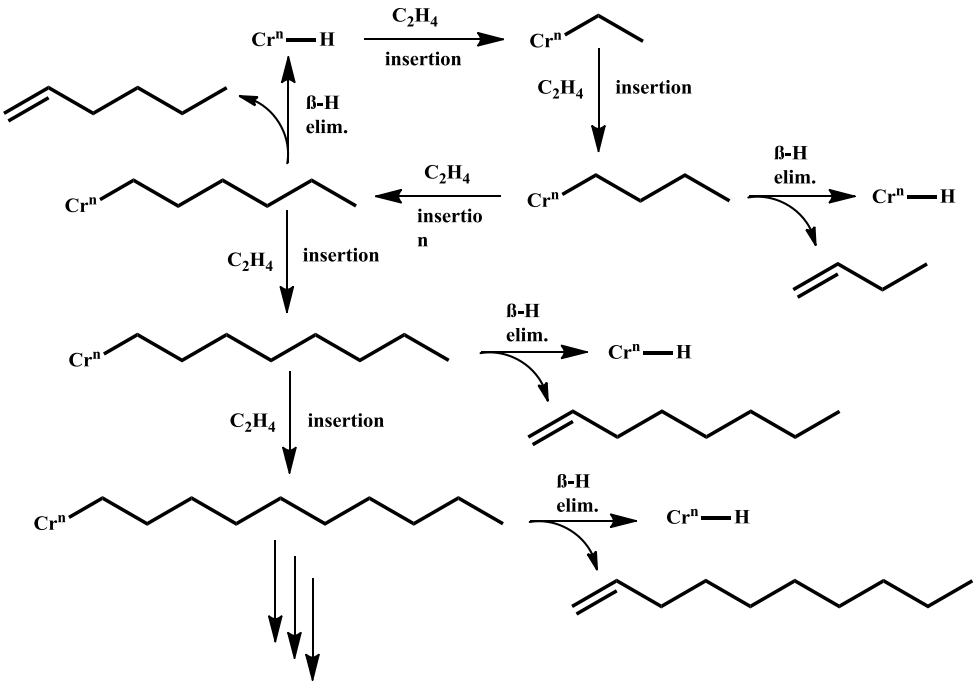

Scheme 1.7. Cossee-Arlman mechanism for non-selective ethylene oligomerization.

1.3.2 Metallacycle "ring expansion" Mechanism ($2e^-$ Redox)

The most widely accepted mechanism to account for high selectivity involves metallacycle intermediates (Scheme 1.8). Initial coordination of two ethylene molecules to the catalytically active metal center M^{+n} is followed by oxidatve coupling to form a metallacyclopentane ring where the metal has increased its oxidation state by two. β-hydrogen elimination from the chromacyclopentane might in principle lead to 1-butene formation. However, the chromacyclopentane ring is strained and ring expansion to a larger ring is thus favored. The resulting metallacycloheptane is flexible enough to undergo β-hydrogen elimination, affording a chromium-alkenyl-hydride species that reductively eliminates 1-hexene and regenerates the original catalytically active species. It has been suggested that the release of 1-hexene from the metallacycloheptane proceeds via a concerted 3,7-hydrogen shift.[71-78] A tetramerization proceeding through metallacycle mechanism would imply expansion of the seven

to a nine membered ring intermediate. In this scenario however, further ring expansion to even larger ring will have only a similar activation barrier. The obvious result will be that the selectivity cannot necessarily reach high levels in this case. It is because of this realization that workers in the field have started thinking about alternative reaction routes in the hope to increase the selectivity of the tetramerization.

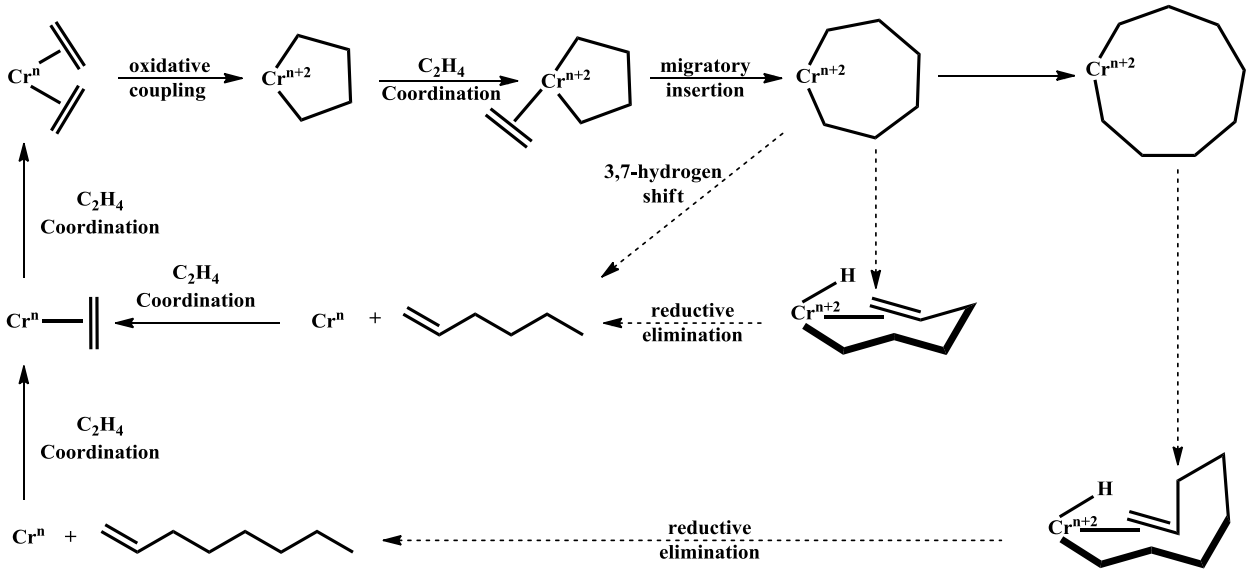

Scheme 1.8. Metallacycle mechanism.

1.3.3 Bimetallic Mechanism: an alternative pathway for 1-octene formation?

Rosenthal and coworkers[79] have envisioned the possibility that a bimetallic complex might be able to selectively afford 1-octene (Scheme 1.9). The idea is intellectually stimulating and triggered research efforts to find supporting evidence. To date, however, the mechanism has never been completely substantiated and further experimerntal evidence is necessary. The mechanism implies the proximity of two catalytically active monovalent chromium centers. The vicinity will have to be limited though in order to prevent formation of Cr-Cr multiple bond and which will obliterate the catalytic activity. Assuming formation of two five-membered

metallacycles, two subsequent reductive eliminations are expected to form the C_8 chain first and 1-octene in the last step.

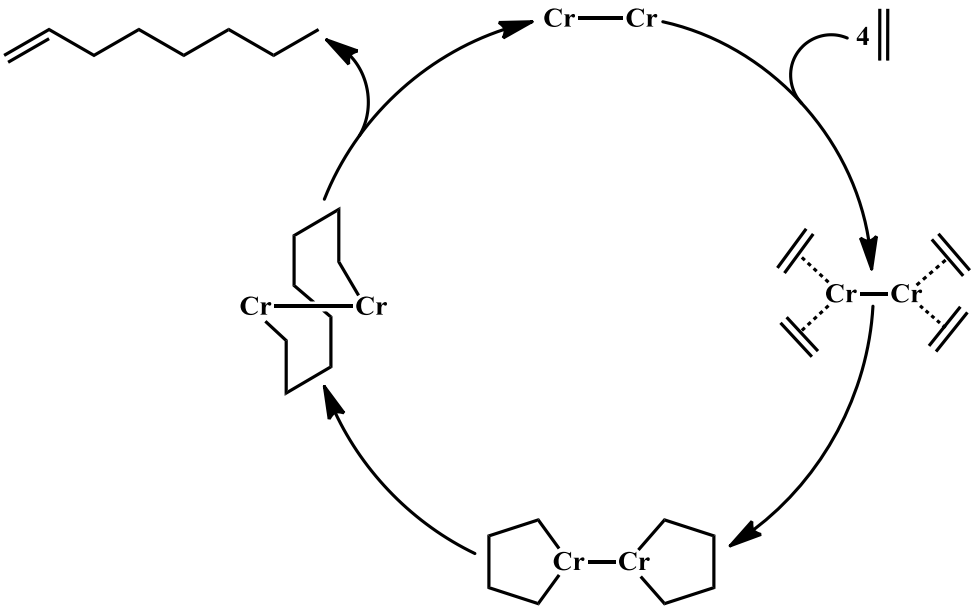

Scheme 1.9. Rosenthal proposed bimetallic mechanism.

1.4 Chromium Based Selective Ethylene Oligomerization

In the collection of the existing selective catalytic systems, chromium by far remains the most preferred element since it produced the most active, selective catalysts within the highest structural diversity.[80-82] The remaining current challenges include the improvement of catalyst performance with respect to lifetime, activity and selectivity. A substantial amount of research work has been carried out to correlate catalytic behaviour to ligand features, solvent, and activator's nature. [36,56,57,83]

The first discovery of chromium based catalysts for selective ethylene oligomerization dated back to 1967, when Manyik, Walker, and Wilson from Union Carbide Corporation observed that during ethylene polymerization with Cr(III)-tris-2-ethylhexonate, activated with partially hydrolyzed tri-isobutylaluminum, a certain amount of 1-hexene (1-C_6) was formed and

then co-polymerized with ethylene.[84] One year later, the same authors proposed a possible mechanism to account for the selective trimerization involving chromium metallacyclic intermediates.[85]

1.4.1 Chevron-Philips System

In the early 1990's, Reagan[86,87] from Phillips Petroleum developed an industrially viable process for the production of 1-hexene. Using the same Cr(III)-tris-2-ethylhexanoate and adding 2,5-dimethylpyrrole as a ligand together with DEAC and TEAL as co-catalyst, a catalytic system of high activity (156,666 g/gCr/h) was obtained with 93% selectivity for 1-hexene (Scheme 1.10). Mitsubishi Chemical made further enhancement to the performance of this catalyst by using non-coordinating Lewis acid $B(C_6F_5)_3$, DMAP and using chlorinated solvent such as hexachloroethane.[88] (Scheme 1.11)

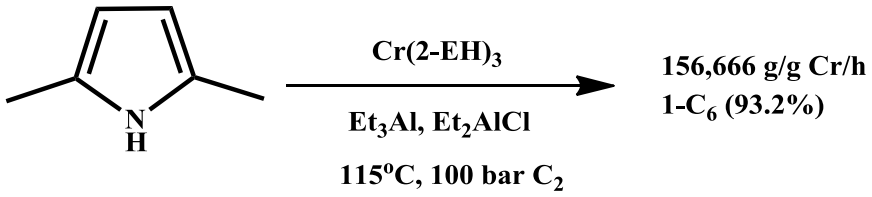

Scheme 1.10. Phillips Pyrrolate system.

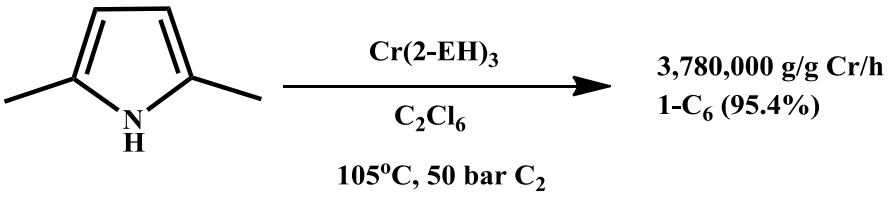

Scheme 1.11. Mitsubishi improved Pyrrolate system.

This highly efficient catalytic system was investigated in our lab in the recent past. By isolating the self activating catalytically active species as generated by the activators, it was

possible to correlate specific chromium oxidation states to the type of catalytic behaviour and unveil the chromium oxidation state responsible for selectivity.[89] (Scheme 1.12)

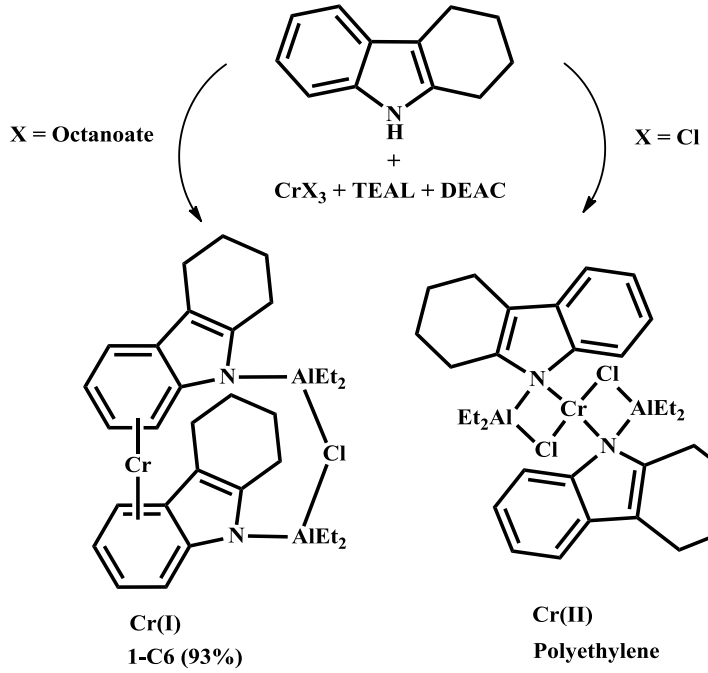

Scheme 1.12. Bulky pyrrolate lignad designed by Gambarotta and co-workers.

1.4.2 Tosoh's Pyrazolylmethane System

The recent literature shows a florilegia of diversified systems. The tris(pyrazolyl)methane chromium derivative as developed by Tosoh corporation researchers[90] was found to be highly active and selective for trimerization upon activation with methylaluminoxane (MAO) (Scheme 1.13). The significance of this system lies in the stability of the ligand, simplifying handling while comparing to the Phillips pyrrolate system.

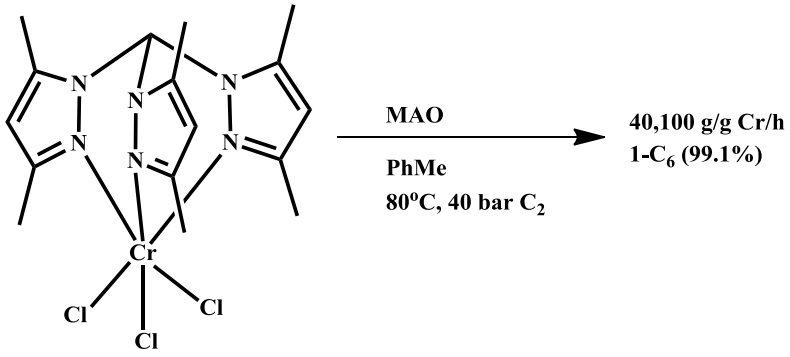

Scheme 1.13. Tosoh's Pyrazolylmethane system.

Further studies on modified heteroscorpionate tridentate pyrazolyl ligands were carried out by Hor and co-workers.[91-93] Upon activation with MAO, both sulfur and oxygen complexes showed selectivity toward ethylene trimerization, the best activity and selectivity being observed for thioether (R = hexyl and R` = Me). (Scheme 1.14)

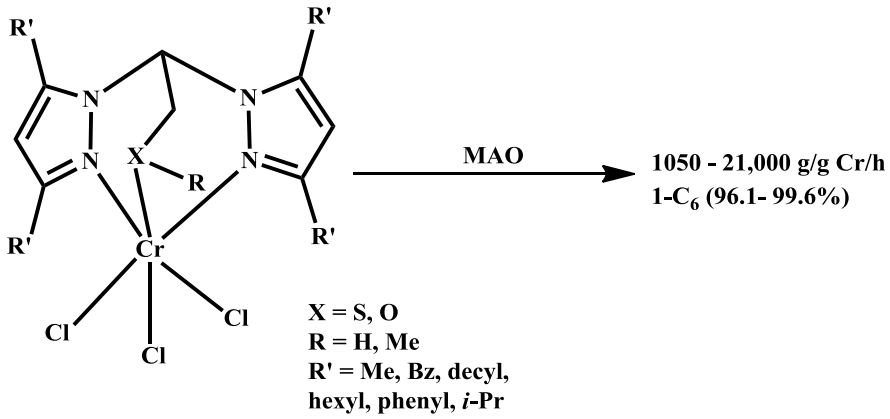

Scheme 1.14. Hor heteroscorpionate pyrazolyl ligands.

1.4.3 Triazacyclononane System

Köhn and co-workers[94,95] developed an NNN heteroscorpionate complex of Cr(III), based on triazacyclononane ligand. Upon activation with MAO, this system also showed selectivity toward 1-hexene. However, the downside of this system is the formation of polymeric material

along with 1-hexene. Thorough investigation of the catalytic system demonstrated that the alkyl substitution on the nitrogen atoms was essential to prevent polymerization. (Scheme 1.15)

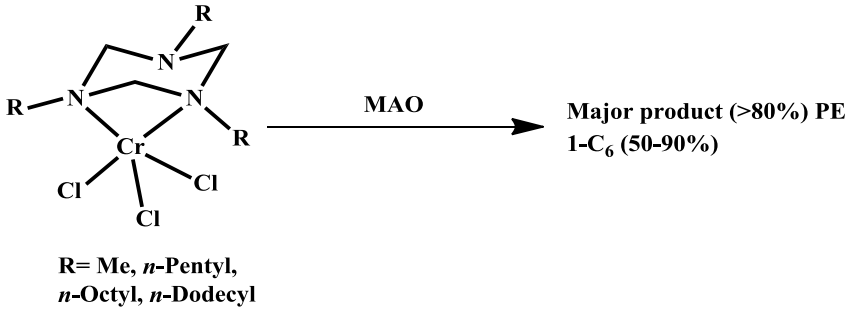

Scheme1.15. Köhn and co-worker NNN heteroscorpionate chromium complex.

1.4.4 British Petroleum *ortho*-methoxy PNP System

PNP type ligands were introduced in the early 2000s and produced a versatile family of selective catalysts. The *ortho*-methoxy PNP (Scheme 1.16) was reported in 2002 by Wass from British Petroleum[96-98] (BP) showing very high activity and selectivity (90%) for 1-hexene. Important from the industrial point of view is that this catalyst produces no undesirable polymeric byproduct.

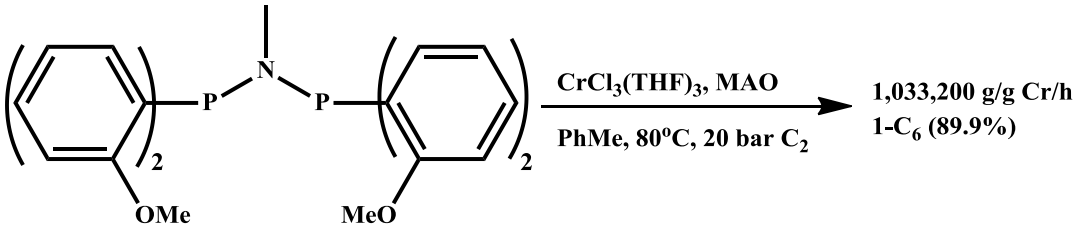

Scheme 1.16. The *ortho*-methoxy PNP catalytic system developed by Wass.

1.4.5 Sasol PNP System

The Sasol Corporation built on the Wass's work on PNP system by introducing substituents on both the nitrogen and phosphorus atoms and changing reaction conditions. By removing the *ortho*-substituent from the phenyl groups, the first example of a tetramerization

catalyst was obtained with a remarkable selectivity for 1-octene of up to 70%. (Scheme 1.17) Increasing the steric of the substituent of the phenyl rings[99,100] affected the selectivity toward 1-octene with bulky groups favoring 1-hexene formation, and less bulky affording mainly 1-octene (Scheme 1.18).[101]

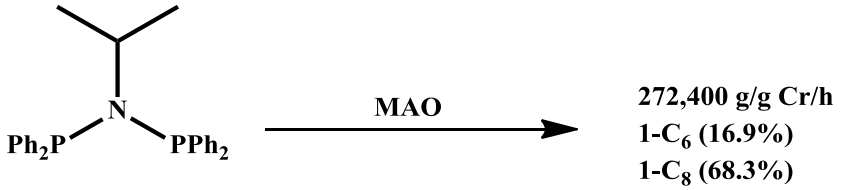

Scheme 1.17. Sasol's PNP ligands system.

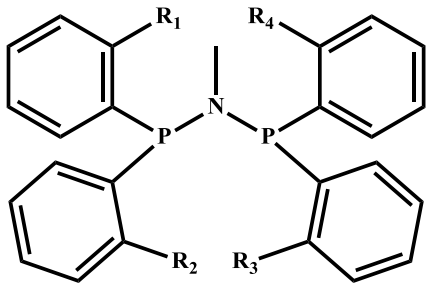

R_1, R_2, R_3, R_4 = H, Me, Et, *i*-Pr

Scheme 1.18. *ortho*-substitution of Sasol PNP system.

By moving the location and number of the methoxy substituents to the *meta* or *para*-positions, the same selectivity displayed by unsubstituted ligands in terms of C_6/C_8 was obtained. Moreover, it was noted that only one *ortho*-methoxy substituent is necessary to shift the selectivity toward trimerization.[101,102] (Scheme 1.19)

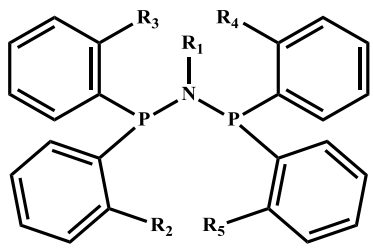

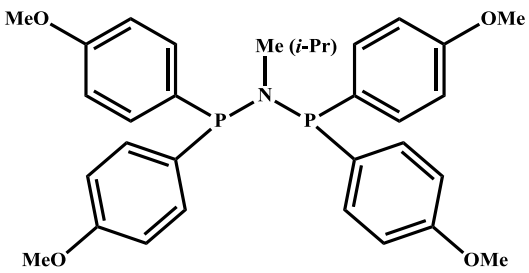

R_1	R_2	R_3	R_4	R_5
Me	**OMe**	**OMe**	**OMe**	**OMe**
Me	**H**	**H**	**H**	**H**
***i*-Pr**	**H**	**H**	**H**	**H**
***i*-Pr**	**OMe**	**H**	**H**	**OMe**
***i*-Pr**	**OMe**	**H**	**H**	**H**
***i*-Pr**	**Et**	**H**	**H**	**H**

Scheme 1.19. *ortho*, *meta* and *para*-substitution of Sasol PNP system.

The role of the *N*-substituent was mainly determining ligand deformation by providing steric bulk, with less-sterically demanding groups leading to 1-hexene.[103-106] The influence of *N*-aryl functions was also examined by Killian et al,[107] finding that the selectivity was more dependent on the steric bulk attached to nitrogen, and less on the group basicity. *Ortho*-substitution, as in classical PNP ligands, was found to be important in maximizing 1-hexene selectivity possibly through coordination to the chromium center. (Scheme 1.20)

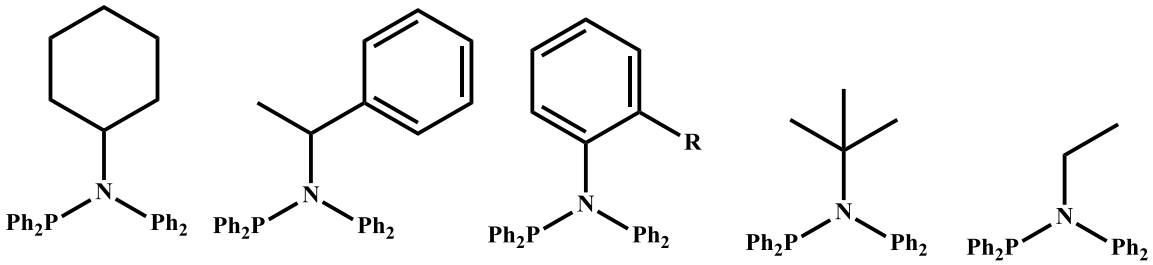

Scheme 1.20. Study of the steric effect of the *N*-substituted PNP catalytic system.

Further modification of the ligand framework included the preparation of multi-site ligands (Scheme 1.21).[108-109] Since no enhancement in selectivity was observed, the involvement

of bimetallic mechanisms was ruled out for catalysts of this specific framework. Nonetheless, increase in activity for the longer chain bridging ligand was observed.

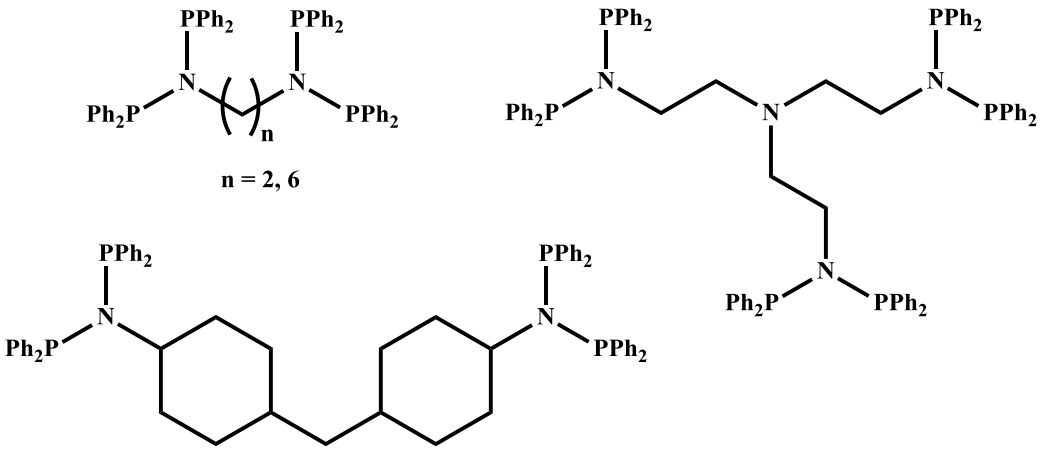

Scheme 1.21. Multi-site PNP ligands.

1.4.6 Cr-PNNP System

The role of the PN linkage was further examined by using a $Ph_2PN(Me)N(Me)PPh_2$ chelating ligand, which afforded tetramerization with similar selectivity, though the activity was only moderate comparing to the previous Sasol PNP catalytic system.[110] (Scheme 1.22)

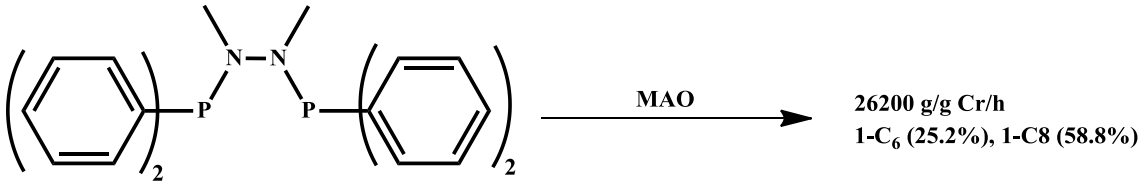

Scheme 1.22. PNNP catalytic system.

1.4.7 Rosenthal System

A modification to the $Ar_2PN(R)PAr_2$ ligands, was implemented by Rosenthal[111-114] who has obtained with $Ph_2PN(i\text{-}Pr)P(Ph)(NHR)$ a selective trimerization catalyst with 99.3% selectivity (Scheme 1.23). The chromium complex of the ligand shows k_2-(P,P) coordination

similar to PNP ligands without pendant donors. An attempt to deprotonate the amine function gave formation of a hetero-dinuclear species, which was assumed to be the active catalyst for ethylene trimerization.

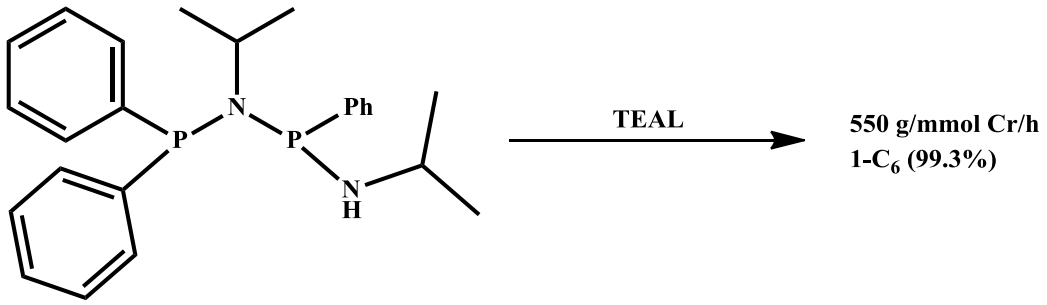

Scheme 1.23. Rosenthal ligand system.

1.4.8 Other PNP Systems

Another class of bidentate ligands featuring a carbon linker separating P and N atoms of the PNP system gave selective trimerization behavior. A $Ph_2PCH_2N(R)CH_2PPh_2$ ligand framework was designed by Le Floch showing coordination to the metal only through the phosphines residues.[115] A modification of this system gave a combined 1-hexene and 1-octene amount of over 90%. As in the previous PNP system, the less sterically hindered substitution of the phosphines led to a decrease in selectivity for C_6 product in favor of C_8. Upon changing the phosphorous substituents from cyclohexyl to n-butyl, the selectivity shifted from 97% C_6 product to 78% C_6 and 21% C_8. (Scheme 1.24)

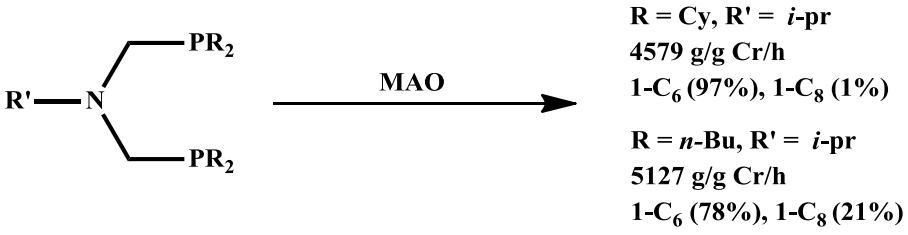

Scheme 1.24. Le Floch PNP ligand system.

A successful modification of this unique ligand framework was implemented by Sasol's workers with the introduction of ethylenic bridges between the N and P hetero atoms.[116] The ligands of general formula $R_2P(CH_2)_2NH(CH_2)_2PR_2$, proved to be excellent supporting systems for a family of potent trimerization catalysts. The organic residues at the P atoms again played an important role. Compared to cyclohexyl and phenyl, the ethyl group-containing ligand was the most selective and produced up to 98% C_6 with 99.1% 1-hexene with a respectable activity of 37400 g/g Cr/h.[117] (Scheme 1.25)

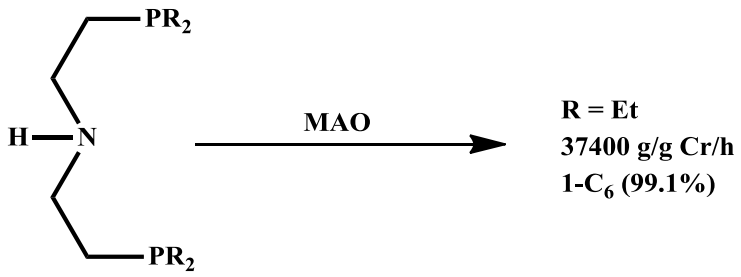

Scheme 1.25. Sasol $Ph_2PCH_2CH_2N(H)CH_2CH_2PPh_2$ ligand system.

In direct analogy with the PNP systems, the nature of the group at the N atom has a great influence on the catalytic behavior. Alkyl groups gave lower selectivity toward 1-hexene and also produced a significant amount of polymer (>30%).[118] Instead the N-H functionality is essential for high activity and selectivity, and the authors speculated that deprotonation at the NH functionality might occur during activation by the aluminate. However, deliberately deprotonated ligands gave catalytically inert complexes.

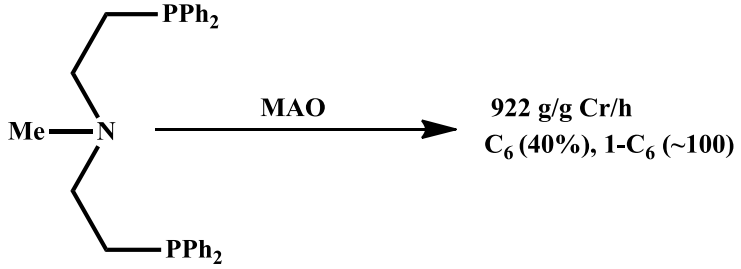

Scheme 1.26. PNHP containing N-alkyl functionality.

Further studies focused on the N-H functionality, the chromium oxidation state as well as on the role of MAO.[119] A chromium (II) complex was prepared and its activity and selectivity was found very similar to the original trivalent complexes. This led to the conclusion that Cr(III) precursors are reduced to the divalent state or lower (Scheme 1.27).

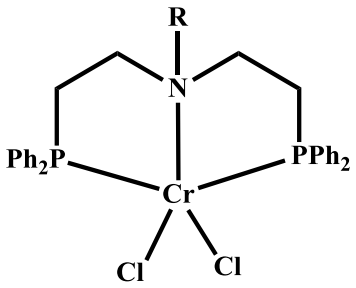

Scheme 1.27. Chromium (II) complex of PN(R)P ligands system.

1.4.9 Imine PNP System

Bluhm[120] and co-worker tested tridentate ligands of central imine and amine donors such as those shown in Scheme 1.28. Upon activation with MAO, ~82-86% 1-hexene was formed with the remainder being polyethylene. Increasing the temperature caused the selectivity to shift toward polymer formation. Furthermore, the amine analogs were tested and found to similarly produce 60-70% polyethylene, with the remainder being 1-hexene.

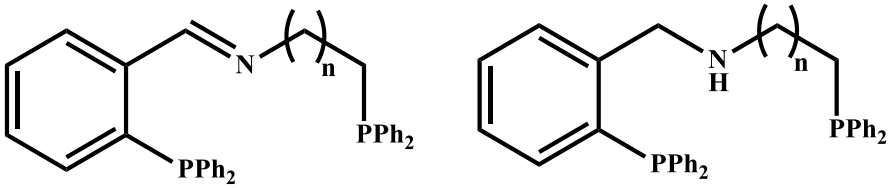

Scheme 1.28. Bluhm tridentates ligands of central imine and amine donors.

1.4.10 Modified PN System

A significant breakthrough was achieved in our lab with the design of a $PN(CH_2)_nNP$ ligand,[121] where n = 2, 3. This ligand motif provided highly selective catalysts for either 1-

hexene or 1-octene depending on the size of the bridge between the two N atoms. (Scheme 1.29) Furthermore, when linking the N-P functionality to pyridine or amine through two carbon atoms,[122] high selectivity toward 1-octene was also obtained. (Scheme 1.30)

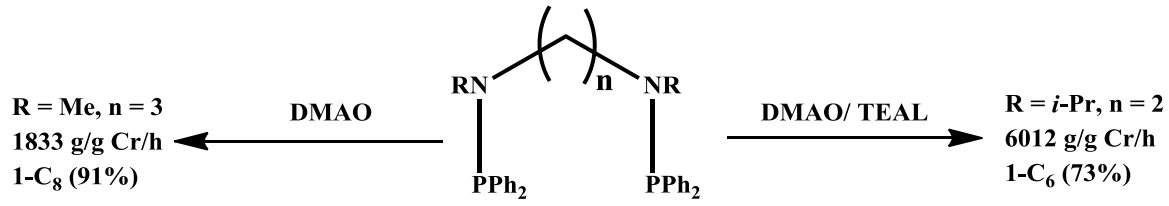

Scheme 1.29. $PN(CH_2)_nNP$ ligands.

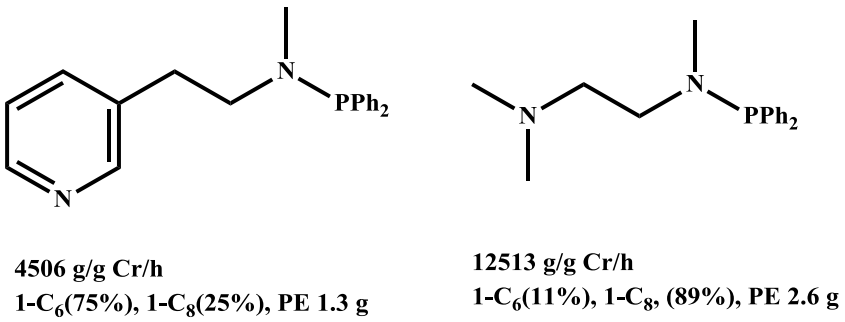

Scheme 1.30. Modified $PN(CH_2)_nNR_2$ ligands.

1.5 Significance of the co-catalyst

Typically, every catalytic system, whether selective or non-selective requires an activator "co-catalyst". Since its discovery by Kaminsky and Sinn, MAO (methylaluminoxane) became the preferred co-catalyst for ethylene oligomerization.[123] MAO is a hydrolyzed form of $AlMe_3$, believed to be composed of –MeAlO- repeated units arranged in a polymeric form and containing variable amounts of free $AlMe_3$ ranging from 10-30%.

MAO plays important roles during the catalytic process as: a) alkylating agent to the metal centre, b) halide or alkyl abstractor from the metal center, generating cationic metal centre,

c) it is also believed that the polymeric nature of the anionic MAO facilitates its separation from the metal center, thereby maintaining the cationization of the active species.

Commercially, MAO solution is prepared through controlled hydrolysis of $AlMe_3$. Hor[124] et al investigated the role of MAO during catalytic process through testing of various catalytically isolated active species of the [NNN] pyrazolyl Cr (III) complexes. In their finding they concluded that the presence of residual $AlMe_3$ in MAO solution is very crucial for metal reduction as well metal-halide activation.

Removal of the TMA component from MAO *in vacuo* at 50 ^{o}C produces DMAO (depleted MAO). Using DMAO fails to produce catalytically active species for the above [NNN] ligand system. On the other hand, when neat $AlMe_3$ is used, only very low activity were obtained indicating that MAO indeed is an important ingredient in the activation process.

1.6 Aim of the Thesis

The literature data summarized above clearly reiterates the fundamental role played by the metal oxidation state in the chromium-catalyzed selective oligomerization. Therefore, in the rational design of new and better performing catalysts, it is critical to identify ligand features capable of stabilizing the monovalent state. While phosphines and carbonyls certainly have a very strong stabilizing effect, not much information is available about the possible role of the pyridine ring. Pyridine in fact may well engage in back bonding interactions and thus might provide a good balance of reactivity and stabilization. In this particular field the information is rather scattered and there is little data suggesting the beneficial effect of this unit on selectivity. Therefore, with this thesis we were aiming towards a more comprehensive study on the role of pyridine as a trapping/stabilizing unit during the interaction of the metal center with the activator. In this research work we have focused on both neutral and ionic pyridine-based

modified ligand systems with a major effort having been carried out to isolate catalytically active species.

In chapter 2, organochromium complexes based on a dianionic $Ph_2PNHPyNHPPh_2$ ligand were prepared and tested as catalyst for ethylene oligomerization and polymerization. We were interested in clarifying a possible role of the pyridine substituent in stabilizing lower oxidation states and ultimately affecting the selectivity of the catalytic cycle. The introduction of the pyridine ring in the PN ligand scaffold afforded nonselective catalytic systems. The stabilizing ability of the pyridine ring affects not only the chromium divalent state but also the Cr- R function. Even when reduction to the divalent state does occur, the pyridine ring most likely prevents further reduction.

Chapter 3 includes the modification of the ligand used in the previous chapter by removing the N-P functionality. Using a neutral classical diphosphino-pyridine pincer ligand, we have attempted to understand how the ligand neutrality affects the aggregation between chromium and aluminates. Although in this case we were able to isolate a complex containing cationic chromium in its monovalent state, its encapsulation in an octahedral ligand field as defined by two ligands is probably responsible for its failure as a catalyst.

Further modification to the PNP was carried out in chapter 4, where we have reconsidered the classical Sasol's PNP scaffold and connected such functions to the two *ortho* positions of a central pyridine ring and examined the reactivity of the chromium derivative with alkyl aluminum. Two alternative modifications of this ligand motif have also been examined, where the tether of pyridine moiety to the central N of the PNP system was modified and the impact on catalytic behavior analyzed.

Chapter 5 describes the isolation of catalytically active chromium polyhydride cluster, one of very rare examples of chromium hydride species reported in the literature. The complex was obtained upon treatment with TIBA activator. The reaction not only reduced the metal to the divalent state but also generated hydride functions assembling an unprecedented hexa-chromium hydride cluster. The nonselecdtive catalytic behaviour of the formed cluster toward ethylene oligomerization was evaluated.

In chapter 6, cyclic PNPN scaffold was separated by methylene linkers. Its chromium precursors when treated with TMA afforded a Cr-Cr multiply bonded mixed valence Cr(I)/Cr(II) species. The complex was isolated and its activity toward ethylene oligomerization evaluated.

References

(1) Malpass, D. B. *Introduction to Industrial Polyethylene: Properties, Catalysts, and Processes*; Co-published by John Wiley & Sons, Inc. Hoboken, New Jersey, and Scrivener Publishing LLC. Salem, Massachusetts, 2010.

(2) Peacock, A. J. *Handbook of Polyethylene: Structures: Properties, and Applications*; Marcel Dekker Inc.: New York, 2000, pp 17-25.

(3) Pechmann, H. V. *Berichte* **1898**, *31*, 2640.

(4) Bamberger, E.; Tschirner, F.; *Chem Ber* **1900**, *33*, 955.

(5) Friedrich, M. E. P.; Marvel, C. S. *J. Am. Chem. Soc.*, **1930**, *52*, 376.

(6) Fawcett, E. W.; Gibson, O. R.; Perrin, M. W.; Patton, J. G.; Williams, E. G. Brit. Pat.# 571,590, 1937.

(7) Chen, E.; Marks, T. *Chem. Rev.* **2000**, *100*, 1391.

(8) Ziegler, K.; Holzkamp, E.; Breil, H.; Martin, H. *Angew. Chem.* **1955**, *67*, 541.

(9) Ziegler, K.; Breil, H.; Matin, H.; Holzkamp, E. GR 973,626, **1960**.

(10) Natta, G.; Pino, P.; Corradini, P.; Danusso, F.; Mantica, E.; Mazzanti, G.; Moraglio, G. *J. Am. Chem. Soc.* **1955**, *77*, 1708.

(11) Boor, Jr. Ziegler-Natta Catalysts and Polymerization. Academic Press: New York, 1979.

(12) Tait, P. J. T. Development in Polymerization, edited by Haward, R. N., Applied Science Publishers Ltd.: London, 1979, Vol. 2.

(13) Stauffer Chemical Co., *Preliminary Titanium Trichloride Technical Data*, 1962.

(14) Tornqvist, E. G. M.; Richardson, J. T.; Wilchinsky, Z. W.; Looney, R. W. *J. Catal.* **1967**, *8*, 189.

(15) Natta, G.; Corradini, P.; Allegra, G. *J. Polym. Sci.* **1961**, *51*, 399.

(16) Cossee, P. *Tetrahedron Lett.* **1960**, *8*, 86.

(17) Cossee, P. In Proceedings of the 6th Int. Congress on Coordination Chemistry. Macmillan: New York, **1961**, p 241.

(18) Arlman, *J. Proc. Int. Congr. Catal. 3rd*, **1964**, 2, p. 957.

(19) Hogan, J. P.; Banks, R. L. U.S. Patent 2,825,721, 1958.

(20) Malpass, D., B. *Introduction to Industrial Polyethylene: Properties, Catalysts, and Processes*; Wiley: 2010, p 62.

(21) Hlatky, G. *Chem. Rev.* **2000**, *100*, 1347.

(22) Collman, J. P.; Hegebus, L. S.; Norton, J. R.; Finke, R. G. *Principles and Applications of Organotransition Metal Chemistry*, University Science Books, Sausalito, CA, 1987, p 165.

(23) Carbtree, R. H. The Organometallic Chemistry of the Transition Metals, Wiley-Interscience, New York, 3rd Ed., 2001, p 130.

(24) Collman, J. P.; Hegebus, L. S.; Norton, J. R.; Finke, R. G. *Principles and Applications of Organotransition Metal Chemistry*, University Science Books, Sausalito, CA, 1987, P 9.

(25) Crabtree, R. H. The organometallic Chemistry of Transition metals, Wiley, 4th Edition, P 140.

(26) Breslow, D. S.; Newberg, N. R. *J. Am. Chem. Soc.* **1957**, *79*, 5072.

(27) Petros, R. A.; Norton, J. R. *Organometallics*, **2004**, 23, 5105.

(28) Sin, H.; Kaminsky, W. *Adv Organomet. Chem.* **1980**, *18*, 99.

(29) Sin, H.; Kaminsky, W.; Wolmer, H. J.; Woldt, R. *Angew. Chem. Int. Ed. Engl.* **1980**, *18*, 390.

(30) Ittel, S. D.; Johnson, L. K.; Brookhart, M. *Chem Rev*. **2000**, *100*, 1169.

(31) Wang, C.; Freidrich, S.; Younkin, T. R.; Li, R. T.; Grubbs, R. H.; Bansleben, D. A.; Day, M. W. *Organometallics* **1998**, *17*, 3149.

(32) Johnson, L. K.; Killian, C. M.; Brookhart, M. *J. Am. Chem. Soc.* **1995**, *117*, 6414.

(33) B. L.; Brookhar, M.; Bennett, A. M. A. *J. Am. Chem. Soc.* **1998**, *120*, 4049.

(34) Britovsek, G. J. P.; Gibson, V. C.; Kimberly, B. S.; Maddox, P. J.; McTavish, S. J.; Solan, G. A.; White, A. J. P.; Williams, D. J. *Chem Commun.* **1998**, 849.

(35) Alpha Olefins (02/03-4), PERP Report, Nexant Chem Systems.

(36) Vogt, D. Oligomerization of ethylene to higher linear α-olefins; In *Applied Homogeneous Catalysis with Organometallic Compounds*; Cornils, B., Herrmann, W. A., Ed.; Wiley-VCH: Weinheim, Germany, 2000; Chapter 2, pp 245-258.

(37) Lappin, G. R.; Sauer, J. D. In *Alpha Olefins Application Handbook*. Vol 37, Marcel Dekkers Inc.: New York, 1989, pp 1-3.

(38) McGuinness, D. *Chem. rev.* **2011**, *111*, 2321 and references cited therein.

(39) Alpha Olefins (06/07-5), PERP Report, Nexant Chem Systems.

(40) Freitas, E. R.; Gum, C. R. *Chem. Eng. Prog*. **1979**, *75*, 73.

(41) Lutz, E. F. (Shell Oil) US 4.528.416, 1985.

(42) Lutz, E. F.; Gautier, P. A. (Shell) EP 177.999, 1986.

(43) Turner, A. H. *J. Am. Oil Chem. Soc.* **1983**, *60*, 594.

(44) Cossee, P. *J. Catal.* **1964**, *3*, 80.

(45) Arlman, E. J.; Cossee, P. *J. Catal.* **1964**, *3*, 99.

(46) Schulz, G. V. Z. *Phys. Chem.* **1935**, *B30*, 379.

(47) Schulz, G. V. Z. *Phys. Chem.* **1936**, *B32*, 27.

(48) Flory, P. J. *J. Am. Chem. Soc.* **1936**, *58*, 1877.

(49) Keim, W.; Kowaldt, F. H.; Goddard, R.; Kruger, G. *Angew. Chem., Int. Ed. Engl.* **1978**, *17*, 466.

(50) Keim, W.; Behr, A.; Limbacker, B.; Kruger, C. *Angew. Chem., Int. Ed. Engl.* **1983**, *22*, 503.

(51) Keim, W.; Behr, A.; Gruber, B.; Hoffmann, B.; Kowaldt, F. H.; Kurschner, U.; Limbacker, B.; Sistig, F. P. *Organometallics* **1986**, *5*, 2356.

(52) Keim, W. *New J. Chem.* **1987**, *11*, 531.

(53) Keim, W. *J. Mol. Catal.* **1989**, 52, 19.

(54) Behr, A.; Keim, W. *Arab J. Sci. Eng.* **1985**, *10*, 377.

(55) Keim, W. *Angew. Chem., Int. Ed. Engl.* **1990**, *29*, 235.

(56) Keim, W. Ann. N.Y. *Acad. Sci.* **1983**, *415*, 191.

(57) Muller, U.; Keim, W.; Kruger, C.; Betz, P. *Angew. Chem. Int. Ed. Engl.* **1989**, *28*, 1011.

(58) Keim, W.; Schulz, R. P. *J. Mol. Catal.* **1994**, *92*, 21.

(59) Muller, U.; Keim, W.; Kruger, C.; Betz, P. *Angew. Chem. Int. Ed. Engl.* **1989**, *28*, 1011.

(60) Peitz, S.; Peulecke, N.; Aluri, B. R.; Hansen, S.; Müller, B. H.; Spannenberg, A.; Rosenthal, U.; Al-Hazmi, M. H.; Mosa, F. M.; Wöhl, A.; Müller, W. *Eur. J. Inorg. Chem.* **2010**, 1167.

(61) Zhang, J.; Braunstein, P.; Hor, T. S. A. *Organometallics* **2008**, *27*, 4277.

(62) Bluhm, M. E.; Walter, O.; Döring, M. *J. Organomet. Chem.* **2005**, *690*, 713.

(63) McGuinness, D. S.; Wasserscheid, P.; Morgan, D. H.; Dixon, J. T. *Organometallics* **2005**, 24, 552.

(64) McGuinness, D. S.; Wasserscheid, P.; Keim, W.; Hu, C.; Englert, U.; Dixon, J. T.; Grove, C. *Chem.Commun.* **2003**, 334.

(65) McGuinness, D. S.; Wasserscheid, P.; Keim, W.; Morgan, D. H.; Dixon, J. T.; Bollmann, A.; Maumela, H.; Hess, F. M.; Englert, U. *J. Am. Chem. Soc.* **2003**, *125*, 5272.

(66) Morgan, D. H.; Schwikkard, H.; Dixon, J. T.; Nair, J. J.; Hunter, R. *Adv. Synth. Catal.* **2003**, *345*, 939.

(67) Carter, A.; Cohen, S. A.; Cooley, N. A.; Murphy, A.; Scutt, J.; Wass, D. F. *Chem. Commun.* **2002**, 858.

(68) Köhn, R. D.; Haufe, M.; Kociok-Köhn, G.; Grimm, S.; Wasserscheid, P.; Keim, W. *Angew. Chem. Int. Ed.* **2000**, *39*, 4337.

(69) Dixon, J. T; Green, M. J.; Hess, F. M.; Morgan, D. H. *J. Organomet. Chem.* **2004**, *689*, 3641.

(70) van Leeuwen, Piet W. N. M; Clément, N. D.; Tschan, M. J.-L. *Coord. Chem. Rev.* **2011**, *255*, 1499.

(71) Blok, A. N. J., Budzelaar, P. H. M.; Gal, A. W. *Organometallics* **2003**, *22*, 2564.

(72) de Bruin, T. J. M.; Magna, L.; Raybaud, P.; Toulhoat, H. *Organometallics* **2003**, *22*, 3404.

(73) Tobisch, S.; Ziegler, T. *Organometallics* **2003**, *22*, 5392.

(74) van rensburg, W. J.; Grove, C.; Steynberg, J. P.; Stark, K. B.; Huyser, J. J.; Steynburg, P. J. *Organometallics* **2004**, *23*, 1207.

(75) Yu, Z. X.; Houk, K. N. *Angew. Chem. Int. Ed.* **2003**, *42*, 808.

(76) Tobisch, S.; Ziegler, T. *Organometallics* **2005**, *24*, 256.

(77) Tobisch, S.; Ziegler, T. *Organometallics* **2004**, *23*, 4077.

(78) Tobisch, S.; Ziegler, T. *J. Am. Chem. Soc.* **2004**, *126*, 9059.

(79) Peitz , S.; Aluri B. R.; Peulecke, N.; Müller, B. H.; Wöhl, A.; Müller, W.; Al-Hazmi M. H.; Mosa, F. M.; Rosenthal, U. C*hem. Eur. J.* **2010**, *16*, 7670.

(80) Liu, S.; Pattacini, R.; Braunstein, P. *Organomettalics* **2011**, *30*, 3549.

(81) McGuinness, D. S.; Suttil, J. A.; Gardiner, M. G.; Davies, N. W. *Organomettalics* **2008**, *27*, 4238.

(82) Junges, F.; Kuhn, M. C. A.; P dos Santos, A. H. D.; Rabello, C. R. K.; Thomas, C. M.; Carpentier, J.-F.; Casagrande Jr, O. L.; *Organomettalics* **2007**, *26*, 4010.

(83) Agapie, T. *Coord. Chem. Rev.* **2011**, *255*, 861.

(84) Manyik, R. M.; Walker, W. E.; Wilson, T. P. US pat. 3300458, 1967.

(85) Manyik, R. M.; Walker, W. E.; Wilson, T. P. *J. Catal.* **1977**, *47*, 197.

(86) Reagen, W. K. EP 0417477 (Phillips Petroleum Company), March 20, 1991.

(87) Reagen, W. K. Symp. Prepr. Conv. Light Olefins, Div. Pet. Chem., *Am Chem. Soc.* **1989**, *34*, 583.

(88) Araki, Y.; Nakamura, H.; Nanba, Y.; Okanu, T. (Mitsubishi Chemical Corporation) US 5,856, 612, 1999.

(89) Jabri, A.; Mason, C. B.; Sim, Y. ; Gambarotta, S.; Burchell, T. J.; Duchateau, R. *Angew. Chem. Int. Ed.* **2008**, *47*, 9717.

(90) Yoshida, T.; Yamamoto, T.; Okada, H.; Murakita, H. (Tosoh Corporation) US 2002 /0035029, 2002.

(91) Zhang, J.; Braunstein, P.; Hor, A. T. S. *Organometallics* **2008**, *27*, 4277.

(92) Zhang, J.; Li, A.; Hor, T. S. A. *Organometallics* **2009**, *28*, 2935.

(93) Zhang, J.; Li, A.; Hor, T. S. A. *Dalton Trans.* **2009**, 9327.

(94) Köhn, R. D.; Haufe, M.; Kociok- Köhn, G.; Grimm, S.; Wasserscheid, P.; Keim, W. *Angew. Chem. Int. Ed.* **2000**, *39*, 4337.

(95) Köhn, R. D.; Haufe, M.; Mihan, S.; Lilge, D. *Chem. Commun.* **2000**, 1927.

(96) Wass, D. F. (BP Chemicals Ltd) WO 02/04119, 2002.

(97) Carter, A,; Cohen, S. A.; Cooley, N. A.; Murphy, A.; Scutt, J.; Wass, D. F. *Chem Commun.* **2002**, 858.

(98) Wass, D. F. *Dalton Trans.* **2007**, 816.

(99) Bollmann, A.; Dixon, J. T.; Hess, F. M.; Killian, E.; Maumela, H.; McGuinness, D. S.; Morgan, D. H.; Neveling, A.; Otto, S.; Overett, M.; Slawin, A. M. Z.; Wasserscheid, P.; Kuhlmann, S. *J. Am. Chem. Soc.* **2004**, *126*, 14712.

(100) Blann, K.; Bollmann, A.; Dixon, J. T.; Neveling, A.; Morgan, D. H.; Maumela, H.; Killian, E.; Hess, F. M.; Otto, S.; Pepler, L.; Mahomed, H.; Overett, M. WO Patent 04056479A1 (Sasol Technology), 2004.

(101) Blann, K.; Bollmann, A.; Dixon, J. T.; Hess, F. M.; Killian, E.; Maumela, H.; Morgan, D. H.; Neveling, A.; Otto, S.; Overett, M. *Chem. Commun.* **2005**, 620.

(102) Overett, M. J.; Blann, K.; Bollmann, A.; Dixon, J. T.; Hess, F. M.; Killian, E.; Maumela, H.; Morgan, D. H.; Neveling, A.; Otto, S. *Chem. Commun.* **2005**, 622.

(103) Blann, K.; Bollmann, A.; de Bod, H.; Dixon, J. T.; Killian, E.; Maumela, M. C.; Maumela, H.; Morgan, D. H.; Prétorius, M.; Kuhlmann, S.; Wasserscheid, P. *J. Catal.* **2007**, *249*, 244.

(104) Jiang, T.; Chen, H., X.; Ning, Y. N.; Chen, W. Chin. *Chem. Chem. Lett.* **2006**, *17*, 358.

(105) Kuhlmann, S.; Blann, K.; Bollmann, A., Dixon, J. T.; Killian, E.; Taccardi, N.; Wasserscheid, P. *J. Catal.* **2007**, *245*, 279.

(106) Jiang, T.; Zhang, S.; Jiang, X.; Yang, C.; Niu, B.; Ning, Y. *J. Mol. Catal. A: Chem.* **2008**, *279*, 90.

(107) Killian, E.; Blann, K.; Bollmann, A.; Dixon, J. T.; Kuhlmann, S.; Maumela, M. C.; Maumela, H.; Morgan, D. H.; Nongodlwana. P.; Overett, M.; Prétorius, M.; Höfener, k; Wasserscheid, P. J. Kol. *Catal. A:Chem.* **2007**, *270*, 214.

(108) Jiang, T.; Chen, H.; Ning, Y.; Chen, W. *Chin. Sci. Bull*. **2006**, *51*, 521.

(109) Mao, G.; Ning, Y.; Hu, W.; Li, S.; Song, X.; Niu, B.; Jiang, T. *Chin. Sci. Bull.* **2008**, *53*, 3511.

(110) Bollmann, A.; Blann, K.; Dixon, J. T.; Hess, F. M.; Killian, E.; Maumela, H.; McGuinness, D. S.; Morgan, D. H.; Neveling, A.; Otto, S.; Slawin, A. M. Z.; Wasserscheid, P.; Kuhlmann, S. *J. Am. Chem. Soc.* **2004**, *126*, 14712.

(111) Aliyev, V. O.; Al-Hazmi, M. H.; Mosa, F. M.; Fritz, P. M.; Bölt, H.; Wöhl, A.; Müller, W.; Winkler, F.; Wellenhofer, A.; Rosenthal, U.; Müller, B. H.; Hapke, M.; Peulecke, N. WO Patent 09/068157 (Linde and Sabic), 2009.

(112) Fritz, P. M.; Bölt, H.; Wöhl, A.; Müller, W.; Winkler, F.; Wellenhofer, A.; Rosenthal, U.; Hapke, M.; Peulecke, N.; Al-Hazmi, M. H.; Aliyev, V. O.; Mosa, F. M. WO Patent 09/006979 (Linde and Sabic), 2009.

(113) de Boer, E. J. M.; Van der Heijden, H.; On, Q. A.; Smit, J. P.; van Zon, A. WO patent 08/077911 (Shell), 2008.

(114) Fei, Z.; Scopelliti, R.; Dyson, P., J. *Eur. J. Inorg. Chem.* **2004**, 530.

(115) Klemps, C.; Payet, E.; Magna, L.; Saussine, L.; Le Goff, X. F.; Le Floch, P. *Chem. A Eur. J.* **2009**, 15, 8259.

(116) Dixon, J. T.; Grove, C.; Wasserscheid, P.; McGuinness, D. S.; Hess, F. M.; Maumela, H.;

Morgan, D. H.; Bollmann, A. WO 03053891 (Sasol Technology (Pty) Ltd), December 20, 2001.

(117) McGuinness, D. S.; Wasserscheid, P.; Keim, W.; Hu, C. H.; Englert, U.; Dixon, J. T.; Grove, C. *Chem. Commun.* **2003**, 334.

(118) McGuinness, D. S.; Wasserscheid, P.; Morgan, D. H.; Dixon, J. T. *Organometallics* **2005**, *24*, 522.

(119) McGuinness, D. S.; Brown, D. B.; Tooze, R. P.; Hess, F. M.; Dixon, J. T.; Slawin, A. M. Z. *Organometallics* **2006**, *25*, 3605.

(120) Bluhm, M. E.; Walter, O.; Döring, M. J. *Organomet. Chem.* **2005**, *690*, 713.

(121) Shaikh, Y.; Albahily, K.; Sutcliffe, M.; Fomitcheva, V.; Gambarotta, S.; Korobkov, I.; Duchateau, R. *Angew. Chem. Int. Ed.* **2012**, *51*, 1366.

(122) Shaikh, Y.; Gurnham, J.; Albahily, K.; Gambarotta, S.; Korobkov, I. *Organometallics* **2012**, *31*, 7427.

(123) Andresen, A.; Cordes, H. G.; Herwig, J.; Kaminksy, W.; Merck, A.; Mottweiler, R.; Pein, J.; Sinn, H.; Vollmer, H. J. *Angew. Chem.* **1976**, *88*, 689.

(124) Zhang, J.; Li, A.; Hor, T.S. A. *Organometallics* **2009**, *28*, 2935.

CHAPTER 2

Synthesis, Structures, and Ethylene Oligomerization Activity of Bis(phosphanylamine)pyridine Chromium/Aluminate Complexes

The results presented in this chapter have been published in

Alzamly, A.; Gambarotta, S.; Korobkov, I. *Organometallics* **2013**, *32*, 7107.

2.1 Introduction

A task of strategic importance in petrochemical industry is the development of large-scale processes for the production of linear α-olefins (LAOs) via ethylene oligomerization.[1] Linear α-olefins are important commodity chemicals marketed for a wide range of applications spanning from plasticizers to surfactants, detergents, and synthetic lubricants.[2] Since their extraction from crude oil cannot satisfy the market demand, there is a compelling case for developing catalysts for their making from abundant ethylene gas.

Trivalent chromium complexes, in the presence of alkyl aluminum co-activators, provide simple and active catalytic systems.[3] The reaction mechanism may follow two conceptually very different paths: redox *versus* non-redox. The metal oxidation state of the catalytically active species was long debated[4] and only in the recent past new data contributed to clarify the complexity of the mechanistic puzzle.[4b,c,e,5] Upon alkylation by the aluminum activator, trivalent chromium species show a rather general inclination to reduction[1,6] toward the divalent state. In this event, non-selective oligomerization is observed with formation of Schulz-Flory distributions of oligomers. When further reduction to the monovalent state occurs,[7] selective oligomerization (>80%) ensues. Which oxidation state leads to polymerization remains unclear even though there is general agreement that it is either the tri- or divalent state.[8] The situation is further complicated by the chromium redox dynamism,[9] *i.e.* the rapid inter-conversion between the three oxidation states during the catalytic cycle through series of dis- and comproportionations. In turn, this well explains the frequent occurrence of catalysts producing distribution of oligomers enriched in either 1-hexene or 1-octene and further contaminated by variable amounts of polymer.[4a,b,10]

The ligand clearly plays a pivotal role in the stabilization of a specific oxidation state and consequently in determining the type of catalytic behavior (selective versus non-selective). For this reason, we and others have embarked on systematic screening of series of ligands aiming at identifying the features of a selective catalyst.[3,11] To this end, it is safe to state that the N-P function of the phosphamine ligands is particularly versatile at enhancing the catalytic behavior of chromium. In fact by using ligands based on this functions, a rather large family of performing catalysts, selective,[12] non-selective[9b,13]and switchable,[9a,14] has been discovered.

In this study, we have examined a pincer-type bis(phosphanylamine)pyridine for the synthesis and oligomerization of chromium catalysts. We were interested in clarifying a possible role of the pyridine substituent in stabilizing lower oxidation states and ultimately affecting the selectivity of the catalytic cycle. Herein we describe our results.

2.2 Experimental Section

All reactions were carried out under inert atmosphere using Schlenk techniques or in a purified nitrogen-filled drybox. Solvents were dried using a purification system composed of aluminum oxide. GC-MS analysis of the oligomers was carried out with a Hewlett-Packard HP 5973 gas chromatograph using an Agilent DB1 column and dual FID and MS detector. Elemental analysis was carried out with a PerkinElmer 2400 CHN analyzer. Magnetic susceptibility measurements were performed with a Johnson Matthey balance at room temperature. The samples were powdered and weighed inside a drybox and transferred to sealed and calibrated tubes for measurements. NMR spectra were recorded on Varian Mercury 400 MHz spectrometer at 300 K. Infrared spectra were recorded on an ABB Bomem FTIR instrument from Nujol mulls prepared in a VAC drybox. All chemical reagents were purchased from commercial sources and used as received. Diethyl aluminum chloride, trimethyl aluminum,

triethyl aluminum and tri-isobutyl aluminum were purchased from Strem and used as received. Methylaluminoxane (MAO, 20% in toluene) was purchased from Albemarle Corporation. TMA-depleted methylaluminoxane (DMAO) was prepared by removing all the volatiles from MAO *in vacuo* (2 mmHg) and with moderate heating (40 °C) for 6 hours. Ligand $Ph_2PNHPyNHPPh_2$,[15] $CrCl_3(THF)_3$[16] and $CrCl_2(THF)_2$[17] were prepared according to literature procedures.

Preparation of {[2,6-$(Ph_2P\text{-}NH)_2C_5H_3N$]$CrCl_3$}$(THF)_2$ (2.1)

A solution of $CrCl_3(THF)_3$ (0.375g, 1.0 mmol) in THF (15 mL) was added to a solution of $Ph_2PNHPyNHPPh_2$ (0.477g, 1.0 mmol) in THF (5 mL). The color of the solution immediately changed to green. The solution was refluxed for 10 min. and stirred at room temperature for 2 h. The volume of the solution was then reduced to 7 mL and the residue allowed to stand at −40 °C for 3 days. Green crystals of **2.1** were thus obtained (0.61 g, 0.96 mmol, 96%). μ_{eff} = 3.83 μ_{BM}. Elemental Analysis % calculated for $C_{37}H_{41}Cl_3CrN_3O_2P_2$ (found): C 54.78 (54.63), H 3.96 (3.91), N 6.61 (6.55). IR (Nujol): $\nu_{N\text{-}H}$= 3205 cm^{-1}

Preparation of {[2,6-$(Ph_2PNH)C_5H_3N(AlClMe_2NPPh_2)$]$CrMe(\mu\text{-}Cl)_2AlMe_2$}$(toluene)_{1.5}$ (2.2)

A solution of $Ph_2PNHPyNHPPh_2$ (0.48 g, 1.0 mmol) in toluene (10 mL) was treated with $CrCl_3(THF)_3$ (0.37 g, 1.0 mmol). After twelve hours of stirring at room temperature, the mixture was cooled to -40 ^oC and trimethylaluminum (0.72 g, 10.0 mmol) was added dropwise. Stirring was continued for 30 min. While reaching room temperature. The suspension was then centrifuged and the supernatant concentrated, layered with hexanes (3 mL) and stored in the freezer at -40 ^oC for 3 days. The resulting brown crystals of **2.2** were filtered, washed with cold hexanes (10 mL) and dried *in vacuo* (0.23 g, 0.31 mmol, 31%). μ_{eff} = 3.88 $_{\mu BM}$. Elemental Analysis % calculated for $C_{78.5}H_{90}Al4Cl_6Cr_2N_6P_4$ (found): C 53.45 (53.12), H 5.15 (4.95), N 5.50(5.49). IR (Nujol): $\nu_{N\text{-}H}$= 3212 cm^{-1}

Preparation of {[2,6-(Ph_2PNH)C_5H_3N($AlClEt_2NPPh_2$)]Cr(μ-Cl)$_2$$AlEt_2$}(toluene) (2.3)

A solution of $Ph_2PNHPyNHPPh_2$ (0.48 g, 1.0 mmol) in toluene (10 mL) was treated with $CrCl_3(THF)_3$ (0.37g, 1.0 mmol). After twelve hours of stirring at room temperature, the mixture was cooled to -40 ^oC and triethylaluminum (0.57 g, 5.0 mmol) was added dropwise. Stirring was continued for 30 min. While reaching room temperature. The suspension was then centrifuged and the supernatant concentrated, layered with hexanes (3 mL) and stored at -40 ^oC for 3 days. The resulting bluish green crystals of **2.3** were filtered, washed with cold hexanes (10 mL) and dried *in vacuo* (0.52 g, 0.65 mmol, 65%). μ_{eff} = 4.81 μ_{BM}. Elemental Analysis % calculated for for $C_{44}H_{52}Al_2Cl_3CrN_3P_2$(found): C 55.20 (54.8), H 5.51 (5.48), N 5.22 (5.16). IR (Nujol): ν_{N-H}= 3244 cm^{-1}.

Preparation of {[2,6-(Ph_2PNH)C_5H_3N(Al-Cl-*i*-Bu_2NPPh_2)]Cr(μ-Cl)$_2$Al*i*-Bu_2}$_2$(toluene) (2.4)

A Solution of $Ph_2PNHPyNHPPh_2$ (0.48 g, 1.0 mmol) in toluene (10 mL) was treated with $CrCl_3(THF)_3$ (0.37g, 1.0 mmol). After twelve hours of stirring at room temperature, the mixture was cooled to -40 ^oC, and triisobutylaluminum (0.99 g, 5.0 mmol) was added dropwise. Stirring was continued for 30 min. While reaching room temperature. The suspension was then centrifuged and the supernatant concentrated, layered with hexanes (3 mL) and stored in a freezer at -40 ^oC for 3 days. The resulting blue crystals of **2.4** were filtered, washed with cold hexanes (10 mL) and dried *in vacuo* (0.25g, 0.27 mmol, 27%). μ_{eff} = 4.92 μ_{BM}. Elemental Analysis % calculated for for $C_{97}H_{128}Al_4Cl_6Cr_2N_6P_4$ (found): C 58.92 (57.88), H 6.59 (6.52), N 4.58 (4.54). IR (Nujol): ν_{N-H}= 3239 cm^{-1}

Preparation of {[2,6-(Ph_2PNH)C_5H_3N($HNPPh_2$)]CrEt(μ-Cl)$_2$$AlEt_2$}$AlEtCl_3$(hexane)$_{0.5}$ (2.5)

A solution of $Ph_2PNHPyNHPPh_2$ (0.48 g, 1.0 mmol) in toluene (10 mL) was treated with $CrCl_3(THF)_3$ (0.37 g, 1.0 mmol). After twelve hours of stirring at room temperature, the mixture was cooled to -40 ^oC, diethylaluminum chloride (1.21 g, 10.0 mmol) was added dropwise. Stirring was continued for 30 min. While reaching room temperature. The suspension was then centrifuged and the supernatant concentrated, layered with hexanes (3 mL) and stored in a freezer at -40 ^oC for 3 days. The resulting brown crystals of **2.5** were filtered, washed with cold hexanes (10 mL) and dried *in vacuo* (0.66 g, 0.67 mmol, 67%). μ_{eff} = 3.85 μ_{BM}. Elemental Analysis % calculated for $C_{38.5}H_{48.5}Al_2Cl_5CrN_3P_2$ (found): C 35.34 (34.93), H 3.61 (3.51), N 3.34 (3.21). IR (Nujol): ν_{N-H}= 3242 cm^{-1}.

Preparation of {[2,6-(Ph_2PNH)C_5H_3N($Cl_2EtAlNPPh_2$)]Cr(μ-Cl)$_2$$AlEt_2$}$_2$(toluene) (2.6)

A solution of $Ph_2PNHPyNHPPh_2$ (0.48 g, 1.0 mmol) in toluene (10 mL) was treated with $CrCl_2(THF)_2$ (0.27 g, 1.0 mmol). After twelve hours of stirring at room temperature, the mixture was cooled to -40 ^oC and diethyl aluminum chloride (0.57 g, 5.0 mmol) was added dropwise. Stirring was continued for 30 min. While reaching room temperature. The suspension was then centrifuged and the supernatant concentrated, layered with hexanes (3 mL) and stored in a freezer at -40 ^oC for 3 days. The resulting brown crystal of **2.6** were filtered, washed with cold hexanes (10 mL) and dried *in vacuo* (0.53 g, 0.65 mmol, 65%). μ_{eff} = 4.88 μ_{BM}. Elemental Analysis % calculated for $C_{77}H_{86}Al_4Cl_8Cr_2N_6P_4$ (found): C 51.81 (51.74), H 4.84 (4.92), N 5.18 (5.11). IR (Nujol): ν_{N-H}= 3275 cm^{-1}.

2.3 X-Ray Data

Table 2.1. Crystal Data and Structure Analysis Results of Complexes **2.1**-**2.6**.

	2.1	**2.2**	**2.3**
Formula	$C_{37}H_{41}Cl_3CrN_3P_2$	$C_{78.50}H_{90}Al_4C_6Cr_2N_6P_4$	$C_{44}H_{52}Al_2Cl_3Cr\ N_3P_2$
FW, gmol^{-1}	780.02	1666.07	897.14
Space group	Triclinic, P-1	Triclinic, P-1	Monoclinic, P2(1)/n
***a* (Å)**	10.1613(6)	14.5638(5)	15.564(2)
***b* (Å)**	10.1843(5)	18.7481(6)	17.882(3)
***c* (Å)**	18.5264(11)	19.6790(7)	18.987(3)
α, (deg)	89.005(4)	89.610(2)	90
β, (deg)	87.369(3)	73.977(2)	100.382(3)
γ, (deg)	79.343(3)	77.743(2)	90
***V* (Å^3)**	1882.09(18)	5039.1(3)	5197.8(14)
Z	2	2	4
Radiation	0.71073	0.71073	0.71073
T (K)	200(2)	200(2)	200(2)
D_{calcd} (mg/m^3)	1.376	1.098	1.146
μ_{calcd} (mm^{-1})	0.639	0.510	0.499
***F*$_{000}$**	810	1730	1872
***R*, *Rw*^{2a}**	0.0499, 0.0846	0.0499, 0.0846	0.0499, 0.0846
GoF	0.911	1.025	1.045

	2.4	**2.5**	**2.6**
Formula	$C_{97}H_{128}Al_4Cl_6Cr_2N_6P_4$	$C_{38.50}H_{48.50}Al_2Cl_5CrN_3P_2$	$C_{77}H_{86}Al_4Cl_8Cr_2N_6P_4$
FW, gmol^{-1}	1926.55	898.45	1714.92
Space group	Monoclinic, P2(1)/c	Triclinic, P-1	Triclinic, P-1
***a* (Å)**	10.4726(2)	10.7401(5)	16.1105(5)
***b* (Å)**	35.8132(7)	12.6900(7)	16.6010(5)
***c* (Å)**	27.6642(6)	17.5709(9)	21.1062(7)
α, (deg)	90	98.8110(10)	99.206(2)
β, (deg)	96.0150(10)	105.1540(10)	99.641(2)
γ, (deg)	90	92.4280(10)	117.8560(10)
***V* (Å^3)**	10318.5(4)	2275.7(2)	4732.9 (3)
Z	4	2	2
Radiation	0.71073	0.71073	0.71073
T (K)	200(2)	200(2)	200(2)
D_{calcd} (mg/m^3)	1.240	1.311	1.203
μ_{calcd} (mm^{-1})	0.508	0.684	0.600
***F*$_{000}$**	4056	931	1772
***R*, *Rw*^{2a}**	0.0638, 0.1618	0.0523, 0.1408	0.0748, 0.2145
GoF	1.019	1.012	1.018

[a] $R = \Sigma|F_o| - |F_c|/\Sigma|F_o|$, $Rw = [\Sigma(|F_o| - |F_c|)2/\Sigma wF_o2]^{1/2}$

2.4 Results and Discussion

The phosphanyl pyridine ligand $Ph_2PNHPyNHPPh_2$ was prepared according to a literature procedure.[15] Treatment of $CrCl_3(THF)_3$ with the ligand in THF afforded the corresponding complex $\{[(2,6\text{-}(Ph_2P\text{-}NH)_2C_5H_3N]CrCl_3\}(THF)_2$ (**2.1**) (Scheme 2.1). The complex has the magnetic moment as expected for the d^3 electronic configuration of trivalent chromium in an octahedral field.

Scheme 2.1

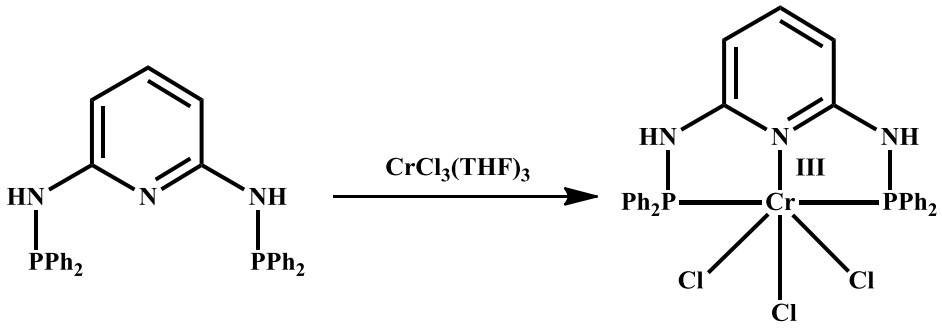

(2.1)

It was possible to grow crystals of sufficient quality for X-ray analysis. The structure of **2.1** (Figure 2.1) shows a distorted-octahedral trivalent chromium center surrounded by three meridionally placed donor atoms of one ligand [Cr(1)-N(2) = 2.108(4) Å, Cr(1)-P(1) = 2.4190(15) Å, N(2)-Cr(1)-P(1) = 80.31(12)^o, P(1)-Cr(1)-P(2) = 160.26(5)^o]. The three chlorine atoms occupy the three remaining positions [Cr(1)-Cl(1) = 2.3010(15) Å, Cr(1)-Cl(2) = 2.2934 (15) Å, Cr(1)-Cl(3) = 2.2969(15) Å, Cl(2)-Cr(1)-Cl(3) = 93.45(6)^o, Cl(3)-Cr(1)-Cl(1) = 172.74 (6)^o].

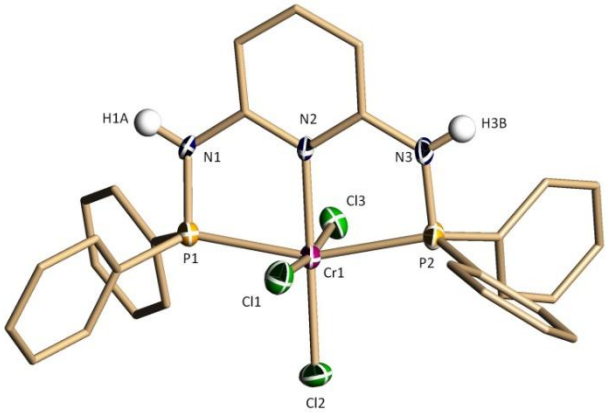

Figure 2.1. Thermal ellipsoid plot of **2.1** with ellipsoids drawn at 50% probability level. Selected bond distances (Å) and angles (deg) for **2.1**: Cr(1)-Cl(1) = 2.3010(15), Cr(1)-P(2) = 2.4503(15), N (1)-P(1) = 1.680(4), N(3)-P(2) = 1.686(4), N(2)-Cr(1)-Cl(2) = 179.15(12), N(2)-Cr(1)-Cl(3) = 87.41(11), N(2)-Cr(1)-Cl(1) = 86.37(11), Cl(2)-Cr(1)-Cl(1) = 92.78(5), Cl(2)-Cr(1)-P(1) = 99.75 (5), Cl(3)-Cr(1)-P(1) = 85.97(5), Cl(1)-Cr(1)-P(1) = 89.28(5), N(2)-Cr(1)-P(2) = 80.15(12), Cl (2)-Cr(1)-P(2) = 99.82(5), Cl(3)-Cr(1)-P(2) = 90.35(5), Cl(1)-Cr(1)-P(2) = 92.28(5), N(1)-P(1)-Cr (1) = 97.75(14), N(3)-P(2)-Cr(1) = 97.13(15).

Upon activation with MAO, complex **2.1** displays a good activity as non-selective oligomerization catalyst. However, a substantial amount of polymeric material was invariably present in the oligomeric mixtures (Table 2.2). This tentatively suggested the presence of dynamism between the di- and trivalent oxidation states during the catalytic cycle. The fact that no enrichment in 1-hexene or 1-octene was observed further suggested that no reduction to the monovalent state occurred. The lower than expected amount of 1-hexene initially suggested incorporation into the polymeric or heavy-oligomer solid material. However, ^{13}C NMR clearly showed only highly linear chains.

Table 2.2. Ethylene catalyzed oligomerization reactions of **2.1**.[a]

Catalyst	Alkenes (g)	PE (g)	M_n, PD (g mol^{-1})	Activity (g/((g of Cr) h))	Linear alpha olefins (mol %)							
					C_4	C_6	C_8	C_{10}	C_{12}	C_{14}	C_{16}	C_{18}
2.1	22	3.2	355/1.6	46029	4.1	13.2	24.5	21.5	15.7	12.3	6.2	2.5

[a]Conditions: 100mL of toluene, loading 20 µmol of catalyst, reaction temperature 80 ˚C, 40 bar of ethylene, reaction time 30 min, 500 (Al:Cr) MAO.

To gain insight into the interaction of complex **2.1** with the activator and aiming at isolating catalytically active species, this complex was reacted with stoichiometric amounts of different alkyl aluminum activators (Scheme 2.2).

Scheme 2.2

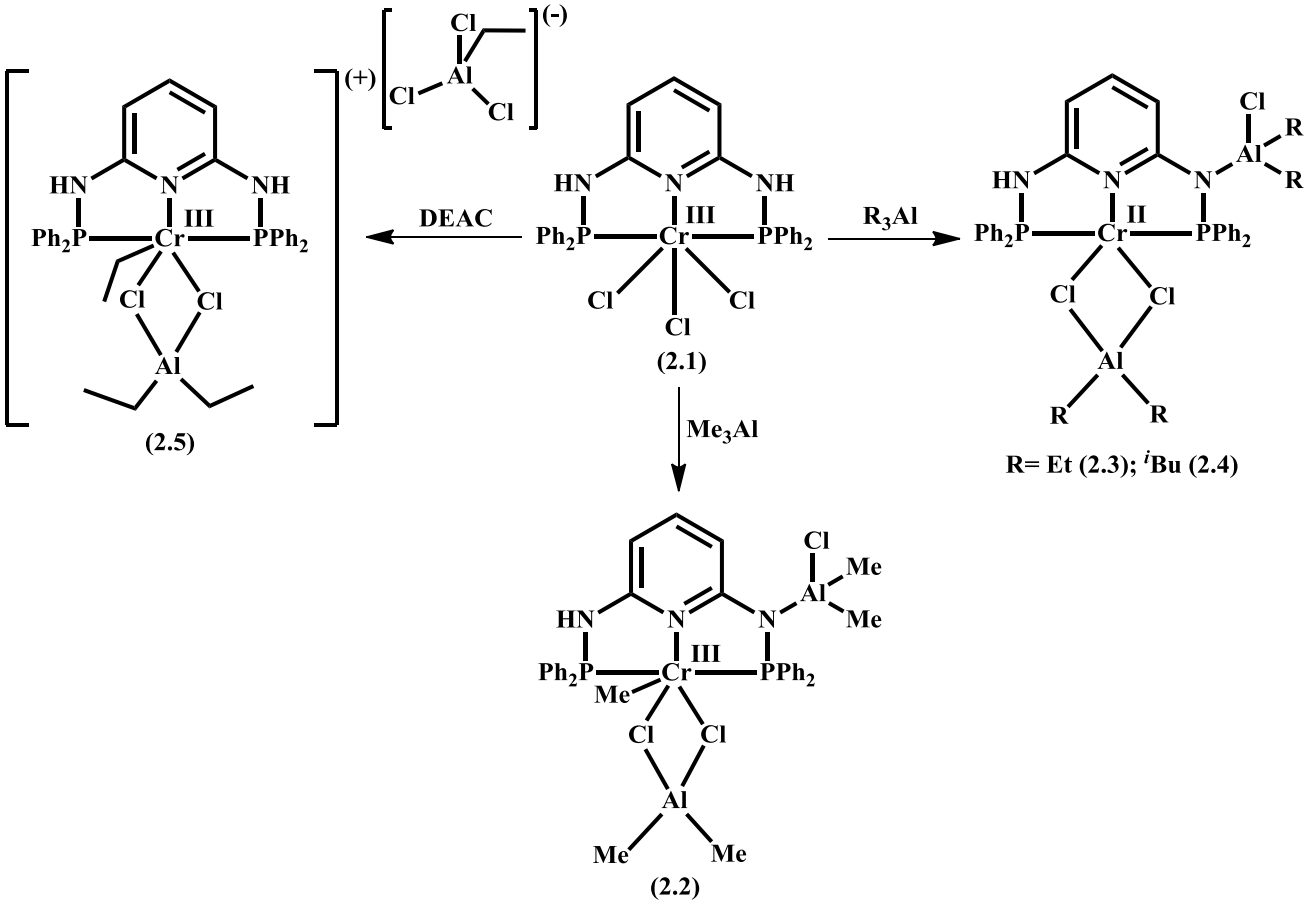

The reactions with MAO invariably gave oily materials, while the active oligomerization catalyst {[2,6-$Ph_2PNHC_5H_3NAlClMe_2NPPh_2$]CrMe($\mu$-Cl)$_2$$AlMe_2$}(toluene)$_{1.5}$ (**2.2**) was obtained in crystalline form upon treating **2.1** with 10 equivalents of Me_3Al. Interestingly, the trivalent oxidation state was preserved during the formation of this complex.

The salient features of the structure of **2.2** are the methylation of the chromium center and the deprotonation of one of the two amino functions whose hydrogen atom was in fact replaced by one $ClAlMe_2$ moiety (Figure 2.2). Unfortunately, the crystal quality was strained by the very high air sensitivity; this was reflected in the borderline values of the convergence parameters. Nonetheless, the connectivity remains demonstrated. The trivalent chromium is in a distorted-octahedral coordination environment [Cr(1)-N(2) = 2.052(6) Å, Cr(1)-Cl(1) = 2.490(3) Å, Cr(1)-P(1) = 2.465(2) Å, N(2)-Cr(1)-Cl(2) = 174.55(19)^o, N(2)-Cr(1)-P(1) = 82.76(17)^o, N(2)-Cr(1)-Cl(1) = 91.41(18)^o)]. The coordination polyhedron is defined by the three donor atoms of the meridionally arranged ligand system [Cr(1)-P(2) = 2.403(2) Å, N(2)-Cr(1)-P(2) = 79.71(17)^o, P(2)-Cr(1)-P(1) = 162.19(9)^o]. The remaining three meridional coordination sites are occupied by one carbon atom of a terminally bonded Me group [Cr(1)-C(30) 2.095(10) Å, N(2)-Cr(1)-C(30) = 87.3(3)^o] and two chlorine atoms. In turn, the two chlorine bridge a Me_2Al residue [Cl(1)-Al(1)-Cl(2) = 90.60(12)^o, Al(1)-Cl(1)-Cr(1) = 92.24(11)^o, Al(1)-Cl(2)-Cr(1) = 93.41(11)^o].

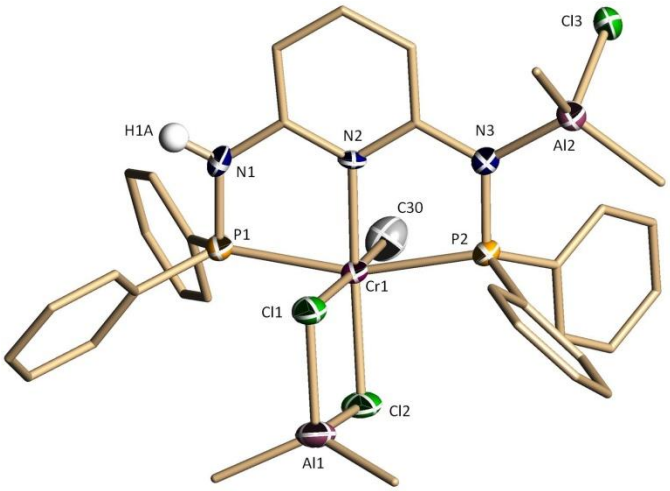

Figure 2.2. Thermal ellipsoid plot of **2.2** with ellipsoids drawn at 50% probability level**.** Selected bond distances (Å) and angles (deg) for **2.2**: Cr(1)-Cl(2) = 2.390(2), Al(1)-Cl(1) = 2.262(3), Al(1)-Cl(2) = 2.321(4), Al(2)-N(3) = 1.964(6), Al(2)-Cl(3) = 2.238(3), N(1)-P(1) = 1.669(7), N(3)-P(2) = 1.671(6), Cl(2)-Cr(1)-P(2) = 98.24(8), Cl(2)-Cr(1)-P(1) = 99.50(8), Cl(2)-Cr(1)-Cl(1) = 83.73(9), P(2)-Cr(1)-Cl (1) = 95.43(8), P(1)-Cr(1)-Cl(1) = 88.10(8), Cl(1)-Al(1)-Cl(2) = 90.60(12), N(3)-Al(2)-Cl(3) = 102.2(2), Al(1)-Cl(1)-Cr(1) = 92.24(11), P(2)-N(3)-Al(2) = 122.2(4), N(1)-P(1)-Cr(1) = 93.5(2), N(3)-P(2)-Cr(1) = 101.4(2), N(2)-Cr(1)-Cl(2) = 174.55(19).

When the more reducing Et_3Al or *i*-Bu_3Al was used, reactions carried out under otherwise identical conditions took an interesting turn. The two activators generated two nearly isostructural *divalent* complexes {[2,6-$Ph_2PNHC_5H_3NAlClEt_2NPPh_2$]Cr($\mu$-Cl)$_2$AlEt$_2$}(toluene) (**2.3**) and {[2,6-$Ph_2PNHC_5H_3NAl$-Cl*i*-Bu_2NPPh_2]Cr(μ-Cl)$_2$Al*i*-Bu$_2$}$_2$(toluene) (**2.4**) (Figure 2.3). Apart from the two different alkyls, the two species are basically identical. The complexes are also similar to **2.2** in the sense that they retained the aluminate residues at the deprotonated N atom and at the two chlorine atoms. Different from **2.2**, the oxidation state of chromium was lowered from the tri- to the divalent. The two alkylaluminum reagents used for the reactions were tested by NMR for the presence of hydrides and found to be hydride-free. Therefore, the reduction may be only ascribed to the more enhanced reducing power of TEAL and TIBA with

respect to that of TMA and the consequently lower stability of the initially formed organochromium function.

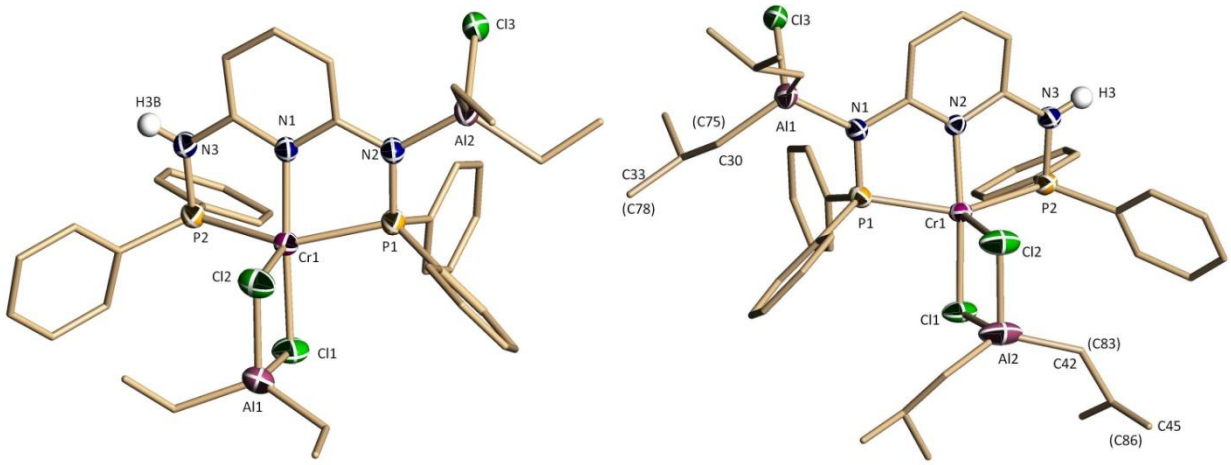

2.3 **2.4**

Figure 2.3. Thermal ellipsoid plots of **2.3** and **2.4** with ellipsoids drawn at 50% probability level**.** Selected bond distances (Å) and angles (deg) for **2.3**: Cr(1)-N(1) = 2.062(2), Cr(1)-Cl(2) = 2.3865(9), Cr(1)-P(1) = 2.3952(8), Cr(1)-P(2) = 2.4290(8), Cr(1)-Cl(1) = 2.5642(9), Al(1)-Cl(1) = 2.2504 (12), Al(1)-Cl(2) = 2.3003(13), Al(2)-N(2) = 1.950(2), Al(2)-Cl(3) = 2.2403(11), P(1)-N(2) = 1.686(2), P(2)-N(3) = 1.683(2), N(1)-Cr(1)-Cl(2) = 174.36(6), N(1)-Cr(1)-P(1) = 77.86 (5), Cl(2)-Cr(1)-P(1) = 99.92(3), N(1)-Cr(1)-P(2) = 80.46(5), Cl(2)-Cr(1)-P(2) = 98.95(3), P(1)-Cr(1)-P(2) = 144.54(3), N(1)-Cr(1)-Cl(1) = 100.43(6), Cl(2)-Cr(1)-Cl(1) = 85.09(3), P(1)-Cr(1)-Cl(1) = 102.66(3), P(2)-Cr(1)-Cl(1) = 108.64(3), Cl(1)-Al(1)-Cl(2) = 94.81(4), N(2)-Al(2)-Cl(3) = 102.84(7), Al(1)-Cl(1)-Cr(1) = 88.29(4), Al(1)-Cl(2)-Cr(1) = 91.61(3), N(2)-P(1)-Cr(1) = 102.18 (7), N(3)-P(2)-Cr(1) = 96.13(7), P(1)-N(2)-Al(2) = 122.49(11). Selected bond distances (Å) and angles (deg) for **2.4**: Cr(1)-N(2) = 2.063(3), Cr(1)-Cl(2) = 2.3874(13), Cr(1)-P(1) = 2.3931(13), Cr(1)-P(2) = 2.4417(13), Cr(1)-Cl(1) = 2.5560(14), Al(1)-N(1) = 1.957(4), Al(1)-Cl(3) = 2.2413(19), Al(2)-Cl(1) = 2.256(2), Al(2)-Cl(2) = 2.298(2), N(1)-P(1) = 1.686(4), N(3)-P(2) = 1.684(4), N(2)-Cr(1)-Cl(2) = 174.24(10), N(2)-Cr(1)-P(1) = 77.38(10), Cl(2)-Cr(1)-P(1) = 99.44(5), N(2)-Cr(1)-P(2) = 80.90(10), Cl(2)-Cr(1)-P(2) = 99.63(5), P(1)-Cr(1)-P(2) = 145.31(5), N(2)-Cr(1)-Cl(1) = 100.58(10), Cl(2)-Cr(1)-Cl(1) = 84.92(5), P(1)-Cr(1)-Cl(1) = 107.12(5), P(2)-Cr(1)-Cl(1) = 103.20(5), N(1)-Al(1)-Cl(3) = 103.16(12), Al(2)-Cl(1)-Cr(1) = 88.63(6), Al(2)-Cl(2)-Cr(1) = 91.92(6), P(1)-N(1)-Al(1) = 122.8(2), N(3)-P(2)-Cr(1) = 95.58(13).

The reaction of **2.1** with the more Lewis acidic DEAC (10 equivalents) afforded instead alkylation and cationization. In this case, no reduction and no deprotonation of the amino functions were observed. As a result, the cationic, trivalent chromium complex {[2,6-Ph_2PNH C_5H_3NHNPPh_2]CrEt(μ-Cl)$_2$AlEt_2}Al$EtCl_3$ (hexane)$_{0.5}$ **(2.5)** (Scheme 2.2) containing an ethyl function directly connected to chromium was obtained in crystalline form.

The structure of **2.5** shows the chromium atom in an octahedral environment and with the intact ligand arranged as in complex **2.1** [Cr(1)-N(1) = 2.062(3) Å, Cr(1)-P(1) = 2.4648(13) Å, P(2)-Cr(1)-P(1) = 159.87(5)^o, N(1)-Cr(1)-P(1) = 80.15(10)^o]. One ethyl group and two chlorine atoms complete the coordination sphere of the metal center [Cr(1)-Cl(1) = 2.5069(12) Å, Cr(1)-C(30) = 2.079(4) Å, Cl(2)-Cr(1)-Cl(1) = 84.51(4)^o, C(30)-Cr(1)-Cl(2) = 89.51(13)^o, C(30)-Cr(1)-Cl(1) = 173.87(13)^o]. An aluminate counter anion is present in the lattice, unconnected to the chromium unit (Figure 2.4).

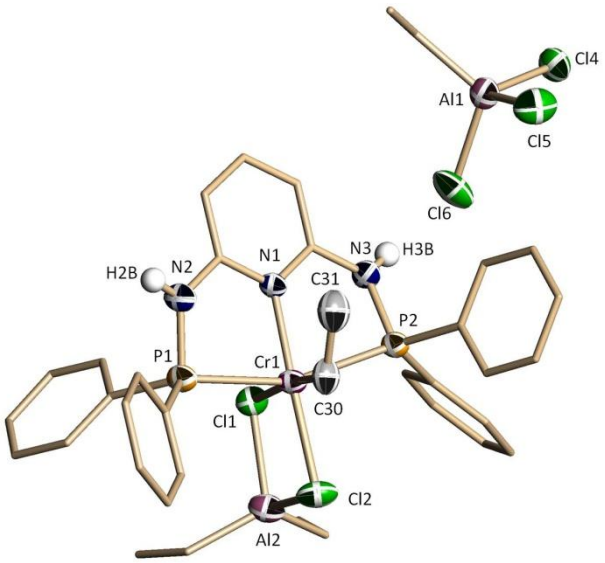

Figure 2.4. Thermal ellipsoid plot of **2.5** with ellipsoids drawn at 50% probability level**.** Selected bond distances (Å) and angles (deg) for **2.5**: Cr(1)-Cl(2) = 2.3992(13), Cr(1)-P(2) = 2.4569(13), Al(1)-Cl(1) = 2.2650(18), Al(1)-Cl(2) = 2.3088(18), Al(2)-Cl(5) = 2.1485(18), Al(2)-Cl(4) =

2.1695(18), Al(2)-Cl(3) = 2.178(2), N(2)-P(1) = 1.690(3), N(1)-Cr(1)-Cl(2) = 173.28(10), Cl(2)-Cr(1)-P(2) = 96.57(5), Cl(2)-Cr(1)-P(1) = 103.55(5), N(1)-Cr(1)-Cl(1) = 89.80(9), P(2)-Cr(1)-Cl(1) = 89.54(4), P(1)-Cr(1)-Cl(1) = 91.73(4), Cl(5)-Al(2)-Cl(3) = 105.54(7), Cl(4)-Al(2)-Cl = (3)105.29 (8), Al(1)-Cl(1)-Cr(1) = 90.28(5), Al(1)-Cl(2)-Cr(1) = 91.98(5), N(2)-P(1)-Cr(1) = 94.94(13), N (3)-P(2)-Cr(1) = 95.24(13), N(1)-Cr(1)-P(2) = 79.76(10)**.**

To probe the stability of the divalent analogue, a similar preparation was carried out by reacting an *in situ* generated divalent adduct with 5 equivalent of DEAC. The reaction afforded the corresponding divalent {[2,6-$Ph_2PNHC_5H_3NCl_2EtAlNPPh_2$]Cr($\mu$-Cl)$_2AlEt_2$}$_2$ (toluene) (**2.6)** (Scheme 2.3). Different from the case of **2.5**, the ligand in **2.6** was deprotonated with the nitrogen atom retaining one additional aluminate residue. In turn, this indicates that the acidity of the ligand amino protons is affected by more than simple inductive effects.

Scheme 2.3

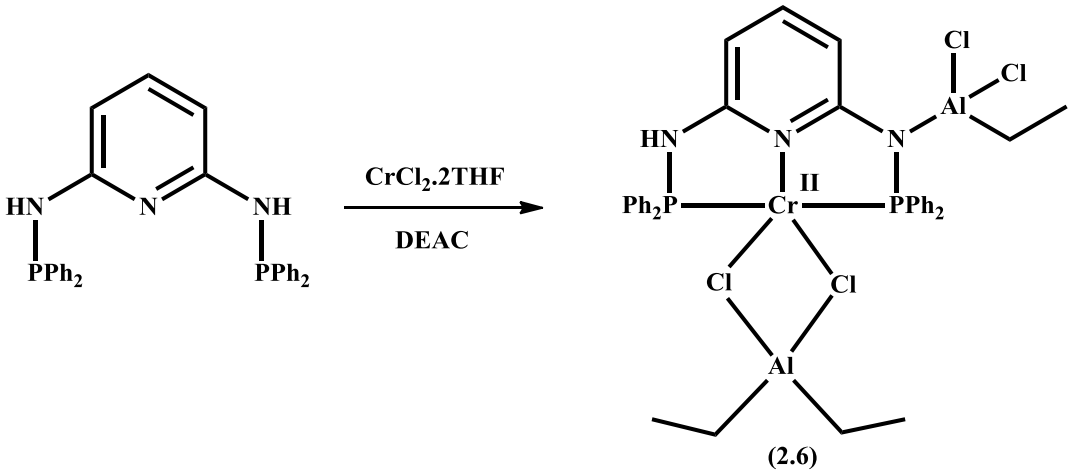

(2.6)

Even in this case, the good crystallinity allowed a crystallographic structural investigation. The molecule features the metal center in a square-pyramidal coordination environment with the ligand donor atoms [Cr(1)-N(1) = 2.074(4) Å, Cr(1)-P(1) = 2.4432(14) Å, N(1)-Cr(1)-P(1) = 80.87(11)^o, P(2)-Cr(1)-P(1) = 149.73(6)^o] and one chlorine [Cr(1)-Cl(2) =

2.3740(16) Å, N(1)-Cr(1)-Cl(2) = 171.09(12)^{o}] defining the basal plane and a second chlorine atom in the axial position [Cr(1)-Cl(1) = 2.5757(17) Å, N(1)-Cr(1)-Cl(1) = 103.93(11)^{o}] (Figure 2.5). One of the two amino functions was deprotonated and the nitrogen atom coordinated a Cl_2AlEt residue [Al(2)-N(3) = 1.932(4)]. The two chlorine atoms also bridge a second Et_2Al moiety [Cl(1)-Al(1)-Cl(2) = 94.32(9)^{o}].

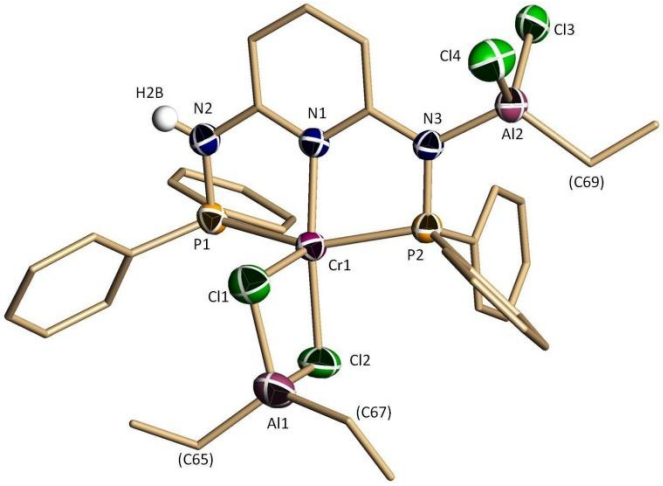

Figure 2.5. Thermal ellipsoid plot of **2.6** with ellipsoids drawn at 50% probability level. Selected bond distances (Å) and angles (deg) for **2.6**: Cr(1)-P (2) = 2.4014(15), Cr(2)-N(4) = 2.068(4), Al (1)-Cl(1) = 2.233(3), Al(1)-Cl(2) = 2.323(3), Al(2)-Cl(4) = 2.150(2), Al(2)-Cl(3) = 2.208(2), P (1)-N(2) = 1.694(4), P(1)-C(12) = 1.805(5), P(2)-N(3) = 1.684(4), N(1)-Cr(1)-P(2) = 78.43(11), Cl(2)-Cr(1)-P(2) = 97.35(6), Cl(2)-Cr(1)-P(1) = 99.85(6), Cl(2)-Cr(1)-Cl(1) = 84.82(6), P(2)-Cr(1)-Cl(1) = 108.69(6), P(1)-Cr(1)-Cl(1) = 97.56(6), N(3)-Al(2)-C(34) = 116.9(2), N(3)-Al(2)-Cl(4) = 106.72(15), N(3)-Al(2)-Cl(3) = 105.55(14), Cl(4)-Al(2)-Cl(3) = 108.34(10), Al(1)-Cl(1)-Cr(1) = 88.54(8), Al(1)-Cl(2)-Cr(1) = 91.52(8), N(2)-P(1)-Cr(1) = 94.76(14), N(3)-P(2)-Cr(1) = 102.43(14), P(2)-N(3)-Al(2) = 119.1 (2).

When activation of the complexes was attempted in methylcyclohexene, no catalytic activity could be detected. This is most likely the result of the insolubility of all these complexes in non-aromatic solvents. Therefore, catalytic runs were necessarily carried out in toluene and the results summarized in Table 2.3.

Table 2.3. Ethylene catalyzed oligomerization reactions of **2-6**.[a]

Catalyst	Alkenes (g)	PE (g)	M_n, PD (g mol^{-1})	Activity (g/((g of Cr) h))	Linear alpha olefins (mol %)							
					C_4	C_6	C_8	C_{10}	C_{12}	C_{14}	C_{16}	C_{18}
2.2	16	2.6	394, 1.9	33875	15.1	23.4	21.1	14.3	10.3	7.2	5.1	3.5
2.3	48	2.5	316, 2.0	92808	9.3	19.9	19.7	15.9	12.7	9.7	7.3	5.5
2.4	35	1.1	407, 2.3	68115	5.2	18.1	20	17.1	13.9	10.9	8.3	6.5
2.5	18	2	406, 2.2	36846	8	12.9	16.6	15.8	14.3	12.5	10.6	9.3
2.6	40	1.7	381, 1.9	76144	4.2	16.8	20.6	17.7	14.4	11.2	8.5	6.6

[a]Conditions: 100mL of toluene, loading 20 μmol of catalyst, reaction temperature 80 ˚C, 40 bar of ethylene , reaction time 30 min, 500 (Al:Cr) MAO.

As anticipated, upon activation with MAO the divalent **2.3**, **2.4**, and **2.6** gave slightly higher activity as nonselective ethylene oligomerization catalysts. Low-molecular-weight polymeric material was invariably present in the reaction mixtures. Their high-temperature NMR spectra and GPC analysis indicated that the broadly dispersed polymer chains were heavier linear α-olefins with a distribution centered over the average values of the molecular weights. In turn, this ruled out that the solid material could simply be the tail of the lighter oligomer distribution. Variable amounts of 1-butene were also formed by the catalytic runs. While the quantification of 1-butene is affected by larger error, its presence is in principle indicative of an S-F distribution. However, the low amount of 1-hexene and the somewhat larger amount of 1-octene (and 1-decene in one case) are reflective of an abnormal unselective oligomerization. To explain this complex behavior, we suggest that more than one mechanism is at play, in turn involving more than one chromium oxidation state. The lack of selectivity, which dominates the distribution, indicates that the divalent state was preserved in these complexes throughout the activation process and without further reduction to the monovalent state. Conversely, the formation of oligomeric/polymeric material might be attributed to the re-forming of trivalent species via

comproportionation.[9c]It is tempting to ascribe this behavior to an increased resiliency of the trivalent state toward reduction to the divalent state which makes the overall catalytic cycle less productive and more inclined toward polymer formation. The small enrichment in 1-octene could be attributed to the monovalent species formed in low concentration, but we remain baffled by the lower than expected amount of 1-hexene. The linearity of the polymeric material discourages the idea that 1-hexene might have been perhaps incorporated.

2.5 Conclusions

In conclusion, we have herein reported the synthesis and characterization of organochromium complexes based on P-N(pyridine) ligand system. The introduction of the pyridine ring in the PN ligand scaffold afforded non-selective catalytic systems. The almost complete obliteration of selectivity, otherwise commonly observed within the large family of N-P ligands, at first glance may look surprising. On the other hand, the stabilizing ability of the pyridine ring not only affects the chromium divalent state but also the Cr-R function. This is clearly visible in **2.2** and especially in **2.5**, containing a relatively rare example[7d] of a Cr^{III}-Et group. Even in the case when reduction to the divalent state does occur, the pyridine ring most likely prevents further reduction. Only in the cases where some enrichment in 1-octene is observed, most likely a small concentration of the chromium intermediates have made their way to the monovalent state. The simultaneous presence of all these species may well account for the complexity of the observed distributions.

References

(1) Skupińska, *Chem. Rev.* **1991**, *91*, 613.

(2) (a) Alpha Olefins (02/03-4), PERP Report, Nexant Chem Systems; (b) Vogt, D. Oligomerization of ethylene to higher linear α-olefins. In *Applied Homogeneous Catalysis with Organometallic Compounds*; Cornils, B., Herrmann, W. A., Eds.; Wiley-VCH: Weinheim, Germany, 2000; Chapter 2, pp 245-258. (c) Lappin, G. R.; Sauer, J. D. In *Alpha Olefins Application Handbook*; Marcel Dekkers: New York, 1989; Vol. 37, pp 1-3.

(3) (a) McGuinness, D. *Chem. Rev.* **2011**, *111*, 2321, and references cited therein. (b) Liu, S.; Pattacini, R.; Braunstein, P. *Organomettalics* **2011**, *30*, 3549. (b) McGuinness, D. S.; Suttil, J. A.; Gardiner, M. G.; Davies, N. W. *Organomettalics* **2008**, *27*, 4238. (c) Junges, F.; Kuhn, M. C. A.; P dos Santos, A. H. D.; Rabello, C. R. K.; Thomas, C. M.; Carpentier, J.-F.; Casagrande Jr, O. L.; *Organomettalics* **2007**, *26*, 4010.

(4) (a) Licciulli, S.; Thapa, I.; Albahily, K.; Korobkov, I.; Gambarotta, S.; Duchateau, R.; Chevalier, R.; Schuhen, K. *Angew. Chem. Int. Ed.* **2010**, *49*, 9225. (b) Bhaduri, S.; Mukhopadhyay, S.; Kulkarni, S. A. *J. Organomet. Chem.* **2009**, *694*, 1297. (c) Budzelaar, P. H. M. *Can. J. Chem.* **2009**, *87*, 832. (d) Jabri, A.; Mason, C. B.; Sim, Y.; Gambarotta, S.; Burchell, T. J.; Duchateau, R. *Angew. Chem., Int. Ed.* **2008**, *47*, 9717. (e) Wass, D. *Dalton Trans.* **2007**, 816, and references therein. (f) Agapie, T.; Bercaw, J. E.; Labinger, J. A. *J. Am. Chem. Soc.* **2007**, *129*, 14281. (g) Bowen, L. E.; Haddow, M. F.; Orpen, A. G.; Wass, D. *Dalton Trans.* **2007**, 1160. (h) Elowe, P. R.; McCann, C.; Pringle, P. G.; Spitzmesser, S. K.; Bercaw, J. E. *Organomeallics* **2006**, *25*, 5255. (i) Overett, M. J.; Blann, K.; Bollmann, A.; Dixon, J. T.; Haasbroek, D.; Killian, E.; Maumela, H.;

McGuinness, D. S.; Morgan, D. H. *J. Am. Chem. Soc.* **2005**, *127*, 10723. (j) van Rensburg, W. J.; Grove, C.; Steynberg, J. P.; Stark, K. B.; Huyser, J. J.; Steynberg, P. J. *Organometallics* **2004**, *23*, 1207. (k) Agapie, T.; Schofer, S. J.; Labinger, J. A.; Bercaw, J. E. *J. Am. Chem. Soc.* **2004**, *126*, 1304. (l) Emrich, R.; Heinemann, O.; Jolly, P. W.; Kruger, C.; Verhovnik, G. P. J. *Organometallics* **1997**, *16*,1511. (m) Briggs, J. R. *Chem. Commun.* **1989**, *11*, 674.

(5) (a) Schofer, S. J.; Day, M. W.; Henling, L. M.; Labinger, J. A.; Bercaw, J. E. *Organometallics* **2006**, *25*, 2743. (b) Jabri, A.; Temple, C.; Crewdson, P.; Gambarotta, S.; Korobkov, I.; Duchateau, R. *J. Am. Chem. Soc.* **2006**, *128*, 9238.

(6) (a) MacAdams, L. A.; Buffone, G. P.; Incarvito, C. D.; Golen, J. A.; Rheingold, A. L.; Theopold, K. H. *Chem. Commun.* **2003**, 1164. (b) Sugiyama, H.; Aharonian, G.; Gambarotta, S.; Yap, G. P. A.; Budzelaar, P. H. *J. Am. Chem. Soc.* **2002**, *124*, 12268. (c) Schulzke, C.; Enright, D.; Sugiyama, H.; LeBlanc, G.; Gambarotta, S.; Yap, G. P. A.; Thompson, K. K.; Wilson, D. R.; Duchateau, R. *Organometallics* **2002**, *21*, 3810. (d) Bhandari, G.; Kim, Y.; McFarland, J. M.; Rheingold, A. L.; Theopold, K. H. *Organometallics* **1995**, *14*, 738. (e) Winter, M. J. Comprehensive Organometallic Chemistry, 2nd ed.; Wilkinson, G., Ed.; Pergamon Press: Oxford, 1995. (f) Kirtley, S. W. Comprehensive Organometallic Chemistry; Wilkinson, G., Ed.; Pergamon Press: Oxford, 1978.

(7) (a) Albahily, K.; Fomitcheva, V.; Shaikh, Y.; Sebastiao, E.; Gorelsky, S. I.; Gambarotta, S.; Korobkov, I.; Duchateau, R. *Organometallics* **2011**, *30*, 4201. (b) Albahily, K.; Fomitcheva, V.; Gambarotta, S.; Korobkov, I.; Murugesu, M.; Gorelsky, S. I. *J. Am. Chem. Soc.* **2011**, *133*, 6380. (c) Albahily, K.; Shaikh, Y.; Sebastiao, E.; Gambarotta, S.;

Korobkov, I.; Gorelsky, S. I. *J. Am. Chem. Soc.* **2011**, *133*, 6388. (d) Licciulli, S.; Albahily, K.; Fomitcheva, V.; Korobkov, I.; Gambarotta, S.; Duchateau, R. *Angew. Chem., Int. Ed.* **2011**, *50*, 2346. (e) Rucklidge, A. J.; McGuinness, D. S.; Tooze, R. P.; Slawin, A. M. Z.; Pelletier, J. D. A; Hanton, M. J.; Webb, P. B. *Organometallics* **2007**, *26*, 2782.

(8) (a) Xu, J.; Gao, W.; Zhang, Y.; Li, J.; Mu, Y. *J. Organomet. Chem.* **2007**, *692*, 1505. (b) Xu, T; Mu, Y.; Gao, W.; Ni, J.; Ye, L.; Tao, Y. *J. Am. Chem. Soc.* **2007**, *129*, 2236. (c) Kreisel, K. A.; Yap, G. P. A; Theopold, K. H. *Organometallics* **2006**, *25*, 4670. (d) Jones, D. J.; Gibson, V. C.; Green, S. M.; Maddox, P. J.; White, A. J. P.; Williams, D. J. *J. Am. Chem. Soc.* **2005**, *127*, 11037. (e) Groppo, E.; Lamberti, C.; Bordiga,S.; Spoto, G.; Zecchina, A. *Chem. Rev.* **2005**, *105*, 115. (f) Zhang, H.; Ma, J.; Qian, Y. L.; Huang, J. *Organometallics* **2004**, *23*, 5681. (g) Small, B. L.; Carney, M. J.; Holman, D. M.; O'Rourke, C. E.; Halfen, J. A. *Macromolecules* **2004**, *12*, 4375. (h) Esteruelas, M. A.; Lopez, A. M.; Mendez,L.; Olivan, M.; Onate, E. *Organometallics* **2003**, *22*, 395. (i) Ogata, K.; Nakayama, Y.; Yasuda, H. *J. Polym. Sci., Part A* **2002**, *40*, 2759. (j) Dohring, A.; Jensen, V. R.; Jolly, P. W.; Thiel, W.; Weber, J. C. *Organometallics* **2001**, *20*, 2234. (k) Ikeda, H.; Monoi, T.; Ogata, K.; Yasuda, H. *Macromol. Chem. Phys.* **2001**, *202*, 1806. (l) Bazan, G. C.; Rogers, J. S.; Fang, C. C. *Organometallics* **2001**, *20*, 2059. (m) Endres, M.; Fernandez, P.; Ludwig, G.; Pritzkow, H. *Organometallics* **2001**, 5005. (n) Kotov, V. V.; Avtomonov, E. V.; Sundermeyer, J.; Aitola, E.; Repo, T.; Lemenovskii, D. A. *J. Organomet.* Chem. **2001**, *640*, 21. (o) Döhring, A.; Göhre, J.; Jolly, P. W.; Kryger, B.; Rust, J.; Verhovnik, G. P. J. *Organometallics* **2000**, *19*, 388. (p) Britovsek, G. J. P.; Gibson, V. C.; Wass, D. F. *Angew. Chem., Int. Ed*. **1999**, *38*, 428. (q) Theopold, K. H.

Eur. J. Inorg. Chem. **1998**, 15. (r) Liang, Y. F.; Yap, G. P. A.; Rheingold, A. L. *Organometallics* **1996**, *15*, 5284. (s) Theopold, K. H. *Acc. Chem. Res.* **1990**, *23*, 263. (t) Thomas, B. J.; Theopold, K. H. *J. Am. Chem. Soc.* **1988**, *110*, 5902. (u) Karapinka, G. L. U.S. Patent 3,709,853, 1973. (v) Karol, F. J.; Karapinka, G. L.; Wu, C.; Dow, A. W.; Jonson, N.; Carrick, W. L *J. Polym. Sci., Part A* **1972**, *10*, 2621. (w) Hogan, J. P. *J. Polym. Sci., Part A-1* **1970**, *8*, 2637. (x) Hogan, J. P.; Banks, R. L. U.S. Patent 2,825,721, 1958.

(9) (a) Thapa, I.; Gambarotta, S.; Duchateau, R.; Kulangara, S. V.; Chevalier, R. *Organometallics* **2010**, *29*, 4080. (b) Albahily, K.; Koç, E.; Al-Baldawi, D.; Savard, D.; Gambarotta, S.; Burchell, T. J.; Duchateau, R. *Angew. Chem. Int. Ed.* **2008**, *47*, 5816. (c) Temple, C.; Jabri, A.; Crewdson, P.; Gambarotta, S.; Korobkov, I.; Duchateau, R. *Angew. Chem. Int. Ed.* **2006**, *45*, 7050. (d) Jabri, A.; Crewdson, P.; Gambarotta, S.; Korobkov, I.; Duchateau, R. *Organometallics* **2006**, *25*, 715.

(10) (a) Kim, S.-K.; Kim, T.-J.; Chung, J.-H.; Hahn, T.-K.; Chae, S.-S.; Lee, H.-S.; Cheong, M.; Kang, S. O. *Organometallics* **2010**, *29*, 5805. (b) Klemps, C.; Payet, E.; Magna, L.; Saussine, L.; Le Goff, X. F.; Le Floch, P. *Chem. Eur. J.* **2009**, *15*, 8259. (c) Zhang, J.; Braunstein, P.; Hor, T. S. A. *Organometallics* **2008**, *27*, 4277.

(11) (a) Dixon, J. T.; Green, M. J.; Hess, F. M.; Morgan, D. H. *J. Organomet. Chem.* **2004**, *689*, 3641. (b) Carter, A.; Cohen, S. A.; Cooley, N. A.; Murphy, A.; Scott, J.; Wass, D. F. *Chem. Commun.* **2002**, 858.

(12) (a) Shaikh, Y.; Gurnham, J.; Albahily, K.; Gambarotta, S.; Korobkov, I. *Organometallics* **2012**, *31*, 7427. (b) Peitz, S.; Peulecke, N.; Müller, B. H.; Spannenberg, A.; Drexler, H.-J.; Rosenthal, U.; Al-Hazmi, M. H.; Al-Eidan, K. E.; Wöhl, A.; Müller, W.

Organometallics **2011**, *30*, 2364. (c) Peitz, S.; Peulecke, N.; Aluri, B. R.; Müller, B. H.; Spannenberg, A.; Rosenthal, U.; Al-Hazmi, M. H.; Mosa, F. M.; Wöhl, A.; Müller, W. *Chem. Eur. J.* **2010**, *16*, 12127. (d) Peitz, S.; Peulecke, N.; Aluri, B. R.; Müller, B. H.; Spannenberg, A.; Rosenthal, U.; Al-Hazmi, M. H.; Mosa, F. M.; Wöhl, A.; Müller, W. *Organometallics* **2010**, *29*, 5263. (e) Aluri, B. R.; Peulecke, N.; Peitz S.; Spannenberg A.; Müller, B. H.; Schulz, S.; Heller, D.; Al-Hazmi, M. H.; Mosa, F. M.; Wöhl, A.; Müller, W.; Rosenthal, U. *Dalton Trans.* **2010**, 7911. (f) Klemps, C.; Payet, E.; Magna, L.; Saussine, L.; Le Goff, X. F.; Le Floch, P. *Chem. Eur. J.* **2009**, *15*, 8259. (g) Killian, E.; Blann, K.; Bollmann, A.; Dixon, J. T.; Kuhlmann, S.; Maumela, M. C.; Maumela, H.; Morgan, D. H.; Nongodlwana, P.; Overett, M. J.; Pretorius, M.; Hofener, K.; Wasserscheid, P. *J. Mol. Catal. A: Chem.* **2007**, *270*, 214. (h) McGuinness, D. S.; Overette, M., Tooze, R. P.; Blann, K.; Dixon, J. T.; Slawin, A. M. Z. *Organometallics* **2007**, *26*, 1108. (i) Kuhlmann, S.; Blann, K.; Bollmann, A.; Dixon, J. T.; Killian, E.; Maumela, M. C.; Maumela, H.; Morgan, D. H.; Pretorius, M.; Taccardi, N.; Wasserscheid, P. *J. Catal.* **2007**, *245*, 279. (j) Kuhlmann, S.; Blann, K.; Bollmann, A.; Dixon, J. T.; Killian, E.; Maumela, M. C.; Maumela, H.; Morgan, D. H.; Pretorius, M.; Taccardi, N.; Wasserscheid, P. *J. Catal.* **2006**, *245*, 279. (k) Jabri, A.; Crewdson, P.; Gambarotta, S.; Korobkov, I.; Duchateau, R. *Organometallics* **2006**, *25*, 715. (1) McGuinness, D. S.; Wasserscheid, P; Morgan, D. H.; Dixon, J. T. *Organometallics* **2005**, *24*, 552. (m) Blann, K.; Bolmann, A.; Dixon, J. T.; Hess, F.; Kilian, E.; Maumela, H.; Morgan, D. H.; Neveling, A.; Otto, S.; Overett, M. *Chem. Commun.* **2005**, 620. (n) Blann, K.; Bollmann,A.; Dixon, J. T.; Hess, F. M.; Killian, E.; Maumela, H.; Morgan, D. H.; Neveling, A.; Otto, S.; Overett, M. J. *Chem. Commun.*

2005, 622. (o) McGuinness, D. S.; Wasserscheid, P.; Keim, W.; Hu, C.; Englert , U.; Dixon, J. T.; Grove, C. *Chem. Commun.* **2003**, 334.

(13) Albahily, K.; Al-Baldawi, D.; Gambarotta, S.; Koç, E.; Duchateau, R. *Organometallics* **2008**, *27*, 5943.

(14) (a) Albahily, K.; Al-Baldawi, D.; Gambarotta, S.; Koç, E.; Duchateau, R. *Organometallics* **2008**, *27*, 5708. (b) Crewdson, P.; Gambarotta, S.; Djoman, M.-C.; Korobkov,I.; Duchateau, R. *Organometallics* **2005**, *24*, 5214.

(15) Schirmer, W; Flörke, U; Haupt, H.-J.; *Z. Anorg. Allgemeine Chemie* **1987**, *545*, 83.

(16) Collman, J. P.; Kittleman, E. T. *Inorg. Synth.* **1966**, *8*, 149.

(17) Kohler, F. H; rossdorf, W. *Z. Natureforsch. Teil B*, **1977**, *32*, 1026.

CHAPTER 3

Polymer-Free Ethylene Oligomerization Using a Pyridine-Based Pincer PNP-Type of Ligand

The results presented in this chapter have been published in

Alzamly, A.; Gambarotta, S.; Korobkov, I. *Organometallics* **2013**, *32*, 7204.

3.1 Introduction

Preventing formation of unwanted polymeric materials is a major task for the profitability of unselective or selective catalytic systems designed to produce either distributions of linear alpha olefins (LAOs)[1] or 1-hexene and 1-octene.[2] The solid material which accompanies the production of these useful chemicals causes reactor fouling which, in turn, results into significant increase of the operating costs. Once solid-free LAOs are obtained, a specific α-olefin may be extracted through an energy-intensive fractionation or more directly prepared through selective catalytic cycles.

A few highly selective trimerization systems have been discovered in the recent past[3] and for which, the metal oxidation state of the catalytically active species,[4] and the reaction mechanism is reasonably well-understood.[4a-c,e,i,l,5] The tetramerization remains instead somewhat elusive[6] since very high selectivity (>91%) has been obtained in only two cases.[6a,c,7] The mechanism for selective tetramerization remains also debated.[6a,g,8] For the non-selective oligomerization instead, and for which a few industrial processes (Idemitsu, SHOP, SABLIN) are being used, the main challenge remains about maximizing productivity and obtaining polymer-free oligomeric mixtures.

The appearance of polymeric residues in chromium catalyzed oligomerization might be linked to the partial instability of this metal oxidation states and their interconversion (redox dynamism), each responsible for a specific performance: selective versus non-selective oligomerization and polymerization.[4i,9] Alternatively, the polymer may simply be a heavier oligomer tail of the statistical distribution. Regardless, complexes based on trivalent chromium remain by far the most preferred catalyst precursors[5a,10] given their good stability, ease of preparation and activation.

We are interested in assessing the ligand anionicity/neutrality and the aggregation between chromium and aluminates vis-à-vis the catalyst selective *versus* non-selective behavior, its activity and formation of polymeric material. Among the several families of ligand systems which have been employed in this chemistry, those based on a combination of N and P donor atom seems to be the most promising.[11] Recently, we have tested a dianionic $Ph_2PNHPyNHPPh_2$ pincer-type of system,[12] where a pyridine donor moiety was introduced to improve the stabilizing power of the ligand and to test its effect on the metal oxidation state. Interestingly, we found that the pyridine ring obliterates the selectivity of the catalytic systems while producing active catalysts for non-selective oligomerization. However, polymeric material was invariably present. We speculated that this was probably the result of an excess of stabilization introduced by the pyridine ring on the chromium divalent state. In this follow-up paper, we have modified the ligand frame by removing the P-N functions and used a classical diphosphino-pyridine pincer ligand.[13] This was an attempt to moderate the ligand stabilizing power and to probe the response of the catalytic system. Herein we describe our results.

3.2 Experimental Section

All reactions were carried out under inert atmosphere using Schlenk techniques or in a purified nitrogen-filled drybox. Solvents were dried using a purification system composed of aluminum oxide. GC-MS analysis of the oligomers was carried out with a Hewlett-Packard HP 5973 gas chromatograph using an Agilent DB1 column and dual FID and MS detector. Elemental analyses were carried out with a PerkinElmer 2400 CHN analyzer. Magnetic susceptibility measurements were performed with a Johnson Matthey balance at room temperature. The samples were powdered and weighed inside a drybox and transferred to sealed and calibrated tubes for measurements. NMR spectra were recorded on Varian Mercury 400

MHz spectrometer at 300 K. All chemical reagents were purchased from commercial sources and used as received. Diethyl aluminum chloride, trimethyl aluminum, triethyl aluminum and tri-isobutyl aluminum were purchased from Strem and used as received. Methylaluminoxane (MAO, 20% in toluene) was purchased from Albemarle Corporation. TMA-depleted methylaluminoxane (DMAO) was prepared by removing all the volatiles from MAO *in vacuo* (2 mmHg) and with moderate heating (40°C) for 6 hours. Ligand $Ph_2PCH_2PyCH_2PPh_2$ was obtained from digital specialty chemicals. $CrCl_3(THF)_3$[14] and $CrCl_2(THF)_2$[15] were prepared according to literature procedures.

Preparation of $[2,6\text{-}(Ph_2PCH_2)_2C_5H_3N]CrCl_3$ (3.1)

A solution of $CrCl_3(THF)_3$ (0.37 g, 1.0 mmol) in THF (15 mL) was added to a solution of PPh_2 $CH_2PyCH_2PPh_2$ (0.47 g, 1.0 mmol) in THF (5 mL). The color of the solution immediately changed to dark-green. Green crystals of **3.1** were obtained by slow evaporation **(**0.52 g, 0.82 mmol, 82%). μ_{eff} = 3.80 μ_{BM}. Elemental Analysis % calculated for $C_{31}H_{27}Cl_3CrNP_2$ (found): C 58.74 (57.65), H 4.29 (4.02), N 2.21 (2.10).

Preparation of $\{[2,6\text{-}(Ph_2CH_2)_2C_5H_3N]CrCl_2\}.(THF)$ (3.2)

A solution of $CrCl_2(THF)_2$ (0.27 g, 1.0 mmol) in THF (15 mL) was added to a solution of PPh_2 $CH_2PyCH_2PPh_2$ (0.47 g, 1 mmol) in THF (5 mL). The color of the solution immediately changed to light-green. The solution was concentrated to about 7 mL and stored at room temperature for two days, upon which green crystals of **3.2** were formed (0.26 g, 0.44 mmol, 44%). μ_{eff} = 4.82 μ_{BM}. Elemental Analysis % calculated for $C_{35}H_{35}Cl_2CrNOP_2$ (found): C 62.22 (62.12), H 4.55 (4.46), N 2.34 (2.31).

Preparation of $[2,6\text{-}(Ph_2CH_2)_2C_5H_3NCrCl(\mu\text{-}Cl)AlClMe_2]$ (3.3)

A solution of $PPh_2CH_2PyCH_2PPh_2$ (0.47 g, 1 mmol) in toluene (10 mL) was treated with $CrCl_3(THF)_3$ (0.37 g, 1.0 mmol). The mixture was stirred at room temperature overnight. After cooling to -40 ^oC, trimethylaluminum (0.721, 10.0 mmol) was added dropwise and the mixture stirred for 30 min. After reaching room temperature, the suspension was centrifuged and the supernatant concentrated, layered with methylcyclohexanes (3 mL) and stored in the glove box at room temperature for 3 days. The resulting green crystal of **3.3** were filtered, washed with cold hexanes (10 mL), dried *in vacuo* (0.46 g, 0.7 mmol, 66%). μ_{eff} = 4.77 μ_{BM}. Elemental Analysis % calculated for $C_{33}H_{33}Al_3Cl_2CrNP$ (found): C 57.37 (58.32), H 4.81 (4.78), N 2.03 (2.01).

Preparation of {[2,6-$(Ph_2CH_2)_2C_5H_3NCrCl(\mu$-Cl)$AlClEt_2$]}.$(toluene)_{0.5}$ (3.4)

A solution of $PPh_2CH_2PyCH_2PPh_2$ (0.47 g, 1.0 mmol) in toluene (10 mL) was treated with $CrCl_2(THF)_2$ (0.27g, 1.0 mmol). The mixture was stirred at room temperature overnight. After cooling to -40 ^oC, diethylaluminum chloride (0.60 g, 5.0 mmol) was added dropwise and the mixture stirred for 30 min. After warming to room temperature, the suspension was centrifuged and the supernatant concentrated and layered with methylcyclohexanes (3 mL). Upon standing in the glove box at room temperature for 3 days, green crystal of **3.4** were obtained and which were filtered, washed with cold hexanes (10 mL), dried *in vacuo*, (0.42 g, 0.59 mmol, 59%). μ_{eff} = 4.82 μ_{BM}. Elemental Analysis % calculated for $C_{38.5}H_{41}AlCl_3CrNP_2$ (found): C 58.47 (58.38), H 5.19 (5.13), N 1.95 (1.86).

Preparation of {2,6-$(Ph_2CH_2)_2C_5H_3NCrEt(\mu$-Cl$)_2AlEt_2$}{$AlCl_3Et$} (3.5)

A solution of $PPh_2CH_2PyCH_2PPh_2$ (0.47 g, 1 mmol) in toluene (10 mL) was treated with $CrCl_3(THF)_3$ (0.37g, 1.0 mmol). The mixture was stirred at room temperature overnight. After cooling to -40 ^oC, diethylaluminum chloride (1.21 g, 10.0 mmol) was added dropwise and the mixture stirred for 30 min. After warming to room temperature, the suspension was centrifuged

and the supernatant concentrated and layered with methycyclohexane (3 mL) and kept standing in the glove box at room temperature for 3 days. The resulting green crystals of **3.5** were filtered, washed with cold hexanes (10 mL) and dried (0.35 g, 0.40 mmol, 40%). μ_{eff} = 3.73 μ_{BM}. Elemental Analysis % calculated for $C_{39}H_{47}Al_2Cl_5CrNP_2$ (found): C 53.54 (53.82), H 5.41 (5.78), N 1.60 (1.71).

Preparation of {2,6-(PPh_2CH_2)C_5H_3N(PPh_2CH)Al(*i*-Bu)$_2$(μ-Cl)Cr(μ-Cl)$_2$Al(*i*-Bu)$_2$}. ($toluene)_{1.5}$ (3.6)

A solution of $PPh_2CH_2PyCH_2PPh_2$ (0.47 g, 1 mmol) in toluene (10 mL) was treated with $CrCl_3(THF)_3$ (0.37g, 1.0 mmol). The mixture was stirred at room temperature overnight. After cooling to -40 ^oC, triisobutylaluminum (0.99 g, 5.0 mmol) was added dropwise and the mixture stirred for 30 min. After warming to room temperature, the suspension was centrifuged and the supernatant concentrated and layered with methycyclohexane (3 mL). Upon standing in the glove box at room temperature for 3 days, green crystals of **3.6** were obtained and which were washed with cold hexanes (10 mL) and dried *in vacuo*, (0.46 g, 0.50 mmol, 50%). μ_{eff} = 3.89 μ_{BM}. Elemental Analysis % calculated for $C_{57.5}H_{74}Al_2Cl_3CrNP_2$ (found): C 61.68 (61.43), H 6.83 (6.75), N 1.53 (1.49).

Preparation of {2,6-(PPh_2CH_2)$_2C_5H_3N]_2$Cr}{(μ-Cl)[(Al(*i*-Bu)$_3$]$_2$} (3.7)

A solution of $PPh_2CH_2PyCH_2PPh_2$ (0.47 g, 1.0 mmol) in toluene (10 mL)) was treated with $CrCl_2(THF)_2$ (0.27 g, 1.0 mmol). The mixture was stirred at room temperature overnight. After cooling to -40 ^oC, triisobutylaluminum (0.99 g, 5.0 mmol) was added dropwise and the mixture stirred for 30 min. After reaching room temperature, the suspension was centrifuged and the supernatant concentrated and layered with hexanes (3 mL). Upon storing in a freezer at -40 ^oC for 3 days, dark-brown crystals of **3.7** were formed which were filtered, washed with cold

hexanes (10 mL) and dried **(**0.388 g, 0.27 mmol, 27%). μ_{eff} = 1.521 μ_{MB}. Elemental Analysis % calculated for $C_{86}H_{108}Al_2ClCrN_2P_4$ (found): C 71.98 (70.54), H 7.59 (7.21), N 1.95 (1.87).

3.3 X-Ray Data

Table 3.1. Crystal Data and Structure Analysis Results of Complexes **3.1-3.7**.

	3.1	**3.2**	**3.3**	**3.4**
Formula	$C_{31}H_{27}Cl_3CrNP_2$	$C_{35}H_{35}Cl_2CrNOP_2$	$C_{33}H_{33}AlCl_2CrNP_2$	$C_{38.5}H_{41}AlCl_3CrNP_2$
FW, gmol^{-1}	633.83	670.48	690.87	764.99
Space group	Triclinic, P-1	Monoclinic, P2(1)/n	Monoclinic, P2(1)/n	Triclinic, P-1
***a* (Å)**	10.8747(15)	9.8344(3)	11.3819(3)	8.675092)
***b* (Å)**	11.6006(15)	14.4109(5)	14.0201(4)	13.8772(3)
***c* (Å)**	12.9880(18)	23.1807(8)	11.7219(3)	16.3811(4)
α, (deg)	97.703(9)	90	90	99.2870(10)
β, (deg)	91.157(9)	91.4440(10)	114.6190(10)	90.1870(10)
γ, (deg)	117.088(8)	90	90	101.0900(10)
***V* (Å^3)**	1439.4(3)	3284.18(19)	1700.49(8)	1908.64(8)
Z	2	4	2	2
Radiation	0.71073	0.71073	0.71073	0.71073
T (K)	200(2)	200(2)	200(2)	200(2)
D_{calcd} (mg/m^3)	1.462	1.356	1.349	1.331
μ_{calcd} (mm^{-1})	0.0810	0.637	0.715	0.645
***F*$_{000}$**	650	1392	700	794
***R, Rw*^{2a}**	0.0848, 0.2343	0.0372,0 .1095	0.0489, 0.1032	0.0571, 0.1205
	3.5	**3.6**	**3.7**	
Formula	$C_{39}H_{47}Al_2Cl_5CrNP_2$	$C_{57.5}H_{74}Al_2Cl_3CrP_2$	$C_{86}H_{108}Al_2ClCrN_2P_4$	
FW, gmol^{-1}	874.93	1053.43	1435.03	
Space group	Triclinic, P-1	Triclinic, P-1	Orthorhombic, P2(1) 2(1)2(1)	
***a* (Å)**	11.0441(2)	18.270(2)	17.5558(12)	
***b* (Å)**	12.5327(2)	30.639(4)	17.556	
***c* (Å)**	16.3772(3)	13.5899(17)	26.847(2)	
α, (deg)	106.4950(10)	90	90	
β, (deg)	95.1430(10)	114.266(7)	90	
γ, (deg)	91.6730(10)	90	90	
***V* (Å^3)**	2161.22(7)	6935.2(16)	8274.3(8)	
Z	2	4	4	
Radiation	0.71073	0.71073	0.71073	
T (K)	200(2)	200(2)	200(2)	
D_{calcd} (mg/m^3)	1.344	1.009	1.152	
μ_{calcd} (mm^{-1})	0.717	0.382	0.312	
***F*$_{000}$**	906	2228	3060	
***R, Rw*^{2a}**	0.0765, 0.1302	0.0930, 0.1800	0.0623, 0.1424	
GoF	1.026	1.034	1.030	

[a] $R = \Sigma j Fo j - j Fc j / \Sigma j Fj$, $Rw = [\Sigma(j Fo j - j Fc j)2/\Sigma wFo2]^{1/2}$

3.4 Results and Discussion

Treatment of either $CrCl_3(THF)_3$ or $CrCl_2(THF)_2$ with $Ph_2PCH_2PyCH_2PPh_2$ in THF afforded the corresponding complexes $[2,6\text{-}(Ph_2P\text{-}CH_2)_2C_5H_3N]CrCl_3$ (**3.1**) and $\{[2,6\text{-}(Ph_2CH_2)_2C_5H_3N]CrCl_2\}.(THF)$ (**3.2**) (Scheme 3.1).

Scheme 3.1

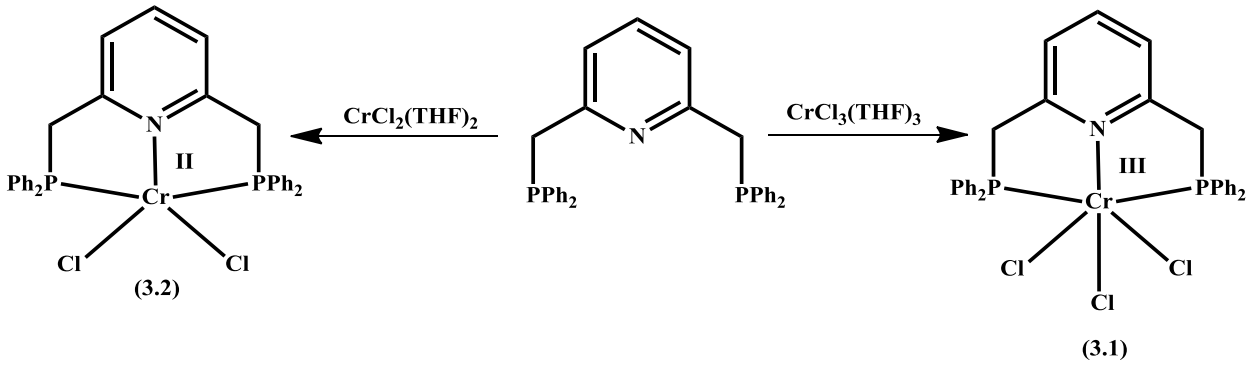

For both species it was possible to grow crystals of sufficient quality for X-ray analysis. The structure of **3.1** (Figure 3.1a) shows a distorted-octahedral trivalent chromium center surrounded by three meridionally placed donor atoms of the ligand [Cr(1)-N(1) = 2.1465(6) Å, Cr(1)-P(1) = 2.431(3) Å, N(1)-Cr(1)-P(2) = 81.00(2)^o, N(1)-Cr(1)-P(1) = 80.8(2)^o, P(2)-Cr(1)-P(1) = 161.8(9)^o]. The three chlorine atoms occupy the three remaining positions [Cr(1)-Cl(2) = 2.281(2) Å, Cr(1)-Cl(3) = 2.314(2) Å, Cr(1)-Cl(1) = 2.3010(15) Å, Cl(2)-Cr(1)-Cl(1) = 92.69 (9)^o,].

The structure of **3.2** (Figure 3.1b) consists of a square-pyramidal divalent chromium center with three ligand donor atoms and one chlorine defining the basal plane [Cr(1)-N(1) = 2.1642(16) Å, Cr(1)-P(1) = 2.4900(6) Å, Cr(1)-Cl(1) = 2.3262(6) Å, N(1)-Cr(1)-P(1) = 78.80

(4)^{o}, P(2)-Cr(1)-P(1) = 142.41(2)^{o}]. The second chlorine atom is located on the apical position [Cr(1)-Cl(2) = 2.4348(6) Å, N(1)-Cr(1)-Cl(2) = 94.63(4)^{o}].

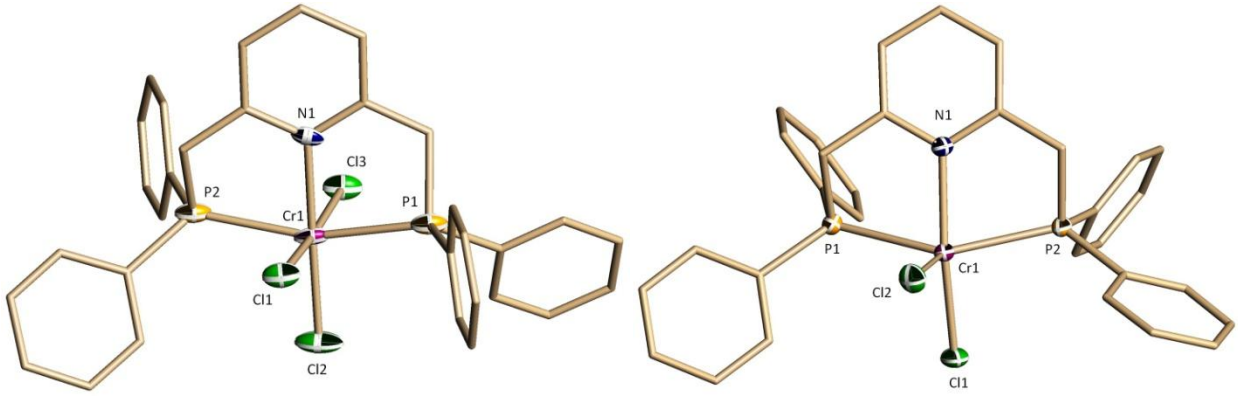

a **b**

Figure 3.1. Thermal ellipsoid plots of **3.1** and **3.2** with ellipsoids drawn at 50% probability. Selected bond distances (Å) and angles (deg) for **3.1**: Cr(1)-Cl(3) = 2.313(2), Cr(1)-P(2) = 2.423(3), N(1)-Cr(1)-Cl(2) = 179.2(2), N(1)-Cr(1)-Cl(1) = 87.37(17), N(1)-Cr(1)-Cl(3) = 87.49 (17), Cl(2)-Cr(1)-Cl(3) = 92.46(9), Cl(1)-Cr(1)-Cl(3) = 174.85(9), Cl(2)-Cr(1)-P(2) = 98.18(10), Cl(1)-Cr(1)-P(2) = 91.99(9), Cl(3)-Cr(1)-P(2) = 87.30(9), Cl (2)-Cr(1)-P(1) = 100.02(10), Cl(1)-Cr(1)-P(1) = 86.96(9), Cl(3)-Cr(1)-P(1) = 92.12(9). Selected bond distances (Å) and angles (deg) for **3.2**: Cr(1)-P(2) = 2.4445(6), N(1)-Cr(1)-Cl(1) = 164.44 (5), Cl(1)-Cr(1)-Cl(2) = 100.93(2), N(1)-Cr(1)-P(2) = 79.70(5), Cl(1)-Cr(1)-P(2) = 93.70(2), Cl(2)-Cr(1)-P(2) = 113.95 (2), N(1)-Cr(1)-P(1) = 78.80(4), Cl(1)-Cr(1)-P(1) = 98.92(2), Cl(2)-Cr(1)-P(1) = 98.23(2).

When activated with MAO, both complexes show catalytic behavior only at temperatures of 80 ^{o}C or higher (Table 3.2). The catalytic cycles produced mixtures of oligomers with good activity and without the presence of visible polymeric material. The output of oligomers, along with the invariable presence of 1-butene, reasonably fits a Schultz-Flory distribution for the heavier oligomers (α ranging from 0.46 to 0.52) with a minor and yet visible excess of 1-hexene in two runs (entry 2 and 4) and a minor deficiency in another (entry 3). The enrichment in 1-hexene might tentatively suggest redox dynamism between the mono- and divalent states of

the metal center during the catalytic cycle. Increasing the temperature from 80 to 110˚C had some effect on the activity and also somewhat modified the distribution of oligomers. This may be attributed to an increased instability at higher temperatures of the organochromium species with respect to further reduction to the monovalent state. At higher temperatures, the catalytic system was completely inactive. Although for convenience reasons the catalytic activities have been measured in 30 minutes runs, we have observed that the catalyst becomes inactive after about 10-15 minutes.

Table 3.2. Ethylene catalyzed oligomerization reactions of **3.1** and **3.2.**

Entry	Catalyst	Alkenes (g)	Activity (g/g Cr . h)	Linear alpha olefins (mol %)								
				C_4	C_6	C_8	C_{10}	C_{12}	C_{14}	C_{16}	C_{18}	α_{av}
1	**3.1**[a]	3	4125	48	29.0	13.2	6.1	2.0	0.9	0.4	0.2	0.46
2	**3.2**[a]	5	6875	73	18.1	7.0	3.7	1.9	1.0	0.5	0.2	0.52
3	**3.1**[b]	4	5500	34	31.3	17.6	8.8	4.7	2.0	1.0	0.5	0.49
4	**3.2**[b]	9	15125	57	25.2	10.5	4.9	2.2	1.1	0.5	0.2	0.47

Conditions: single runs in 100mL of toluene, loading 20 µmol of catalyst, 40 bar of ethylene, [a] T = 80 ˚C, [b] T = 110 ˚C, reaction time 30 min, (Al:Cr) MAO = 500.

To understand the interaction of these complexes with alkyl aluminum activators and in the possible view of isolating catalytically active species, both **3.1** and **3.2** were reacted with moderate excesses of different alkyl aluminums (Schemes 3.2-3.5).

As is often the case, the reactions with MAO gave oily materials while, upon treating the trivalent **3.1** with 10 equivalents of Me_3Al and the divalent **3.2** with 5 equivalents of DEAC, nearly isostructural oligomerization catalysts [2,6-$(Ph_2CH_2)_2C_5H_3NCrCl(\mu\text{-}Cl)AlClMe_2$] **(3.3)** and {[(2,6-$(Ph_2CH_2)_2C_5H_3NCrCl(\mu\text{-}Cl)AlClEt_2$]}.$(toluene)_{0.5}$ **(3.4)** were obtained in crystalline forms (Scheme 3.2).

Scheme 3.2

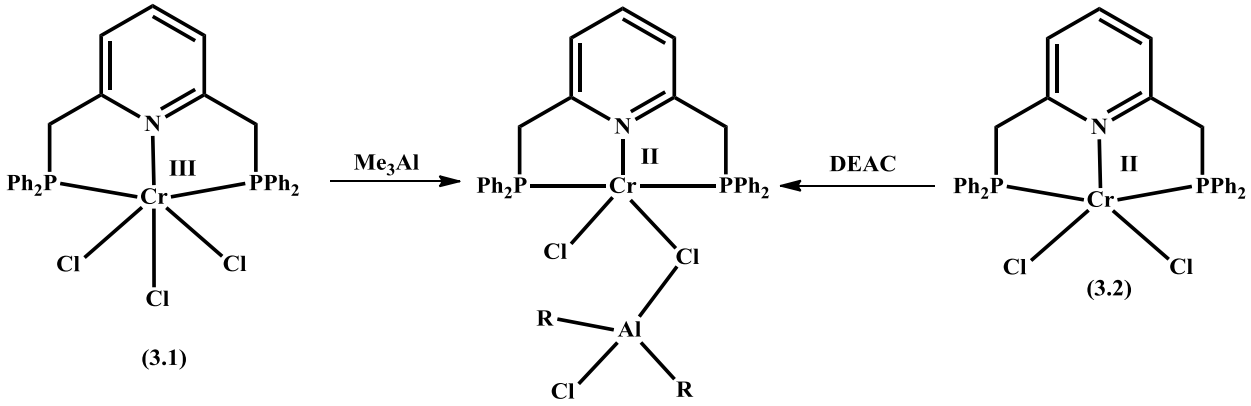

R= Me (3.3); Et (3.4)

Both complexes exhibit the same square-pyramidal geometry (Figure 3.2) with one chlorine atom and the ligand donor atoms defining the basal plane [**3.3**: Cr(1)-N(1) = 2.128(3) Å, Cr(1)-Cl(1) = 2.3107(10) Å, Cr(1)-P(1) = 2.4532(10), Cl(1)-Cr(1)-P(2) = 95.76(4)^{o}, N(1)-Cr(1)-P(1) = 80.29(9)^{o}, P(2)-Cr(1)-P(1) = 143.78(4)^{o}. **3.4**: Cr(1)-N(1) = 2.128(3) Å, Cr(1)-Cl(2) = 2.5695(11) Å, Cr(1)-P(1) = 2.4532(10) Å, N(1)-Cr(1)-P(1) = 80.29(9)^{o}, P(2)-Cr(1)-P(1) = 143.78 (4)^{o}, N(1)-Cr(1)-Cl(2) = 94.80(8)^{o}]. The apical position is occupied by a second chlorine atom which in turn bridges an aluminate residue [**3.3**: Cr(1)-Cl(2) = 2.5695(11) Å, Cl(1)-Cr(1)-Cl(2) = 93.70(4)^{o}. **3.4**: Cr(1)-Cl(1) = 2.3107(10) Å, Cl(1)-Cr(1)-Cl(2) = 93.70(4)^{o}].

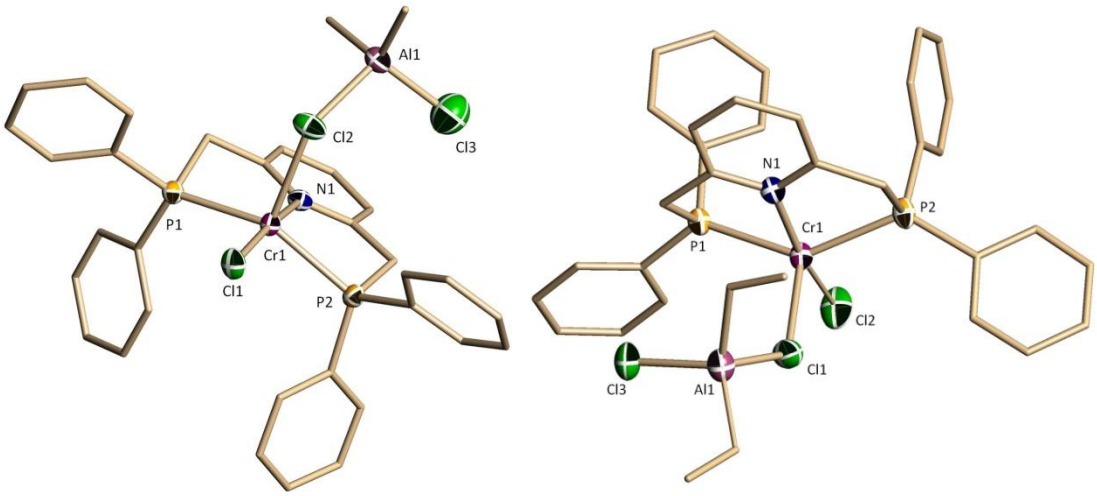

a **b**

Figure 3.2. Thermal ellipsoid plots of **3.3** and **3.4** with ellipsoids drawn at 50% probability level. Selected bond distances (Å) and angles (deg) for **3.3**: Cr(1)-P(2) = 2.4265(10), Al(1)-Cl(3) = 2.111(2), Al(1)-Cl(2) = 2.2872(16), N(1)-Cr(1)-Cl(1) = 171.48(8), N(1)-Cr(1)-P(2) = 81.03(8), Cl(1)-Cr(1)-P(1) = 98.20(4), N(1)-Cr(1)-Cl(2) = 94.80(8), P(2)-Cr(1)-Cl(2), 109.25(4) = P(1)-Cr(1)-Cl(2) = 103.01(4), Cl(3)-Al(1)-Cl(2) = 105.95(8), Al(1)-Cl(2)-Cr(1) = 125.76(6). Selected bond distances (Å) and angles (deg) for **3.4**: Cr(1)-P(2) = 2.4265(10), Cr(1)-Cl(2) = 2.5695(11), Al(1)-Cl(3) = 2.111(2), Al(1)-Cl(2) = 2.2872(16), N(1)-Cr(1)-Cl(1) = 171.48(8), N(1)-Cr(1)-P(2) = 81.03(8), Cl(1)-Cr(1)-P(1) = 98.20(4), N(1)-Cr(1)-Cl(2) = 94.80(8), P(2)-Cr(1)-Cl(2) = 109.25(4), P(1)-Cr(1)-Cl(2) = 103.01(4), Cl(3)-Al(1)-Cl(2) = 105.95(8), Al(1)-Cl(2)-Cr(1) = 125.76(6).

When the trivalent **3.1** was treated with 10 equivalents of DEAC, a cationic complex {2, 6-$(Ph_2CH_2)_2C_5H_3NCrEt(\mu\text{-}Cl)_2AlEt_2\}\{AlCl_3Et\}$ **(3.5)**, (Scheme 3.3) also trivalent and containing an ethyl group terminally bonded to chromium was formed. The failure of DEAC to reduce these systems is in sharp contrast with the ease of reduction to the monovalent state as observed in the Phillips-Chevron system.[4c] This can be ascribed in this case to the larger stabilizing effect of the two P donor atom of the pincer ligand.

Scheme 3.3

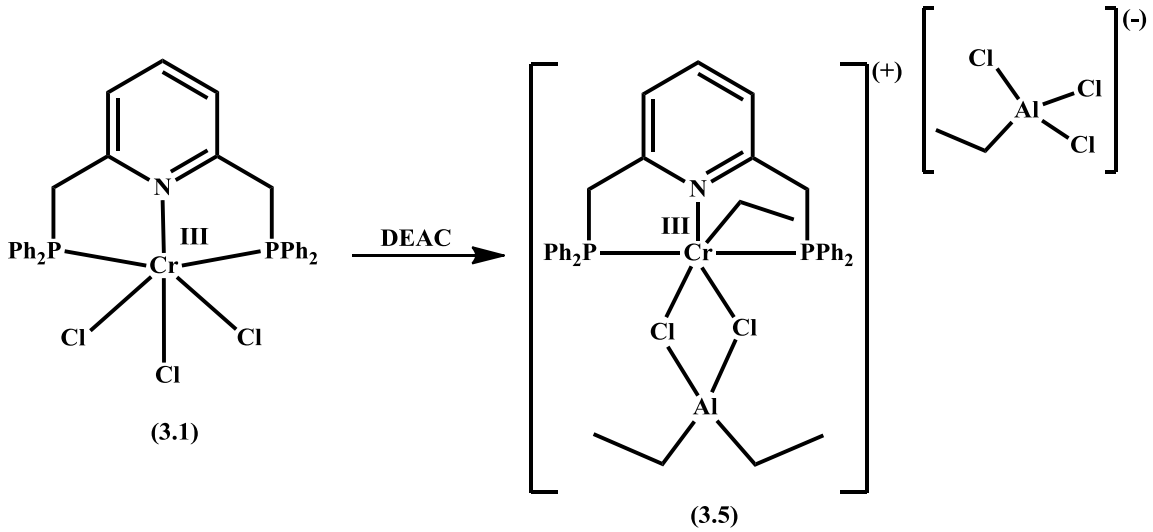

The geometry around the chromium center in **3.5** is distorted octahedral (Figure 3.3) with the equatorial plane defined by the three donor atoms of the ligand [Cr(1)-N(1) = 2.0955(19) Å, Cr(1)-P(1) = 2.4683(6) Å, N(1)-Cr(1)-P(1) = 80.75(5)^{o}, P(2)-Cr(1)-P(1) = 161.27(3)^{o}] and one chlorine [Cr(1)-Cl(2) = 2.4072(7) Å, N(1)-Cr(1)-Cl(2) = 173.33(6)^{o}]. The second chlorine [Cr(1) -Cl(1) = 2.5428(7) Å, N(1)-Cr(1)-Cl(1) = 90.60(5)^{o}] and the ethyl group carbon atom are located on the axial vector [Cr(1)-C(32) = 2.088(3) Å, C(32)-Cr(1)-Cl(1) = 175.37(8)^{o}]. Different from the previous complex, both chlorine atoms bridge the aluminate residue.

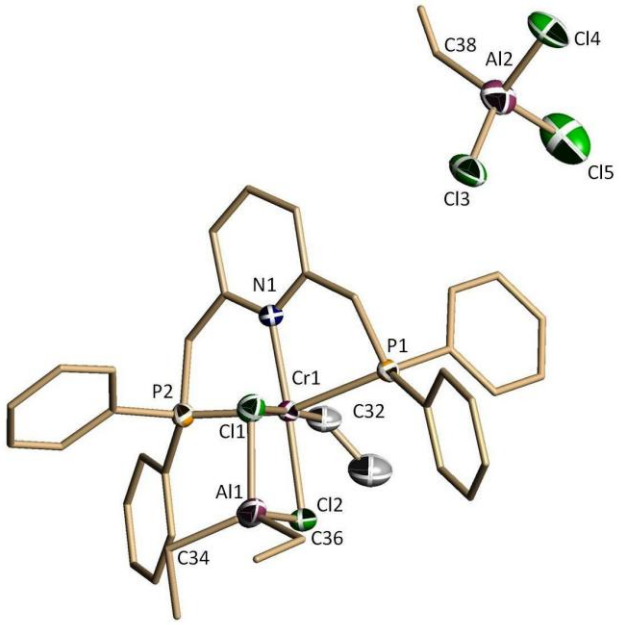

Figure 3.3. Thermal ellipsoid plot of **3.5** with ellipsoids drawn at 50% probability. Selected bond distances (Å) and angles (deg) for **3.5**: Cr(1)-Cl(2) = 2.4072(7), Cr(1)-P(2) = 2.4642(7), Al(1)-Cl(1) = 2.2463(11), Al(1)-Cl(2) = 2.2944(13), Al(2)-Cl(5) = 2.1330(16), Al(2)-Cl(4) = 2.1593 (12), Al(2)-Cl(3) = 2.1619(14), C(32)-Cr(1)-N(1) = 93.26(10), C(32)-Cr(1)-Cl(2) = 93.41(8), C(32)-Cr(1)-P(2) = 88.14(7), N(1)-Cr(1)-P(2) = 80.55(5), Cl(2)-Cr(1)-P(2) = 99.47(2), C(32)-Cr(1)-P(1) = 91.70(7), Cl(2)-Cr(1)-P(1) = 99.24(2), Cl(2)-Cr(1)-Cl(1) = 82.74(3), P(2)-Cr(1)-Cl(1) = 95.03(2), P(1)-Cr(1)-Cl(1) = 86.39(2), Cl(5)-Al(2)-Cl(4) = 106.38(6), Cl(5)-Al(2)-Cl(3) = 106.15(6), Cl(4)-Al(2)-Cl(3) = 107.37(6), Al (1)-Cl(1)-Cr(1) = 90.39(4), Al(1)-Cl(2)-Cr(1) = 92.75(3).

When the more reducing TIBA was used, the trivalent **3.1** was reduced to the divalent state affording {2,6-$(PPh_2CH_2)C_5H_3N(PPh_2CH)Al(i\text{-}Bu)_2(\mu\text{-}Cl)Cr(\mu\text{-}Cl)_2Al(i\text{-}Bu)_2$}.$(toluene)_{1.5}$ **3.6** (Scheme 3.4)**.** Unexpectedly**,** one of the two methylene links was deprotonated with consequent anionization and direct alumination of the ligand system. We found no evidence for any further reduction towards the monovalent state.

Scheme 3.4

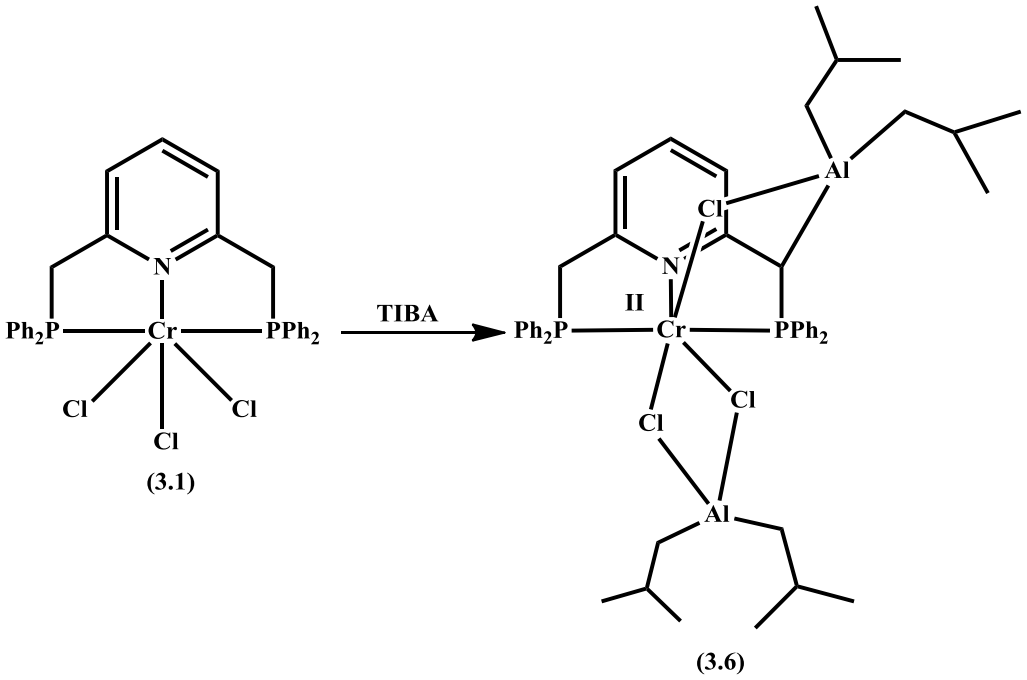

The structure of **3.6** (Figure 3.4) shows a distorted octahedral arrangement around the chromium center with the three ligand donor atoms [Cr(1)-N(1) = 2.110(3) Å, Cr(1)-P(1) = 2.4943(11) Å, N(1)-Cr(1)-P(1) = 78.77(8)^{o}, P(2)-Cr(1)-P(1) = 155.37(4)^{o}] and one chlorine [Cr (1)-Cl(1) = 2.4318(10), N(1)-Cr(1)-Cl(1) = 175.68(8)^{o}] in equatorial position. The two residual chlorine atoms occupy the axial position [Cr(1)-Cl(2) = 2.8258(12) Å, N(1)-Cr(1)-Cl(3) = 97.98 (8)^{o}, Cl(3)-Cr(1)-Cl(2) = 161.82(3)^{o}]. One equatorial and one axial chlorine bridge a (*i*-Bu)$_2$ Al residue, while the second axial chlorine is also bridging a second aluminate residue and which is in turn bonded to the deprotonated methylene group of the ligand. This additional bonding interaction is probably responsible for the visible deviation from the octahedral geometry.

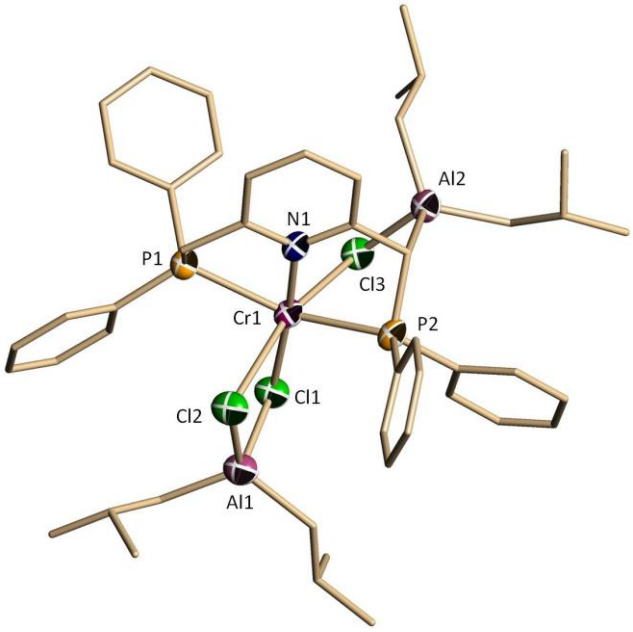

Figure 3.4. Thermal ellipsoid plot of **3.6** with ellipsoids drawn at 50% probability. Selected bond distances (Å) and angles (^{o}) for **3.6**: Cr(1)-P(2) = 2.4891(11), Cr(1)-Cl(3) = 2.7637(10), Al(1)-Cl(2) = 2.2153(16), Al(1)-Cl(1) = 2.3022(15), Al(2)-Cl(3) = 2.2632(15), N(1)-Cr(1)-P(2) = 76.93(8), Cl (1)-Cr(1)-P(2) = 106.46(4), Cl(1)-Cr(1)-P(1) = 97.65(4), Cl(1)-Cr(1)-Cl(3) = 85.22 (3), P(2)-Cr(1)-Cl(3) = 82.76(3), P(1)-Cr(1)-Cl(3) = 104.62(3), N(1)-Cr(1)-Cl(2) = 98.53(8), Cl (1)-Cr(1)-Cl(2) = 78.72(3), P(2)-Cr(1)-Cl(2) = 93.62(4), P(1)-Cr(1)-Cl(2) = 86.06(4), Al(1)-Cl (1)-Cr(1) = 96.13 (5), Al(1)-Cl(2)-Cr(1) = 87.78(5), Al(2)-Cl(3)-Cr(1) = 97.83(4).

When the divalent precursor **3.2** was treated with TIBA, the reaction took an interesting turn in the sense that a monovalent complex {[2,6-$(PPh_2CH_2)_2C_5H_3N]_2Cr$}{($\mu$-Cl)[Al($i$-$Bu_3$)]$_2$} (**3.7)** (Scheme 3.5) was obtained.

Scheme 3.5

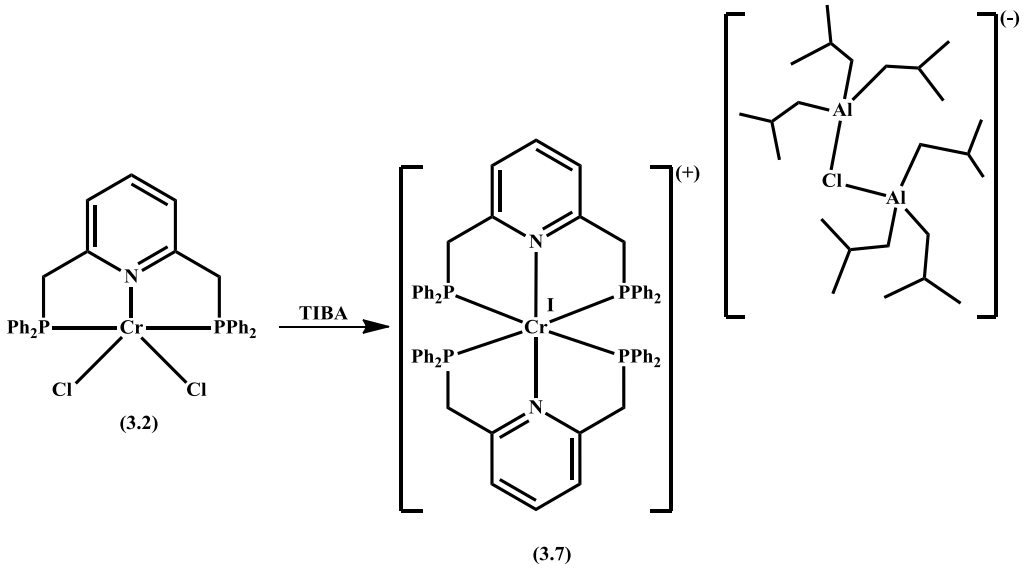

The structure of **3.7** shows an encapsulated Cr(I) atom in an octahedral arrangement as defined by the two meridionally arranged ligands (Figure 3.5) [Cr(1)-N(1) = 2.120(3) Å, Cr(1)-P(1) = 2.3923(10) Å, N(1)-Cr(1)-N(2) = 179.05(12)^{o}, N(1)-Cr(1)-P(1) = 78.27(8)^{o}, P(3)-Cr(1)-P(4) = 157.70(4)^{o}]

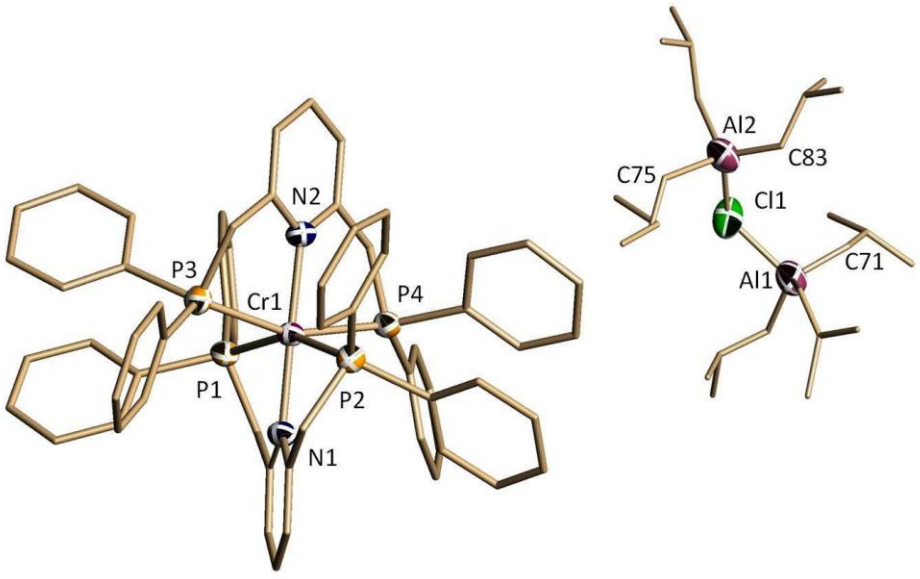

Figure 3.5. Thermal ellipsoid plot of **3.7** with ellipsoids drawn at 50% probability**.** Selected bond distances (Å) and angles (deg) for **3.7**: Cr(1)-N(2) = 2.127(3),Cr(1)-P(3) = 2.3773(10), Cr(1)-

P(2) = 2.3887(10), Cr(1)-P(4) = 2.4031(10), Al(2)-Cl(1) = 2.200(6), N(1)-Cr(1)-P(3) = 99.68(8), N(2)-Cr(1)-P(3) = 79.57(9), N(1)-Cr(1)-P(2) = 79.03(8), N(2)-Cr(1)-P(2) = 100.37(8), P(3)-Cr(1)-P(2) = 91.18(4), N(2)-Cr(1)-P(1) = 102.34(8), P(3)-Cr(1)-P(1) = 93.80(4), P(2)-Cr(1)-P(1) = 157.27(4), N(1)-Cr(1)-P(4) = 102.61(8), N(2)-Cr(1)-P(4) = 78.13(9), P(2)-Cr(1)-P(4) = 93.21(4), P(1)-Cr(1)-P(4) = 90.54(4), Al(2)-Cl(1)-Al(1) = 120.2(2).

Complexes **3.3-3.7** were tested for oligomerization activity. Catalytic runs were performed in toluene by using crystalline samples of the complexes and at temperatures of 110 ^{o}C. No activity was observed when methylcyclohexane and DMAO were used, most likely due to the very sparse solubility. Instead, when activated with MAO in toluene, all these species produced distributions of oligomers. The presence of 1-butene and the distribution fits reasonably with a S-F behavior. The modest excess in either 1-octene or 1-hexene observed in entry 1, 2 and 3, suggests that a redox mechanism involving Cr(I)/Cr(III) might also operate to a minor extent and in parallel during the cycle. We are unable to explain the lower than expected amount if 1-hexene observed in entry 3. The fact that the monovalent **3.7** is catalytically inactive does not counter this argument. The lack of reactivity is certainly due to the encapsulation of the metal center which, albeit allows the isolation and characterization of a monovalent derivative, does not permit any further activation.

Table 3.3. Ethylene catalyzed oligomerization reactions of **3.3** and **3.7**.[a]

Entry	Catalyst	Alkenes (g)	Activity (g/((g of Cr) h))	Linear alpha olefins (mol %)								
				C_4	C_6	C_8	C_{10}	C_{12}	C_{14}	C_{16}	C_{18}	α_{av}
1	**3.3**	3	4125	67	20.2	8.7	5.0	2.8	1.6	0.9	0.5	0.56
2	**3.4**	6	9625	46	29.1	14.1	6.2	4.0	2.3	1.0	0.5	0.46
3	**3.5**	2	2750	38	28.1	17.3	9.2	4.0	2.0	1.0	0.4	0.50
4	**3.6**	3	4125	40	34.3	15.2	6.1	3.4	1.0	0.5	0.5	0.45

[a]Conditions: 100 mL of toluene, loading 20 µmol of catalyst, reaction temperature 110 ^{o}C, 40 bar of ethylene, reaction time 30 min, (Al:Cr) MAO = 500.

3.5 Conclusions

In conclusion, we have herein reported the isolation and characterization of chromium complexes and organochromium/aluminate complexes of a pincer diphosphino-pyridine ligand. All the complexes were catalytically active producing desirable, S-F distributions of oligomers free of insoluble materials. The fact that not even traces of polymers may be visible possibly suggests that the trivalent state does not last the activation process and does not participate in the redox dynamism. In one case it was possible to isolate a monovalent species thus confirming that this oxidation state may indeed be part of the catalytic cycle. The fact that complex **3.7** is not catalytically active does not counterargument the involvement of monovalent chromium in the selective portion of the catalytic cycle. The excessive stabilization of the monovalent **3.7** via abstraction of one additional ligand and cationization, simply results in the encapsulation of the metal center providing a stabilizing octahedral ligand field which prevents further activation.

References

(1) (a) Alpha Olefins (02/03-4), PERP Report, Nexant Chem Systems; (b) Vogt, D. Oligomerization of ethylene to higher linear R-olefins. In *Applied Homogeneous Catalysis with Organometallic Compounds*; Cornils, B., Herrmann, W. A., Eds.; Wiley-VCH: Weinheim, Germany, 2000; Chapter 2, pp 245-258. (c) Lappin, G. R.; Sauer, J. D. In *Alpha Olefins Application Handbook*; Marcel Dekkers: New York, 1989; Vol. 37, pp 1-3.

(2) McGuinness, D. *Chem. rev.* **2011**, *111*, 2321 and references cited therein.

(3) (a) Peitz, S.; Peulecke, N.; Aluri, B. R.; Hansen, S.; Müller, B. H.; Spannenberg, A.; Rosenthal, U.; Al-Hazmi, M. H.; Mosa, F. M.; Wöhl, A.; Müller, W. *Eur. J. Inorg. Chem.* **2010**, 1167. (b) Zhang, J.; Braunstein, P.; Hor, T. S. A. *Organometallics* **2008**, *27*, 4277. (c) Bluhm, M. E.; Walter, O.; Döring, M. *J. Organomet. Chem.* **2005**, *690*, 713. (d) McGuinness, D. S.; Wasserscheid, P.; Morgan, D. H.; Dixon, J. T. *Organometallics* **2005**, 24, 552. (e) McGuinness, D. S.; Wasserscheid, P.; Keim, W.; Hu, C.; Englert, U.; Dixon, J. T.; Grove, C. *Chem.Commun.* **2003**, 334. (f) McGuinness, D. S.; Wasserscheid, P.; Keim, W.; Morgan, D. H.; Dixon, J. T.; Bollmann, A.; Maumela, H.; Hess, F. M.; Englert, U. *J. Am. Chem. Soc.* **2003**, *125*, 5272. (g) Morgan, D. H.; Schwikkard, H.; Dixon, J. T.; Nair, J. J.; Hunter, R. *Adv. Synth. Catal.* **2003**, *345*, 939. (h) Carter, A.; Cohen, S. A.; Cooley, N. A.; Murphy, A.; Scutt, J.; Wass, D. F. *Chem.Commun.* **2002**, 858. (i) Köhn, R. D.; Haufe, M.; Mihan, S.; Lilge, D. *Chem. Commun.* **2000**, 1927. (j) Köhn, R. D.; Haufe, M.; Kociok-Köhn, G.; Grimm, S.; Wasserscheid, P.; Keim, W. *Angew. Chem. Int. Ed.* **2000**, *39*, 4337.

(4) (a) Bhaduri, S.; Mukhopadhyay, S.; Kulkarni, S. A. *J. Organomet. Chem.* **2009**, *694*, 1297. (b) Budzelaar, P. H. M. *Can. J. Chem.* **2009**, *87*, 832. (c) Jabri, A.; Mason, C. B.; Sim, Y.; Gambarotta, S.; Burchell, T. J.; Duchateau, R. *Angew. Chem. Int. Ed.* **2008**, *47*, 9717. (d) Agapie, T.; Labinger, J. A.; Brecaw, J. E. *J. Am. Chem. Soc.* **2007**, *129*, 14281. (e) Wass, D. *Dalton Trans.* **2007**, 816. and references therein. (f) van Rensburg, W. J.; Berg, J.-A.; Steynberg, P. J. *Organometallics* **2007**, *26*, 1000. (g) Bowen, L. E.; Haddow, M. F.; Orpen, A. G.; Wass, D. *Dalton Trans.* **2007**, 1160. (h) Elowe, P. R.; McCann, C.; Pringle, P. G.; Spitzmesser, S. K.; Bercaw, J. E. *Organomeallics* **2006**, *25*, 5255. (i) Temple, C.; Jabri, A.; Crewdson, P.; Gambarotta, S.; Korobkov, I.; Duchateau, R. *Angew. Chem. Intl. Ed.* **2006**, *45*, 7050. (j) Jabri, A.; Temple, C.; Crewdson, P.; Gambarotta, S.; Korobkov, I.; Duchateau, R. *J. Am. Chem. Soc.* **2006**, *128*, 9238. (k) Overett, M. J.; Blann, K.; Bollmann, A.; Dixon, J. T.; Haasbroek, D.; Killian, E.; Maumela, H.; McGuinness, D. S.; Morgan, D. H. *J. Am. Chem. Soc.* **2005**, *127*, 10723. (l) van Rensburg, W. J.; Grove, C.; Steynberg, J. P.; Stark, K. B.; Huyser, J. J.; Steynberg, P. J. *Organometallics* **2004**, *23*, 1207. (m) Agapie, T.; Schofer, S. J.; Labinger, J. A.; Bercaw, J. E. *J. Am. Chem. Soc.* **2004**, *126*, 1304. (n) Briggs, J. R. *Chem. Commun.* **1989**, 674.

(5) (a) Schofer, S. J.; Day, M. W.; Henling, L. M.; Labinger, J. A.; Bercaw, J. E. *Organometallics* **2006**, *25*, 2743. (b) Dixon, J. T.; Green, M. J.; Hess, F. M.; Morgan, D. H. *J. Organomet. Chem.* **2004**, *689*, 3641.

(6) (a) Shaikh, Y.; Albahily, K.; Sutcliffe, M.; Fomitcheva, V.; Gambarotta, S.; Korobkov, I.; Duchateau, R. *Angew. Chem. Int. Ed.* **2012**, *51*, 1366. (b) Dulai, A.; McMullin, C. L.; Tenza, K.; Wass, D. F. *Organometallics* **2011**, *30*, 935. (c) Licciulli, S.; Thapa, I.;

Albahily, K.; Korobkov,I.; Gambarotta, S.; Duchateau, R.; Chevalier, R.; Schuhen, K. *Angew. Chem. Int. Ed.* **2010**, *49*, 9225. (d) Kim, S. K.; Kim, T. J.; Chung, J. H.; Hahn, T. K.; Chae, S. S.; Lee, H. S.; Cheong, M.; Kang, S. O. *Organometallics* **2010**, *29*, 5805. (e) Overett, M. J.; Blann, K.; Bollmann, A.; Villiers, R. de; Dixon, J. T.; Killian, E.; Maumela, M. C.; Maumela, H.; McGuinness, D. S.; Morgan, D. H. *J. Mol. Catal. A* **2008**, *283*, 114. (f) Han, T. K.; Ok, M. A.; Chae, S. S.; S. O. Kang (SK Energy Corporation), WO 2008/088178, 2008. (g) Bollmann, A.; Blann, K.; Dixon, J. T.; Hess, F. M.; Killian, E.; Maumela, H.; McGuinness, D. S.; Morgan, D. H.; Neveling, A.; Otto, S.; Overett, M.; Slawin, A. M. Z.; Wasserscheid, P.; Kuhlmann, S. *J. Am. Chem. Soc.* **2004**, *126*, 14712.

(7) Schuhen, K.; Chevalier, R.; Gambarotta, S.; Licciulli, S.; Thapa, I.; Duchateau, R. PCT Int. Appl. Patent WO 2011085951A1, 2011.

(8) Peitz , S.; Aluri B. R.; Peulecke, N.; Müller, B. H.; Wöhl, A.; Müller, W.; Al-Hazmi M. H.; Mosa, F. M.; Rosenthal, U. C*hem. Eur. J.* **2010**, *16*, 7670.

(9) (a) Thapa, I.; Gambarotta, S.; Duchateau, R.; Kulangara, S. V.; Chevalier, R. *Organometallics* **2010**, *29*, 4080. (b) Albahily, K.; Koç, E.; Al-Baldawi, D.; Savard, D.; Gambarotta, S.; Burchell, T. J.; Duchateau, R. *Angew. Chem. Int. Ed.* **2008**, *47*, 5816.

(10) (a) Peitz, S.; Peulecke, N.; Bernd, H.; Müller, H.; Spannenberg, A.; Drexler, H.-J.; Rosenthal, U.; Al-Hazmi, M. H.; Al-Eidan, K. E.; Wöhl, A.; Müller, W. *Organometallics* **2011**, *30*, 2364. (b) Licciulli, S.; Albahily, K.; Fomitcheva, V.; Korobkov, I.; Gambarotta, S.; Duchateau, R. *Angew. Chem. Int. Ed.* **2011**, *50*, 2346. (c) Agapie, T.; Day, M. W.; Henling, L. M.; Labinger, J. A.; Bercaw, J. E. *Organometallics* **2006**, *25*, 2733. (d) Mohamed, H.; Bollmann, A.; Dixon, J.; Gokul, V.; Griesel, L.; Grove, C.; Hess, F.;

Maumela, H.; Pepler, L. *Appl. Catal., A* **2003**, *255*, 355. (e) Grove, J. J. C.; Mohamed, H. A.; Griesel, L. (Sasol Technology (Pty) Ltd) WO 03/ 004158, 2002. (f) Yoshida, T.; Yamamoto, T.; Okada, H.; Murakita, H. (Tosoh Corporation) US 0035029, 2002. (g) Wass, D. F. (BP Chemicals Ltd) WO 02/04119, 2002. (h) Dixon, J. T.; Wasserscheid, P.; McGuinness, D. S.; Hess, F. M.; Maumela, H.; Morgan, D. H.; Bollmann, A. (Sasol Technology (Pty) Ltd) WO 03053890, 2001. (i) Köhn, R. D.; Haufe, M.; Kociok-Köhn, G.; Grimm, S.; Wasserscheid, P.; Keim, W. *Angew. Chem. Int. Ed.* **2000**, *39*, 4337. (j) Freeman, J. W.; Buster, J. L.; Kundsen, R. D. (Phillips Petroleum Company) US 5,856,257, 1999. (k) Mimura, H.; Aoyama, T.; Yamamoto, T.; Oguri, M.; Koie, Y. (Tosoh Corporation) JP 09268133, 1997. (l) Wu, F. J. (Amoco Corporation) US 5,811,618, 1995. (m) Tanaka, E.; Urata, H.; Oshiki, T.; Aoshima, T.; Kawashima, R.; Iwade, S.; Nakamura, H.; Katsuki, S.; Okanu, T. (Mitsubishi Chemical Corporation) EP 0611743, 1994. (n) Reagan, W. K. (Phillips Petroleum Company) EP 0417477, 1991.

(11) (a) Shaikh, Y.; Gurnham, J.; Albahily, K.; Gambarotta, S.; Korobkov, I. *Organometallics* **2012**, *31*, 7427. (b) van Leeuwen, P. W. N. M.; Clément, N. D.; Tschan, M. J.-L. *Coord .Chem. Rev.* **2011**, *255*, 1499. (c) Agapie, T. *Coord. Chem. Rev.* **2011**, *255*, 861. (d) Peitz, S.; Peulecke, N.; Müller, B. H.; Spannenberg, A.; Drexler, H.-J.; Rosenthal, U.; Al-Hazmi, M. H.; Al-Eidan, K. E.; Wöhl, A.; Müller, W. *Organometallics* **2011**, *30*, 2364. (e) Peitz, S.; Peulecke, N.; Aluri, B. R.; Müller, B. H.; Spannenberg, A.; Rosenthal, U.; Al-Hazmi, M. H.; Mosa, F. M.; Wöhl, A.; Müller, W. *Organometallics* **2010**, *29*, 5263. (f) Aluri, B. R.; Peulecke, N.; Peitz S.; Spannenberg A.; Müller, B. H.; Schulz, S.; Heller, D.; Al-Hazmi, M. H.; Mosa, F. M.; Wöhl, A.; Müller, W.; Rosenthal, U. *Dalton Trans.* **2010**, 7911. (g) Peitz, S.; Peulecke, N.; Aluri, B. R.; Müller, B. H.; Spannenberg, A.;

Rosenthal, U.; Al-Hazmi, M. H.; Mosa, F. M.; Wöhl, A.; Müller, W. *Chem. Eur. J.* **2010**, *16*, 12127. (h) Han, T. K.; Chae, S. S.; Kang, S. O.; Wee, K. R.; Kim, S. K. (SK Energy). Patent WO 2009/022770, 2009. (i) Klemps, C.; Payet, E.; Magna, L.; Saussine, L.; Le Goff, X. F.; Le Floch, P. *Chem. Eur. J.* **2009**, *15*, 8259. (j) Jiang, T.; Zhang, S.; Jiang, X.; Yang, C.; Niu, B.; Ning, Y. *J. Mol. Catal. A: Chem*. **2008**, *279*, 90. (k) Albahily, K.; Al-Baldawi, D.; Gambarotta, S.; Koç, E.; Duchateau, R. *Organometallic*s **2008**, *27*, 5708. (l) Kuhlmann, S.; Blann, K.; Bollmann, A.; Dixon, J. T.; Killian, E.; Maumela, M. C.; Maumela, H.; Morgan, D. H.; Pretorius, M.; Taccardi, N.; Wasserscheid, P. *J. Catal.* **2007**, *245*, 279. (m) Blann, K.; Bollmann, A.; de Bod, H.; Dixon, J. T.; Killian. E.; Nongodlwana, P.; Maumela, M. C.; Maumela, H.; McConnell, A. E.; Morgan, D. H.; Overett, M.; Pretorius, M.; Kuhlmann, S.; Wasserscheid, P. *J. Catal.* **2007**, *249*, 244. (n) Killian, E.; Blann, K.; Bollmann, A.; Dixon, J. T.; Kuhlmann, S.; Maumela, M. C.; Maumela, H.; Morgan, D. H.; Nongodlwana, P.; Overett, M. J.; Pretorius, M.; Höfener, K.; Wasserscheid, P. *J. Mol. Catal. A: Chem.* **2007**, *270*, 214. (o) McGuinness, D. S.; Overett, M.; Tooze, R. P.; Blann, K.; Dixon, J. T.; Slawin, A. M. Z. *Organometallics* **2007**, *26*, 1108. (p) Jabri, A.; Crewdson, P.; Gambarotta, S.; Korobkov, I.; Duchateau, R. *Organometallics* **2006**, 25, 715. (q) Blann, K.; Bollmann, A.; Dixon, J. T.; Hess, F. M.; Killian, E.; Maumela, H.; Morgan, D. H.; Neveling, A.; Otto, S.;Overett, M. J. *Chem. Commun.* **2005**, 622. (r) Crewdson, P.; Gambarotta, S.; Djoman, M.-C.; Korobkov,I.; Duchateau, R. *Organometallics* **2005**, *24*, 5214. (s) Blann, K.; Bolmann, A.; Dixon, J. T.; Hess, F.; Kilian, E.; Maumela, H.; Morgan, D. H.; Neveling, A.; Otto, S.; Overett, M. *Chem. Commun.* **2005**, 620.

(12) Alzamly, A.; Gambarotta, S.; Korobkov, I. *Organometallics* **2013**, *32*, 7107.

(13) (a) Vogt, M.; Rivada-Wheelaghan, O.; Iron, M. A.; Leitus, G.; Diskin-Posner, Y.; Shimon Ljw, Ben-David, Y.; Milstein, D. *Organometallics* **2013**, *32*, 300. (b) Chen, L.; Ai, P.; Gu, J.; Jie, S.; Li, B.-G. *J. Organomet. Chem.* **2012**, *716*, 55. (c) Arashiba, K.; Sasaki, K.; Kuriyama, S.; Miyake, Y. ; Nakanishi, H.; Nishibayashi, Y. *Organometallics* **2012**, *31*, 2035. (d) van der Vlugt, J. I.; Pidko, E. A.; Vogt, D.; Lutz, M.; Spek, A. L.; Meetsma, A. *Inorg. Chem.* **2008**, 47, 4442. (e) Muller, G.; Klinga, M.; Leskela, M.; Rieger, B. *Z. Anorg. Allg. Chem.* **2002**, *628*, 2839.

(14) Collman, J. P.; Kittleman, E. T. *Inorg. Synth.* **1966**, *8*, 149.

(15) Kohler, F. H; rossdorf, W. *Z. Natureforsch. Teil B*, **1977**, *32*, 1026.

CHAPTER 4

Reactivity with Alkyl Aluminum of Chromium Complexes of Pyridine-Containing PNP Ligands: A Unique Case of Redox N-P Bond Cleavage

Part of the results presented in this chapter has been published in

Alzamly, A.; Gambarotta, S.; Korobkov, I. *Organometallics* **2014**, *33*, 1602.

4.1 Introduction

Since its inception, catalytic ethylene oligomerization has steadily attracted the attention of scientists from both the industrial and academic sectors.[1] This topic is even today a surprisingly vibrant field of research, where unveiling the relationship between the nature of the catalytically active species and chemical behavior is central not only to understand but also to guide the search for new and more performing catalytic systems.[2]

As a result of a considerable body of research available, today we know that the combination of chromium with ligand systems containing the P-N functionality[3] is particularly effective, having provided selective tri-[3d,g,4] and tetramerization[3a,b,5] catalysts, potent non-selective oligomerization[6] catalysts and even polymerization[7] systems. Thus, questions arise about the versatility of these complexes and the role played by aluminates during catalyst activation (alkylating, cationizing, etc.). The literature provides a sizeable collection of crystal structures of compounds obtained from the direct interaction between catalyst precursors and activators.[3a,8-13] In addition to straightforward chromium alkylation,[9] the Cr-aluminate interaction features a remarkable variety of transformations such as metal reduction,[10] ligand scrambling,[11] coordination of aluminum residues at both nitrogen and P atom,[9b,12] ligand metallation[9a,13] and multiple coordination.[6a,13] Although solid-state structures are not necessarily representative of the dynamic solution state, they may at least provide some hints about possible features of the catalytically active species, the metal oxidation state[9b,c,14] and the role of the aluminum cocatalysts.

In two recent works,[9a,b] we have introduced a pyridine ring in the PN ligand scaffold and then removed the N donor atoms for the purpose of trapping intermediates, finding that the selectivity of the catalytic cycle and in one case even the ubiquitous presence of polymer could

be substantially affected. The activators attacked those complexes in a variety of modes, resulting in reduction of the metal center to the di- and monovalent state and in one case performing direct ligand metallation at the C atom.[9a,b] In this work, we have examined the classical Sasol PNP[15] scaffold and which came on the scene due to the ability of some of its derivatives to promote selective tri- and tetramerization.[3e,f,4g,h,14h,15,16] We have now connected two such functions to the two *ortho* positions of a central pyridine ring (L1) and examined the reactivity of the chromium derivative with alkyl aluminum. Two alternative modifications of this ligand motif have also been examined, (L2 and L3) where the tether of pyridine moiety to the central N of the PNP system was modified and the impact on catalytic behavior analyzed.

4.2 Experimental Section

All reactions were carried out under inert atmosphere using Schlenk techniques or in a purified nitrogen-filled drybox. Solvents were dried using a purification system composed of aluminum oxide. GC-MS analysis of the oligomers was carried out with a Hewlett-Packard HP 5973 gas chromatograph using an Agilent DB1 column and dual FID and MS detector. Elemental analysis was carried out with a PerkinElmer 2400 CHN analyzer. Magnetic susceptibility measurements were performed with a Johnson Matthey balance at room temperature. The samples were powdered and weighed inside a drybox and transferred to sealed and calibrated tubes for measurements. NMR spectra were recorded on Varian Mercury 400 MHz spectrometer at 300 K. Infrared spectra were recorded on an ABB Bomem FTIR instrument from Nujol mulls prepared in a VAC drybox. All chemical reagents were purchased from commercial sources and used as received. Diethyl aluminum chloride and triethyl aluminum were purchased from Strem and used as received. Methylaluminoxane (MAO, 20% in toluene) was purchased from Albemarle Corporation. TMA-depleted methylaluminoxane

(DMAO) was prepared by removing all the volatiles from MAO *in vacuo* (2 mmHg) and with moderate heating (40 °C) for 6 hours. Ligands 2,6-$[(Ph_2)_2PN]_2C_5H_3N$,[17] $PyN(CH_2PPh_2)_2$,[18] and $(Ph_2P)_2NCH_2Py$,[19] as well as $CrCl_3(THF)_3$[20] were prepared according to literature procedures.

Preparation of {2,6-$[(Ph_2)_2PN]_2C_5H_3N$}$CrCl_3.THF_{2.5}$ (4.1)

A solution of $CrCl_3(THF)_3$ (0.37 g, 1.0 mmol) in THF (15 mL) was added to a solution of a 2,6-$[(Ph_2)_2PN]_2C_5H_3N$ ligand (0.84 g, 1.0 mmol) also in THF (5 mL). The color of the solution immediately changed to reddish brown. The solution was allowed to stand for 3 days at room temperature, after which, reddish brown crystals of **4.1** were obtained (0.67 g, 0.66 mmol, 66%). μ_{eff} = 3.74 μ_B. Elemental Analysis % calculated for $C_{63}H_{63}Cl_3CrN_3O_{2.5}P_4$ (found): C, 63.39 (62.63); H, 4.32 (4.28); N, 4.18 (4.11).

Preparation of {2,6-$(Ph_2PNH)[(Et_2ClAl)NPPh_2]C_5H_3N$}$CrCl(PEtPh_2).(toluene)_{0.5}$ (4.2)

A solution of 2,6-$[(Ph_2)_2PN]_2C_5H_3N$ ligand (0.84 g, 1.0 mmol) in toluene (10 mL) was treated with $CrCl_3(THF)_3$ (0.37 g, 1.0 mmol). The mixture was stirred at room temperature overnight. After the mixture was cooled to -40 ^oC, triethylaluminum (0.57 g, 5.0 mmol) was added dropwise and the suspension stirred for 30 min. After reaching room temperature, the suspension was centrifuged and the supernatant concentrated, layered with heptanes (5 mL) and stored in a freezer at -40 ^oC for 3 days. The resulting reddish brown crystals were filtered, washed with cold hexanes (10 mL), dried *in vacuo*, affording **4.2** (0.68 g, 0.76 mmol, 76%). μ_{eff} = 4.89μ_B. Elemental Analysis % calculated for $C_{48.75}H_{51}AlCl_2CrN_3P_3$ (found): C, 62.81 (62.31); H, 5.5 (5.45); N, 4.68 (4.63). IR (Nujol): ν_{N-H}= 3195 cm^{-1}

Preparation of {2,6-$(Ph_2PNH)[(EtCl_2Al)NPPh_2]C_5H_3N$}$CrCl(PEtPh_2).(toluene)_{0.5}$ (4.3)

A solution of 2,6-$[(Ph_2)_2PN]_2C_5H_3N$ ligand (0.84 g, 1.0 mmol) in toluene (10 mL) was treated with $CrCl_3(THF)_3$ (0.37 g, 1.0 mmol). The mixture was stirred at room temperature overnight. After the mixture was cooled to -40 ^oC, diethylaluminum chloride (0.605, 5.0 mmol) was added dropwise and the suspension stirred for 30 min. After reaching room temperature, the suspension was centrifuged and the supernatant concentrated, layered with heptanes (5 mL) and stored in a freezer at -40 ^oC for 3 days. The resulting reddish brown crystals were filtered, washed with cold hexanes (10 mL), dried *in vacuo*, affording **4.3** (0.27 g, 0.31 mmol, 30%). μ_{eff} = 4.81 μ_B. Elemental Analysis % calculated $C_{48.5}H_{48}AlCl_3CrN_3P_3$ for (found): C, 59.71 (59.11); H, 4.90 (4.86); N, 4.64 (4.60). IR (Nujol): ν_{N-H}= 3225 cm^{-1}

Preparation of $PyN(CH_2PPh_2)_2CrCl_3THF.(THF)_2$ (4.4)

A solution of $CrCl_3(THF)_3$ (0.37 g, 1.0 mmol) in THF (15 mL) was added to a solution of $PyN(CH_2PPh_2)_2$ (0.49 g, 1.0 mmol) in the same solvent (5 mL). The color of the solution immediately changed to dark-green. Green crystals of **4.4** were obtained by slow evaporation (0.47 g, 0.6 mmol, 65%). μ_{eff} = 3.88 μ_{BM}. Elemental Analysis calculated for $C_{43}H_{52}Cl_3CrN_2O_3P_2$ (found): C 58.39 (57.95), H 4.90 (4.85), N 3.89 (3.85).

Preparation of $(Ph_2P)_2NCH_2PyCrCl_3THF$ (4.5)

A Solution of $(Ph_2P)_2NCH_2Py$ (0.48 g, 1.0 mmol) in dichloromethane (10 mL) was treated with $CrCl_3(THF)_3$ (0.37 g, 1.0 mmol). The mixture was stirred at room temperature overnight. The resulting dark blue solution was centrifuged and kept at -40 ^oC. The resulting blue crystals of **4.5** were filtered, washed with cold hexanes (10 mL), dried *in vacuo* (0.44g, 0.62 mmol, 62%). μ_{eff} = 3.87 μ_{BM}. Elemental Analysis calculated for $C_{34}H_{34}Cl_3CrN_2OP_2$ (found): C 57.85 (57.56), H 4.71 (4.67), N 3.97 (3.93).

Preparation of $[Me_3AlPyCH_2N(PPh_2)_2Cr(\mu\text{-}Cl)AlMe_2(\mu\text{-}Cl)AlMe_3]_2(\mu\text{-}Cl)_2$ (4.6)

A solution of $(Ph2P)_2NCH_2Py$ (0.48 g, 1.0 mmol) in toluene (10 mL) was treated with $CrCl_3(THF)_3$ (0.37 g, 1.0 mmol). The mixture was stirred at room temperature overnight. After cooling to -40 ^oC, trimethylaluminum (0.22 g, 3.0 mmol) was added dropwise and the mixture stirred for 30 min. After reaching room temperature, the suspension was centrifuged and the supernatant concentrated and layered with hexanes (3 mL) and stored in a freezer at -40 ^oC for 3 days. The resulting green crystals of **4.6** were filtered, washed with cold hexanes (10 mL), dried *in vacuo*, (0.33 g, 0.19 mmol, 19%). μ_{eff} = 4.85 μ_{BM} per Cr. Elemental Analysis calculated for $C_{76}H_{100}Al_6Cl_6Cr_2N_4P_4$ (found): C, 54.49 (53.94); H, 6.03 (5.96); N, 3.35 (3.30).

4.3 X-Ray Data

Table 4.1. Crystal Data and Structure Analysis Results of Complexes **4.1-4.6**.

	4.1	**4.2**	**4.3**
Formula	$C_{63}H_{63}Cl_3CrN_3O_{2.5}P_4$	$C_{48.75}H_{51}AlCl_2CrN_3P_3$	$C_{47.45}H_{46.80}AlCl_3CrN_3P_3$
FW, gmol^{-1}	1184.39	921.71	937.32
Space group	Triclinic, P-1	Triclinic, P-1	Monoclinic, P 21/c
***a* (Å)**	10.3183(4)	12.634(3)	16.004(4)
***b* (Å)**	12.5463(5)	13.792(3)	16.615(4)
***c* (Å)**	24.2213(10)	15.021(3)	19.488(5)
α, (deg)	86.477(2)	81.438(8)	90
β, (deg)	88.342(2)	68.115(8)	93.209(9)
γ, (deg)	73.417(2)	83.586(8)	90
***V* (Å^3)**	2999.3(2)	2397.3(8)	5174(2)
Z	2	2	4
Radiation	0.71073	0.71073	0.71073
T (K)	200(2)	200(2)	200(2)
D_{calcd} (mg/m^3)	1.311	1.277	1.203
μ_{calcd} (mm^{-1})	0.477	0.504	0.519
***F*$_{000}$**	1234	961	1942
***R*, *Rw*^{2a}**	0.0767, 0.1910	0.1172, 0.1202	0.0778, 0.1643
GoF	1.015	1.039	1.075

	4.4	**4.5**	**4.6**
Formula	$C_{43}H_{52}Cl_3CrN_2O_3P_2$	$C_{34}H_{34}Cl_3CrN_2OP_2$	$C_{76}H_{100}Al_6Cl_6Cr_2N_4P_4$
FW, gmol^{-1}	865.16	706.92	1670.27
Space group	Monoclinic, P2(1)/n	Orthorhombic, Pbca	Triclinic, P-1
***a* (Å)**	11.5113(6)	15.7846(15)	11.2745(8)
***b* (Å)**	19.3069(7)	18.8213(18)	12.3363(9)
***c* (Å)**	19.1839(8)	21.936(2)	16.9833(12)
α, (deg)	90	90	97.223(4)
β, (deg)	93.596(3)	90	100.703(4)
γ, (deg)	90	90	98.1365(5)
***V* (Å^3)**	4255.2(3)	6517.0(11)	2269.4(3)
Z	4	8	1
Radiation	0.71073	0.71073	0.71073
T (K)	200(2)	200(2)	200(2)
D_{calcd} (mg/m^3)	1.350	1.441	1.222
μ_{calcd} (mm^{-1})	0.573	0.726	0.566
***F*$_{000}$**	1812	2920	870
***R*, *Rw*^{2a}**	0.1327, 0.1094	0.0479, 0.0967	0.0901, 0.1653
GoF	1.003	1.005	1.165

[a] $R = \Sigma|F_o| - |F_c|/\Sigma|F_o|$, $Rw = [\Sigma(|F_o| - |F_c|)2/\Sigma wF_o2]^{1/2}$

4.4 Results and Discussion

The 2,6-$[(Ph_2)_2PN]_2C_5H_3N$ **(L1)** ligand was prepared according to a literature procedure.[17] Its reaction with $CrCl_3(THF)_3$ in THF afforded the corresponding adduct {2,6-$[(Ph_2)_2PN]_2C_5H_3N$} $CrCl_3.THF_{2.5}$ **(4.1)** (Scheme 4.1).

Scheme 4.1

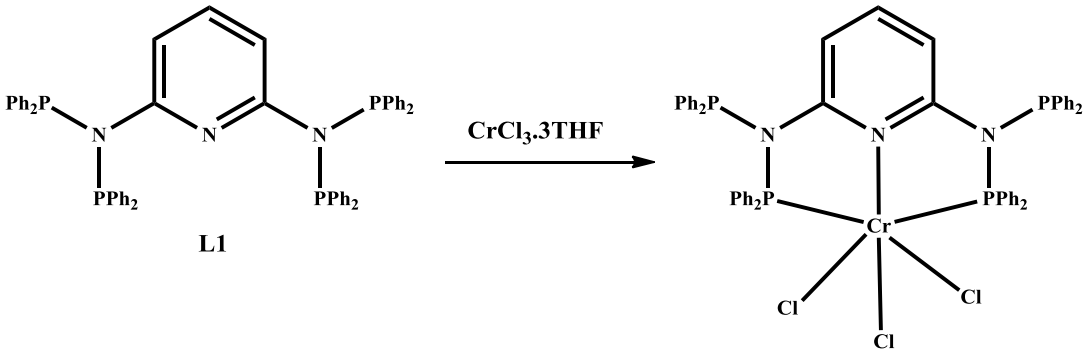

The X-ray structure of **4.1** (Figure 4.1) shows a distorted-octahedral trivalent chromium center surrounded by three meridionally placed pyridine nitrogen atom and two phosphorus atoms of the two PNP functions. [Cr(1)-N(2 = 2.091(2) Å; Cr(1)-P(2) = 2.4204(7) Å; Cr(1)-P(4) = 2.4047(7) Å; P(4)-Cr(1)-P(2) = 161.61(3)^o; N(2)-Cr(1)-P(4) = 80.66(6)^o N(2)-Cr(1)-P(2) = 81.38(6)^o]. The three chlorine atoms occupy the three remaining positions [Cr(1)-Cl(2) = 2.2823(8) Å; Cr(1)-Cl(1) = 2.3089(8) Å; Cr(1)-Cl(3) = 2.3173(8) Å; Cl(2)-Cr(1)-Cl(3) = 95.79(3)^o; Cl(1)-Cr(1)-Cl(3) = 171.17(3)^o; Cl(2)-Cr(1)-Cl(1) = 92.86(3)^o].

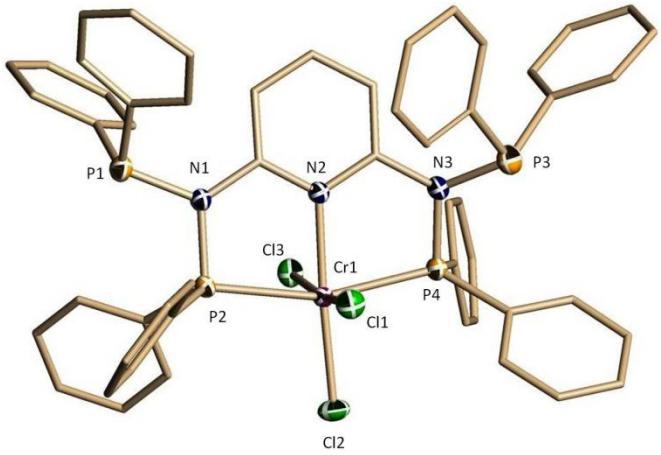

Figure 4.1. Thermal ellipsoid plot of **4.1** with ellipsoids drawn at 50% probability level. Selected bond distances (Å) and angles (deg) for **4.1**: N(1)-C(1) = 1.415(3), N(1)-P(2) =1.727(2), N(1)-P(1) = 1.757(2), N(3)-P(4) = 1.725(2), N(3)-P(3) = 1.782(3), P(2)-N(1)-P(1) = 114.39(12), P(4)-N(3)-P(3) = 119.84(14), N(1)-P(2)-Cr(1) = 98.29(7), N(3)-P(4)-Cr(1) = 98.38(8).

Since the PNP-based catalytic systems have always shown interesting activity upon activation with methylaluminoxane,[14-16] complex **4.1** was also activated in a similar manner. Different from the Sasol systems, however, only an average activity as nonselective ethylene oligomerization was found in this case. Moreover, a rather significant amount of solid material was also present in the oligomeric mixtures (Table 4.2). The NMR and GPC analysis showed this solid to consist of narrowly dispersed linear heavy α-olefins. On the ground of previous observations,[9a,b] we tentatively suggest that this behavior might be ascribed to the chelating, pincer-type geometry adopted by the ligand system, which might provide high stability to the square-planar divalent state of intermediate chromium species.

Table 4.2. Ethylene catalyzed oligomerization reactions of **4.1-4.3**.[a]

Catalyst	Alkenes (g)	PE (g)	M_n (g mol^{-1})	Activity (g/((g of Cr) h))	Linear Alpha Olefins (mol %)								
					C_4	C_6	C_8	C_{10}	C_{12}	C_{14}	C_{16}	C_{18}	α
4.1	29	4.0	435	59942	5	11	16	17	16	14	11	10	0.79
4.2	28	5.1	449	59308	7	15	18	16	14	12	10	8	0.83
4.3	34	4.4	491	70337	10	20	19	15	12	10	8	6	0.75

[a]Conditions: 100mL of toluene, loading 20 μmol of catalyst, reaction temperature 80 ˚C, 40 bar of ethylene , reaction time 30 min, 500 (Al:Cr) MAO.

With the ultimate goal of isolating catalytically active species and to verify the above hypothesis, we have reacted complex **4.1** with different alkyl aluminum activators. As it is often the case, MAO gave only oily and ill-defined materials. However, in the case of treatment with 5 equivalents of Et_3Al, an active oligomerization catalyst formulated as {2,6-(Ph_2PNH) [(Et_2ClAl) $NPPh_2$]C_5H_3N}$CrCl(PEtPh_2)$**.**$(toluene)_{0.5}$ **(4.2)** (Scheme 4.2) was obtained in crystalline form. The utilization of excess aluminate is necessary for the complete consumption of the starting material. The salient features of this suprising complex are: (1) the anticipated reduction from the tri- to the divalent state, (2) the removal of a phosphino residue from each of the two original PNP ligands, (3) the protonation of one nitrogen atom, (4) the retention of the aluminate residue at the remaining deprotonated N atom, and (5) the coordination at the chromium atom of *in situ*-generated diphenylethyl phosphine.

Scheme 4.2

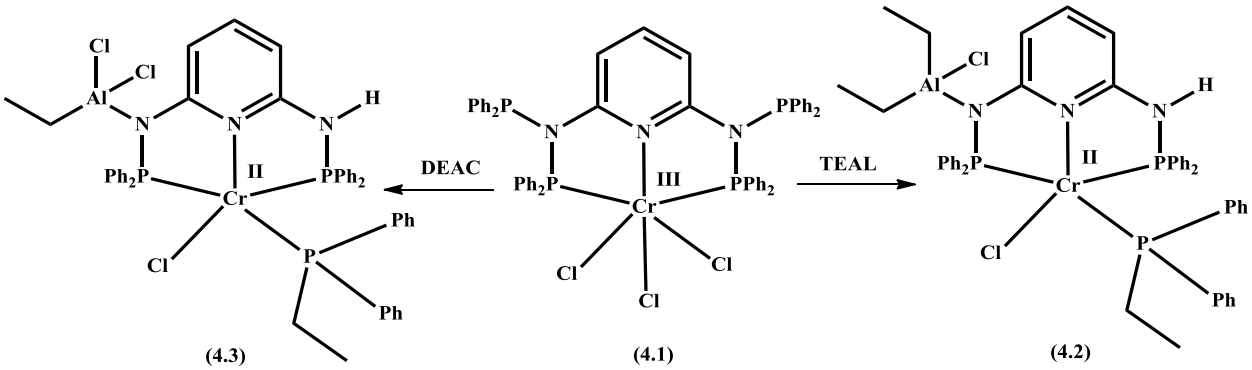

The crystal structure shows the metal center in a distorted trigonal bipyramidal environment (Figure 4.2) [N(1)-Cr(1)-P(1) = 77.87(9)^{o}, N(1)-Cr(1)-P(2) = 76.20(9)^{o}, Cl(1)-Cr(1)-P(3) = 93.12(5)^{o}, N(1)-Cr(1)-P(3) = 98.85(9)^{o}]. The pyridine nitrogen atom and the chlorine atom are at the apical positions [Cr(1)-N(1) = 2.103(3)Å, Cr(1)-Cl(1) = 2.3157(13)Å, N(1)-Cr(1)-Cl(1) = 168.03(9)^{o}] while the three P atoms, two from the ligand [Cr(1)-P(2) = 2.4130(13) Å, Cr(1)-P(3) = 2.6303(14)Å] and one from the coordinated Ph_2EtP molecule [Cr(1)-P(1) = 2.4550(13)Å], define the equatorial plane [P(2)-Cr(1)-P(1) = 135.90(5)^{o}, P(1)-Cr(1)-P(3) = 104.43(5)^{o}, P(2)-Cr(1)-P(3) = 114.32(5)^{o}].

Reaction of **4.1** with 5 equivalent of Et_2AlCl (Scheme 4.2) gave the almost identical complex {2,6-$(Ph_2PNH)[(EtCl_2Al)NPPh_2]C_5H_3N$}$CrCl(PEtPh_2)$**.**$(toluene)_{0.5}$ **(4.3)**, the only difference from **4.2** consisting of the presence of two chlorine atoms around Al instead of one (Figure 4.2).

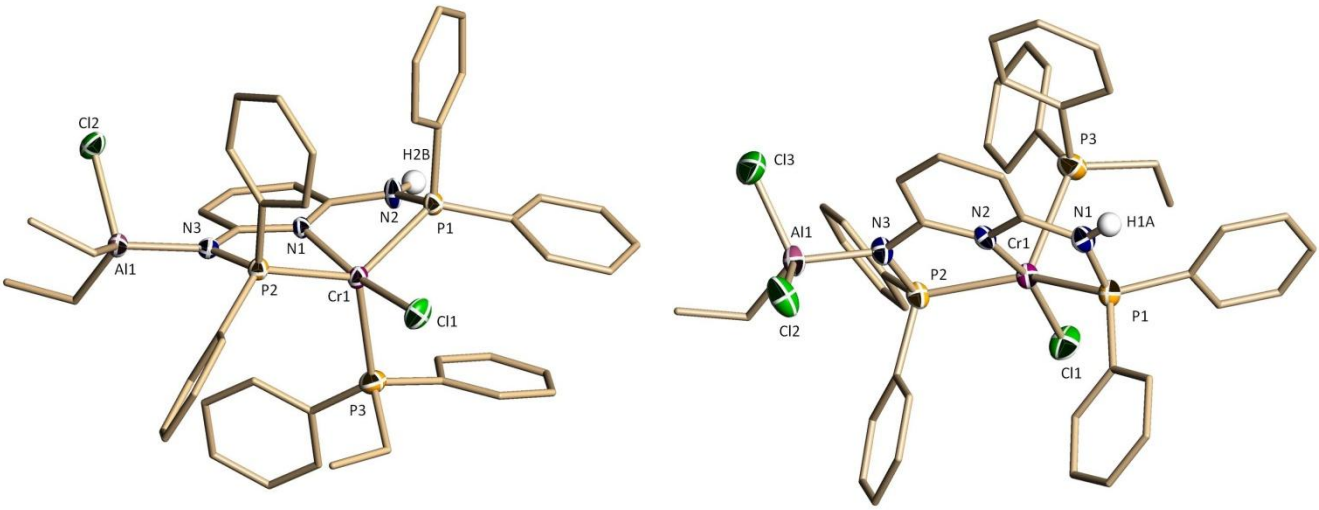

4.2 **4.3**

Figure 4.2. Thermal ellipsoid plot of **4.2** and **4.3** with ellipsoids drawn at 50% probability level. Selected bond distances (Å) and angles (deg) for **4.2**: Al(1)-N(3) = 1.952(3), Al(1)-Cl(2) = 2.2444(16), P(1)-N(2) = 1.690(3), P(2)-N(3) = 1.693(3), N(1)-Cr(1)-Cl(1) = 168.03(9), Cl(1)-Cr(1)-P(2) = 98.82(5), Cl(1)-Cr(1)-P(1) = 99.29(5), N(3)-Al(1)-Cl(2) = 103.68(10), N(2)-P(1)-Cr(1) = 95.61(12), N(3)-P(2)-Cr(1) = 103.47(12), P(2)-N(3)-Al(1) = 122.13(17). Selected bond distances (Å) and angles (deg) for **4.3**: Cr(1)-N(2) = 2.091(3), Cr(1)-Cl(1) = 2.2903(11), Cr(1)-P(2) = 2.4045(11), Cr(1)-P(1) = 2.4348(11), Cr(1)-P(3) = 2.6471(12), Al(1)-N(3) = 1.920(3), N(1)-P(1) = 1.686(3), N(3)-P(2) = 1.695(3), N(2)-Cr(1)-Cl(1) = 64.37(8), N(2)-Cr(1)-P(2) = 76.91(7), Cl(1)-Cr(1)-P(2) = 97.14(4), N(2)-Cr(1)-P(1) = 79.66(8), Cl(1)-Cr(1)-P(1) = 97.29(4), P(2)-Cr(1)-P(1) = 141.35(4), N(2)-Cr(1)-P(3) = 94.38(8), Cl(1)-Cr(1)-P(3) = 101.17(4), P(2)-Cr(1)-P(3) = 116.83(4), P(1)-Cr(1)-P(3) = 95.12(4), N(1)-P(1)-Cr(1) = 95.62(10), N(3)-P(2)-Cr(1) = 103.57(10). N(3)-Al(1)-Cl(3) = 108.52(10), N(3)-Al(1)-Cl(2) = 107.70(10), Cl(3)-Al(1)-Cl(2) = 106.11(6), P(2)-N(3)-Al(1) = 120.27(15).

The formation of the two complexes is the result of a nontrivial transformation. A possible rationalization for the formation of **4.2** and **4.3** is offered in Scheme 4.3. The preliminary step may be regarded as a three-center metathetic attack performed by one aluminate alkyl group, which alkylates the P atom (forming $EtPPh_2$) and extracts one chlorine atom from

chromium to retain electroneutrality. The resulting anionic nitrogen becomes thus available for coordinating an intact aluminate molecule. The elimination of the second phosphino residue and its replacement by an H atom is also accompanied by reduction of the chromium center to the divalent state.

This might be explained by assuming alkylation at the Cr center and formation of a Cr-Et group, which does not perform reduction via a standard homolytic splitting of the Cr-C bond. Instead, β-hydrogen transfer atom from the ethyl group to nitrogen may produce the final complex by eliminating ethylene and, conceivably, diphosphine. We could not find conclusive evidence for the presence of diphosphine but its strong coordinating power might generate other ill-defined chromium containing species. However, we detected a small amount of ethylene in the reaction mother liquor, thus lending some support to the suggested rationalization.

Scheme 4.3

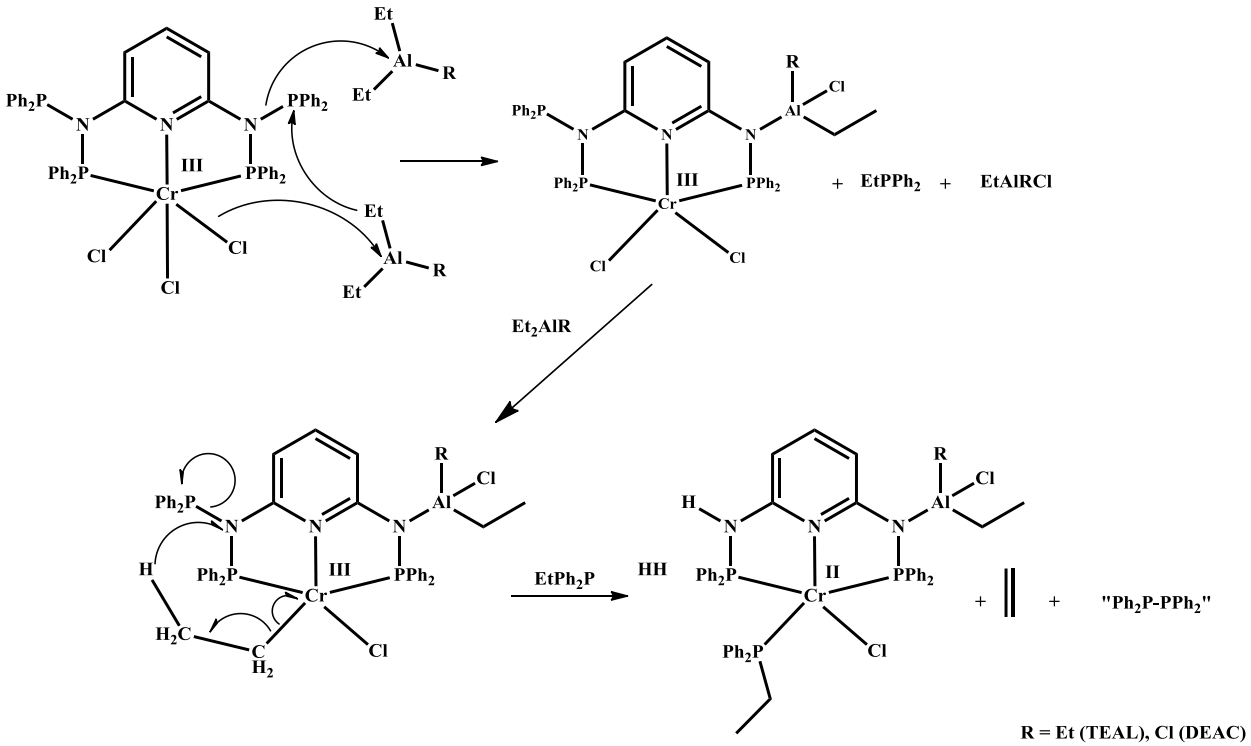

Complexes **4.2** and **4.3** display a catalytic behavior rather similar to that of **4.1,** affording sort of S-F distributions of oligomers, polluted by substantial amount of solid material, and surprisingly low in 1-hexene. The lack of 1-hexene is not easily explained, and the linearity of the polymeric material excludes its incorporation. Questions arise about this strange oligomer distribution. A conventional linear chain growth mechanism should not lead to the present short-chain distribution with C8 > C6 > C4. This leaves us with a ring expansion mechanism as possibly responsible for the formation of this anomalous distribution. On the other hand, chromium is able to interconvert among several oxidation states while in the presence of aluminates.[21]In such event, several catalytically active species might be at work, in the end producing a complex distribution. We have previously noticed this behavior in two related systems and whose common ligand motif was the incorporation of either a pyridine ring as a part of the NP scaffold[9a] or of an aromatic ring in a regular pincer di-phoshphine system.[9b]

In an attempt to evaluate the possibility that ligand fragmentation could be a general behavior for the PNP Sasol's scaffold, we have introduced two modifications. In the first we have placed a -CH_2- spacer between the P and central N atom. The $PyN(CH_2PPh_2)_2$ ligand **(L2)** was prepared according to a literature procedure.[18] The reaction of $CrCl_3(THF)_3$ in THF with **L2** afforded the corresponding complex $PyN(CH_2PPh_2)_2\ CrCl_3THF.(THF)_2$ (**4.4**) in crystalline form (Scheme 4.4). The simple adduct structure was confirmed by X-ray analysis. showing a distorted-octahedral geometry, as defined by the two phorphorus donor atoms of the ligand [(Cr(1)-P(1) = 2.4794(10)Å, Cr(1)-P(2) = 2.5129(10)Å, P(1)-Cr(1)-P(2) = 86.92(3)^o], three chlorine [(Cr(1)-Cl(3) = 2.2860(10)Å, Cr(1)-Cl(2) = 2.2997(9)Å, Cr(1)-Cl(1) = 2.3342(9)Å, Cl(3)-Cr(1)-Cl(2) = 92.54(4)^o, Cl(2)-Cr(1)-Cl(1) = 94.02(4)^o, Cl(3)-Cr(1)-Cl(1) = 173.42(4)^o]

and one THF molecule [Cr(1)-O(1) = 2.091(2)Å, O(1)-Cr(1)-P(1) = 177.64(7)^{o}, O(1)-Cr(1)-P(2) = 91.45(7)^{o}] (Figure 4.3).

Scheme 4.4

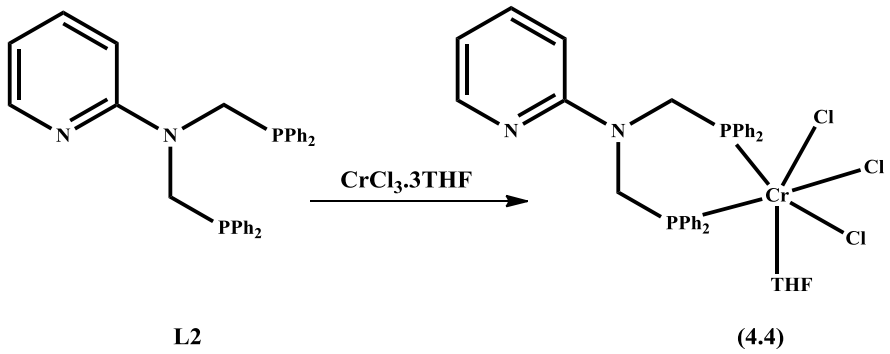

L2 **(4.4)**

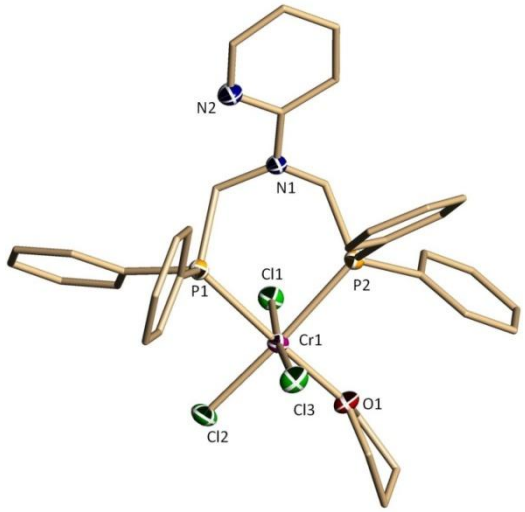

Figure 4.3. Thermal ellipsoid plot of **4.4** with ellipsoids drawn at 50% level. Selected bond lengths (Å) and angles (deg) for **4.4**: O(1)-Cr(1)-Cl(3) = 88.38(7), O(1)-Cr(1)-Cl(2) = 91.02(7), O(1)-Cr(1)-Cl(1) = 91.02(7), Cl(3)-Cr(1)-P(1) = 93.34(3), Cl(2)-Cr(1)-P(1) = 90.51(3), Cl(1)-Cr(1)-P(1) = 87.09(3), Cl(3)-Cr(1)-P(2) = 91.03(3), Cl(2)-Cr(1)-P(2) = 175.72(4), Cl(1)-Cr(1)-P(2) = 82.43(3).

In a second modification, the –CH_2- spacer was placed between the PNP-s nitrogen atom and the pyridine ring. The ligand $PyCH_2Ph_2PNPPh_2$ ligand **(L3)** was prepared according to a literature procedure.[19] The reaction of **L3** with $CrCl_3(THF)_3$ in THF, afforded the expected

adduct $(Ph_2P)_2NCH_2PyCrCl_3THF$ (**4.5**) (Scheme 4.5). Complex **4.5** exhibits a distorted-octahedral geometry as defined by the N and P donor atoms of the ligand [Cr(1)-N(2) = 2.1255(15)Å, Cr(1)-P(1) = 2.4366(5)Å, N(2)-Cr(1)-P(1) = 91.41(4)^o], three chlorine atoms (Cr(1)-Cl(3) = 2.2959(6), Cr(1)-Cl(2) = 2.3047(6)Å, Cr(1)-Cl(1) = 2.3247(5)Å, Cl(3)-Cr(1)-Cl(2) = 93.04(2)^o, Cl(3)-Cr(1)-Cl(1) = 94.04(2)^o, Cl(2)-Cr(1)-Cl(1) = 172.72(2)^o] and one THF molecule [Cr(1)-O(1) = 2.0991(13)Å, O(1)-Cr(1)-N(2) = 92.42(6)^o, O(1)-Cr(1)-P(1) = 175.47(4) ^{o}] (Figure 4.4).

Scheme 4.5

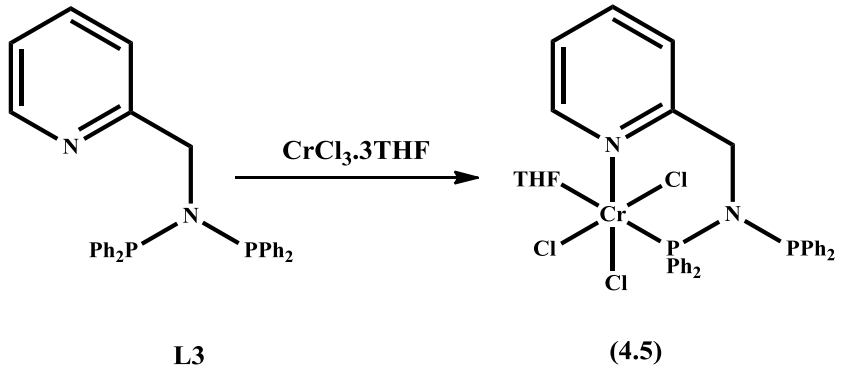

L3 **(4.5)**

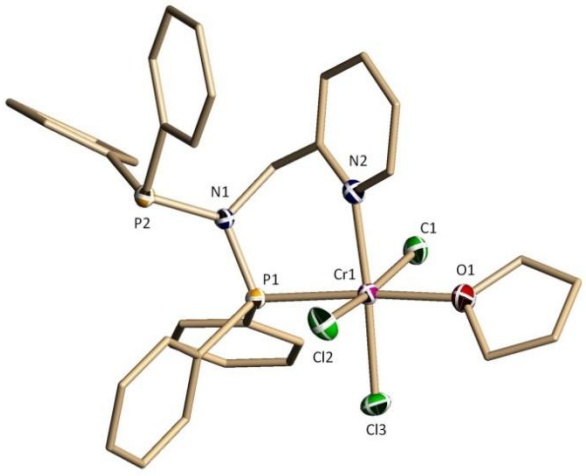

Figure 4.4. Thermal ellipsoid plot of **4.5** with ellipsoids drawn at 50% level. Selected bond lengths (Å) and angles (deg) for **4.5**: P(1)-N(1) = 1.7007(14), O(1)-Cr(1)-Cl(3) = 91.58(4), N(2)-Cr(1)-Cl(3) = 176.00(4), O(1)-Cr(1)-Cl(2) = 88.67(4), N(2)-Cr(1)-Cl(2) = 86.98(4O (1)-Cr(1)-

Cl(1) = 89.45(4), N(2)-Cr(1)-Cl(1) = 86.08(4), Cl(3)-Cr(1)-P(1) = 84.592(19),Cl(2)-Cr(1)-P(1) = 89.117(19), Cl(1)-Cr(1)-P(1) = 93.221(19), N(1)-P(1)-Cr(1) = 106.17(5), P(1)-N(1)-P(2) = 127.5 2(8).

When the trivalent complex **4.5** was treated with 5 equivalents of TMA, a dimetallic and Octanuclear complex **4.6** $[Me_3AlPyCH_2N(PPh_2)_2Cr(\mu\text{-}Cl)AlMe_2(\mu\text{-}Cl)AlMe_3](\mu\text{-}Cl)_2$ was obtained (Scheme 4.6) also in crystalline form. The geometry around each chromium is distorted square-pyramidal with two phosphorus [Cr(1A)-P(1) = 2.472(3)Å, Cr(1A)-P(2) = 2.481(3)Å, P(1)-Cr(1A)-P(2) = 67.45(10)^o] donor atoms of the ligand and two bridging chlorine atoms [Cr(1A)-Cl(1) = 2.359(3)Å, Cl(1)-Cr(1A)-P(1) = 163.36(13)^o, Cl(1)-Cr(1A)-P(2) = 100.25(11)^o] occupying the basal plane. The remaining chlorine atom, connected to the dinuclear aluminate residue occupies the axial position [Cr(1A)-Cl(3) = 2.579(4)Å, P(1)-Cr(1A)-Cl(3) = 94.08(12)^o, P(2)-Cr(1A)-Cl(3) = 88.29(11)^o] (Figure 4.5).

Scheme 4.6

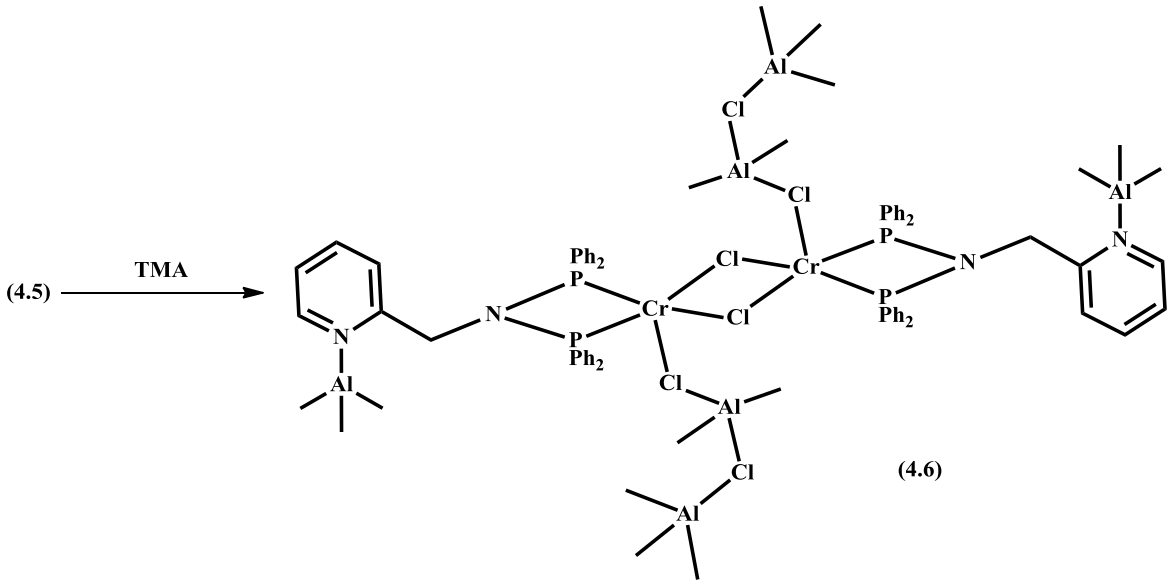

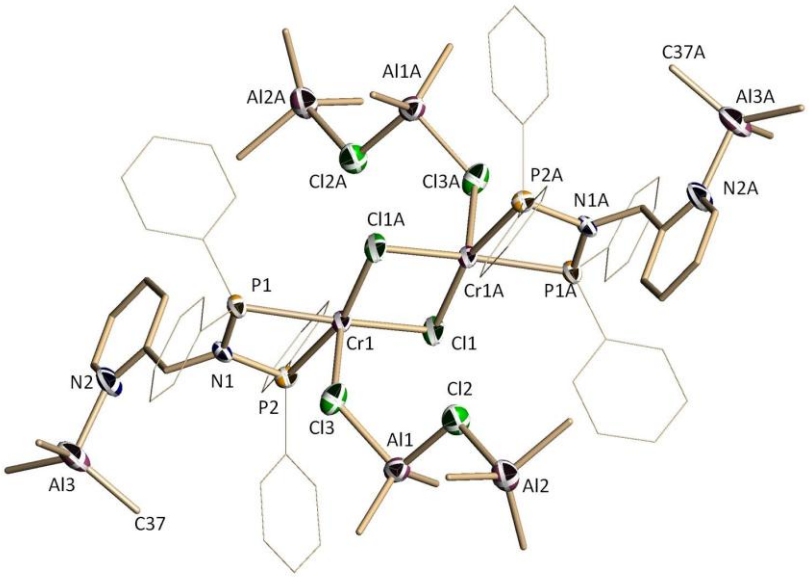

Figure 4.5. Thermal ellipsoid plot of **4.6** with ellipsoids drawn at 50% level. Selected bond lengths (Å) and angles (deg) for **4.6**: Cl(2)-Al(1) = 2.271(5), Cl(2)-Al(2) = 2.431(5), Cl(3)-Al(1) = 2.248(5), P(1)-N(1) = 1.718(8), P(2)-N(1) = 1.692(8), Al(3)-N(2) = 2.071(11), Cl(1)-Cr(1)-Cl(3) = 96.78(13), Al(1)-Cl(2)-Al(2) = 116.0(2), Al(1)-Cl(3)-Cr(1) = 124.67(16), N(1)-P(1)-Cr(1) = 92.3(3), N(1)-P(2)-Cr(1) = 92.7(3), P(2)-N(1)-P(1) = 107.5(5), Cl(4)-Al(3)-N(2) = 104.2(8). Methyl group C(37) is occupationally disordered with Cl atom in the same position with the occupancy split at 70% : 30%, Cl atom omitted for clarity.

Upon activation with MAO and in toluene as a solvent, all complexes showed moderate activity toward ethylene oligomerization with variable amount of polymeric material always present in the oligomeric mixtures (Table 4.3). The oligomer distributions are quite flat but seem to have in 1-octene the main product. Butene is also visible in the reaction mixture thus indicating a chain growth mechanism at least as a significant contributor of the catalytic cycle.

Table 4.3. Ethylene catalyzed oligomerization reactions of **4-6**.[a]

Entry	Catalyst	Alkenes (g)	PE (g)	Activity (g/g Cr . h)	Linear alpha olefins (mol %)								
					C_4	C_6	C_8	C_{10}	C_{12}	C_{14}	C_{16}	C_{18}	α_{av}
1	**4.4**[a]	25	2.0	24471	11	15	17	16	14	11	9	7	0.74
2	**4.5**[a]	24	4.3	50894	10	13	20	16	14	12	9	6	0.75
3	**4.5**[b]	2	10.1	21980	6	29	57	2	2	2	1	1	
4	**4.6**[a]	19	3.8	41683	8	9	15	16	15	14	12	11	0.87
5	**4.6**[b]	1	8.2	17144	8	25	58	3	2	2	1	1	

[a]Conditions: 100mL of solvent, loading 20 μmol of catalyst, 40 bar of ethylene, T = 80 ˚C, [a](Al:Cr) MAO = 500, [a]Solvent = Toluene, [b](Al:Cr) DMAO = 500, [b]Solvent = methylcyclohexane, reaction time 30 min.

When activation of the complexes was attempted in methylcyclohexene no catalytic activity could be detected for **4.4**. Instead complex **4.6** (entry 5) and its precursor **4.5** were catalytically active (entry 3). In both cases, the polymeric material was the main component of the reaction outcome. However, 1-octene stood up as the main product among the light oligomers. The switching of selectivity from a general distribution of oligomers in toluene to a blend of polymerization and rather selective oligomerization in MeCy may be ascribed to two effects simultaneously occurring as a result of the activation. The selective behavior has to be ascribed to the monovalent state and which is normally highly selective and poorly active. On the other hand the regeneration of trivalent chromium through comproportionation is probably affording a highly active and longer living polymerization catalyst. This reasonable hypothesis may well explain the strange distribution. In toluene instead, the poisoning of the monovalent species completely prevents selectivity and introduces a preferential stability for the divalent state, mainly responsible for the observed non-selective behavior.

4.5 Conclusions

In conclusion, we have herein reported the synthesis and characterization of organo-chromium complexes based on three ligand systems containing a combination of pyridine ring and the PNP Sasol ligand motif. The interaction with aluminate activators has been also examined. The outcome of the reaction allows highlighting an unanticipated weakness of the PNP scaffold, which was fragmented to form a phosphine. The reduction of the metal center is instead in line with a trend of reduction of chromium complexes to the divalent state, although the proposed nitrogen-assisted β-hydrogen transfer from the alkyl aluminum is unprecedented.

When using neutral pyridine modified ligands L2 and L3, there was no sign of ligand fragmentation. On the other hand, it was clear that the divalent oxidation state was generated and preserved during catalytic cycles in toluene as a solvent. In Me-Cy instead, selectivity was observed. On the other hand, in case of complexes **4.5** and **4.6**, the presence of visible amount of 1-octene as the most abundant light olefin diagnosed that Cr (I) was generated and stabilized.

References

(1) (a) Alpha Olefins (02/03-4), PERP Report, Nexant Chem Systems; (b) Vogt, D. Oligomerization of ethylene to higher linear α-olefins. In *Applied Homogeneous Catalysis with Organometallic Compounds*; Cornils, B., Herrmann, W. A., Eds.; Wiley-VCH: Weinheim, Germany, 2000; Chapter 2, pp 245-258. (c) Lappin, G. R.; Sauer, J. D. In *Alpha Olefins Application Handbook*; Marcel Dekkers: New York, 1989; Vol. 37, pp 1-3.

(2) McGuinness, D. *Chem. Rev.* **2011**, *111*, 2321, and references cited therein. (b) Dixon, J. T.; Green, M. J.; Hess, F. M.; Morgan, D. H. *J. Organomet. Chem.* **2004**, *689*, 3641.

(3) (a) Shaikh, Y.; Gurnham, J.; Albahily, K.; Gambarotta, S.; Korobkov, I. *Organometallics* **2012**, *31*, 7427. (b) van Leeuwen, P. W. N. M.; Clément, N. D.; Tschan, M. J.-L. *Coord. Chem. Rev.* **2011**, *255*, 1499. (c) Agapie, T. *Coord. Chem. Rev.* **2011**, *255*, 861. (d) Klemps, C.; Payet, E.; Magna, L.; Saussine, L.; Le Goff, X. F.; Le Floch, P. *Chem. Eur. J.* **2009**, *15*, 8259. (e) Kuhlmann, S.; Blann, K.; Bollmann, A.; Dixon, J. T.; Killian, E.; Maumela, M. C.; Maumela, H.; Morgan, D. H.; Pretorius, M.; Taccardi, N.; Wasserscheid, P. *J. Catal.* **2007**, *245*, 279. (f) Killian, E.; Blann, K.; Bollmann, A.; Dixon, J. T.; Kuhlmann, S.; Maumela, M. C.; Maumela, H.; Morgan, D. H.; Nongodlwana, P.; Overett, M. J.; Pretorius, M.; Hofene r, K.; Wasserscheid, P. *J. Mol. Catal. A: Chem.* **2007**, *270*, 214. (g) McGuinness, D. S.; Overett, M.; Tooze, R. P.; Blann, K.; Dixon, J. T.; Slawin, A. M. Z. *Organometallics* **2007**, *26*, 1108.

(4) (a) Peitz, S.; Peulecke, N.; Müller, B. H.; Spannenberg, A.; Drexler, H.-J.; Rosenthal, U.; Al-Hazmi, M. H.; Al-Eidan, K. E.; Wöhl, A.; Müller, W. *Organometallics* **2011**, *30*, 2364. (b) Peitz, S.; Peulecke, N.; Aluri, B. R.; Müller, B. H.; Spannenberg, A.;

Rosenthal, U.; Al-Hazmi, M. H.; Mosa, F. M.; Wöhl, A.; Müller, W. *Chem. Eur. J.* **2010**, *16*, 12127. (c) Peitz, S.; Peulecke, N.; Aluri, B. R.; Müller, B. H.; Spannenberg, A.; Rosenthal, U.; Al-Hazmi, M. H.; Mosa, F. M.; Wöhl, A.; Müller, W. *Organometallics* **2010**, *29*, 5263. (d) Aluri, B. R.; Peulecke, N.; Peitz S.; Spannenberg A.; Müller, B. H.; Schulz, S.; Heller, D.; Al-Hazmi, M. H.; Mosa, F. M.; Wöhl, A.; Müller, W.; Rosenthal, U. *Dalton Trans.* **2010**, 7911. (e) Kuhlmann, S.; Blann, K.; Bollmann, A.; Dixon, J. T.; Killian, E.; Maumela, M. C.; Maumela, H.; Morgan, D. H.; Pretorius, M.; Taccardi, N.; Wasserscheid, P. *J. Catal.* **2006**, *245*, 279. (f) Jabri, A.; Crewdson, P.; Gambarotta, S.; Korobkov, I.; Duchateau, R. *Organometallics* **2006**, *25*, 715. (g) Blann, K.; Bolmann, A.; Dixon, J. T.; Hess, F.; Kilian, E.; Maumela, H.; Morgan, D. H.; Neveling, A.; Otto, S.; Overett, M. *Chem. Commun.* **2005**, 620. (h) Blann, K.; Bollmann, A.; Dixon, J. T.; Hess, F. M.; Killian, E.; Maumela, H.; Morgan, D. H.; Neveling, A.; Otto, S.; Overett, M. J. *Chem. Commun.* **2005**, 622. (i) McGuinness, D. S.; Wasserscheid, P; Morgan, D. H.; Dixon, J. T. *Organometallics* **2005**, *24*, 552.

(5) Shaikh, Y.; Albahily, K.; Sutcliffe, M.; Fomitcheva, V.; Gambarotta, S.; Korobkov, I.; Duchateau, R. *Angew. Chem. Int. Ed.* **2012**, *51*, 1366.

(6) (a) Albahily, K.; Ahmed, Z.; Gambarotta, S.; *Koç, E.; Duchateau, R.*; Borobkov, I. *Organometallics* **2011**, *30*, 6022. (c) Thapa, I.; Gambarotta, S.; Duchateau, R.; Kulangara, S. V.; Chevalier, R. *Organometallics* **2010**, *29*, 4080.

(7) (a) Albahily, K.; Koç, E.; Al-Baldawi, D.; Savard, D.; Gambarotta, S.; Burchell, T. J.; Duchateau, R. *Angew. Chem. Int. Ed.* **2008**, *47*, 5816. (b) Albahily, K.; Al-Baldawi, D.; Gambarotta, S.; Koç, E.; Duchateau, R. *Organometallics* **2008**, *27*, 5943.

(8) (a) Albahily, K.; Fomitcheva, V.; Gambarotta, S.; Korobkov,I.; Murugesu, M.; Gorelsky, S. I. *J. Am. Chem. Soc.* **2011**, *133*, 6380. (b) Thapa, I.; Gambarotta, S.; Korobkov, I.; Duchateau, R.; Kulangara, S. V.; Chevalier, R. *Organometallics* **2010**, *29*, 4080. (c) Albahily, K.; Al-Baldawi, D.; Gambarotta, S.; Koç, E.; Duchateau, R. *Organometallic*s **2008**, *27*, 5708.

(9) (a) Alzamly, A.; Gambarotta, S.; Borobkov, I. *Organometallics* **2013**, *32*, 7204. (b) Alzamly, A.; Gambarotta, S.; Borobkov, I. *Organometallics* **2013**, *32*, 7107. (c) Jabri, A.; Temple, C.; Crewdson, P.; Gambarotta, S.; Korobkov, I.; Duchateau, R. *J. Am. Chem. Soc.* **2006**, *128*, 9238. (d) Schulzke, C.; Enright, D.; Sugiyama, H.; LeBlanc, G.; Gambarotta, S.; Yap, G. P. A.; Thompson, K. K.; Wilson, D. R.; Duchateau, R. *Organometallics* **2002**, *21*, 3810.

(10) (a) Sugiyama, H.; Aharonian, G.; Gambarotta, S.; Yap, G. P. A.; Budzelaar, P. H. *J. Am. Chem. Soc.* **2002**, *124*, 12268. (b) Bhandari, G.; Kim, Y.; McFarland, J. M.; Rheingold, A. L.; Theopold, K. H. *Organometallics* **1995**, *14*, 738. (c) Winter, M. J. Comprehensive Organometallic Chemistry, 2nd ed.; Wilkinson, G., Ed.; Pergamon Press: Oxford, 1995. (d) Kirtley, S. W. Comprehensive Organometallic Chemistry; Wilkinson, G., Ed.; Pergamon Press: Oxford, 1978.

(11) Albahily, K.; Licciulli, S.; Gambarotta, S.; Korobkov, I; Chevalier, R.; Schuhen, K.; Duchateau, R. *Organometallics* **2011**, *30*, 3346.

(12) (a) Albahily, K.; Al-Baldawi, D.; Gambarotta, S.; Duchateau, R.; Koç, E.; Burchell, T. J. *Organometallics* **2008**, *27*, 5711. (b) Albahily, K.; Koç, E.; Al-Baldawi, D.; Savard, D.; Gambarotta, S.; Burchell, T. J. *Angew. Chem.* **2008**, *120*, 5900.

(13) (a) Albahily, K.; Fomitcheva, V.; Shaikh, Y.; Sebastiao, E.; Gorelsky, S. I.; Gambarotta, S.; Korobkov, I.; Duchateau, R. *Organometallics* **2011**, *30*, 4201.

(14) (a) Bhaduri, S.; Mukhopadhyay, S.; Kulkarni, S. A. *J. Organomet. Chem.* **2009**, *694*, 1297. (b) Budzelaar, P. H. M. *Can. J. Chem.* **2009**, *87*, 832. (c) Jabri, A.; Mason, C. B.; Sim, Y.; Gambarotta, S.; Burchell, T. J.; Duchateau, R. *Angew. Chem. Int. Ed.* **2008**, *47*, 9717. (d) Agapie, T.; Labinger, J. A.; Brecaw, J. E. *J. Am. Chem. Soc.* **2007**, *129*, 14281. (e) Wass, D. *Dalton Trans.* **2007**, 816. and references therein. (f) van Rensburg, W. J.; Berg, J.-A.; Steynberg, P. J. *Organometallics* **2007**, *26*, 1000. (g) Bowen, L. E.; Haddow, M. F.; Orpen, A. G.; Wass, D. *Dalton Trans.* **2007**, 1160. (h) Elowe, P. R.; McCann, C.; Pringle, P. G.; Spitzmesser, S. K.; Bercaw, J. E. *Organomeallics* **2006**, *25*, 5255. (i) Overett, M. J.; Blann, K.; Bollmann, A.; Dixon, J. T.; Haasbroek, D.; Killian, E.; Maumela, H.; McGuinness, D. S.; Morgan, D. H. *J. Am. Chem. Soc.* **2005**, *127*, 10723. (j) Agapie, T.; Schofer, S. J.; Labinger, J. A.; Bercaw, J. E. *J. Am. Chem. Soc.* **2004**, *126*, 1304.

(15) Bollmann, A.; Blann, K.; Dixon, J. T.; Hess, F. M.; Killian, E.; Maumela, H.; McGuinness, D. S.; Morgan, D. H.; Neveling, A.; Otto, S.; Overett, M.; Slawin, A. M. Z.; Wasserscheid, P.; Kuhlmann, S. *J. Am. Chem. Soc.* **2004**, *126*, 14712.

(16) (a) Blann, K.; Bollmann, A.; de Bod, H.; Dixon, J. T.; Killian. E.; Nongodlwana, P.; Maumela, M. C.; Maumela, H.; McConnell, A. E.; Morgan, D. H.; Overett, M.; Pretorius, M.; Kuhlmann, S.; Wasserscheid, P. *J. Catal.* **2007**, *249*, 244. (b) Weng, Z.; Teo, S.; Hor. T. S. A. *Dalton Trans* **2007**, 3493.

(17) Biricik, N.; Fei, Z.; Scopelliti, R.; Dyson, P. J. *Helv. Chim. Acta* **2003**, *86*, 3281.

(18) Zhang, J.-F; Xin, G.; Fu, W.-F.; Xu, H.; Li, L. *Inorg. Chem. Acta.* **2010**, *363*, 338.

(19) Nermin Biricik; Feyyaz Durap; Cezmi Kayan; Bahattin Gümgüma; Nevin Gürbüz; Ismail Özdemir; Wee Han Ang; Zhaofu Fei; Rosario Scopelliti. *J. Organomet. Chem.* **2008**, *693*, 2693.

(20) Collman, J. P.; Kittleman, E. T. *Inorg. Synth.* **1966**, *8*, 149.

(21) (a) Temple, C.; Jabri, A.; Crewdson, P.; Gambarotta, S.; Korobkov, I.; Duchateau, R. *Angew. Chem. Intl. Ed.* **2006**, *45*, 7050. (b) Jabri, A.; Temple, C.; Crewdson, P.; Gambarotta, S.; Korobkov, I.; Duchateau, R. *J. Am. Chem. Soc.* **2006**, *128*, 9238.

CHAPTER 5

Isolation of a Hexanuclear Chromium Cluster with a Tetrahedral Hydridic Core

The results presented in this chapter have been submitted to

Alzamly, A.; Gambarotta, S.; Korobkov, I.; Murugesu, M.; LeRoy, J. J.; Budzelaar, P. *Inorg. Chem.*

5.1 Introduction

The Cr-Cr interaction in dimetallic units is probably the most unique and intriguing feature that can be encountered in M-M bond chemistry. Low-valent chromium has provided in fact the shortest ever found intermetallic contacts,[1] initially leading to the conclusion that such interactions should be strong.[2] However, a large body of work both theoretical[3] and experimental[1,4] has clearly highlighted the paradoxical weakness of such interactions.[5] In turn, this hinted that ligand features (chelating geometry, bite, steric interactions, etc.) rather than M-M bond strength may be the factors at play in determining the extent of the Cr-Cr separation.[1b,3f,6]

The two oxidation states occasionally displaying this intriguing behavior are the mono-[1b,f,i,k,r,7] and divalent ones.[8] The monovalent state is particularly noticeable in the sense that it has produced record short Cr-Cr bonds,[1j] thought to be quintuple. However, DFT work has also shown that there is the possibility for singlet open-shell AF-coupled configurations and which may reduce the formal M-M bond order.[1d,3d,9]

Interestingly, both Cr(II) and Cr(I) play an important role in catalytic ethylene oligomerization and it is still debated whether selective catalytic oligomerization to either tri- or tetramerization should be ascribed to the monovalent state.[10] In any event, the ligand system must be able to prevent formation of strong Cr-Cr interactions which may introduce excessive stability and ultimately obliterates the catalytic behavior. Thus, assuming that monovalent chromium is truly responsible for selective oligomerization, it was argued that ligands capable of holding two metal centers at appropriate distance might be the winning key to produce highly desirable selective tetramerization catalysts.[11] Such catalysts remain to date exceedingly rare.[12]

The employment of ligands based on phosphorus or sulfur donor atoms appears to be mandatory if mononuclear and monovalent species of sufficiently long life-time to initiate a

catalytic cycle are being targeted. In addition, amino- and pyridine functionalities may also help to obtain selective catalytic systems. Following the work of McGuinness,[13] Wass[14] and Rosenthal,[15] we have also developed ligand systems based on those functionalities. Of primary interest to us was the isolation of catalytically active species, generated by the direct interaction of trivalent chromium precursors with aluminates.[16]

For the present work, we have selected a 2-[N(H)CH_2PPh_2]C_5H_4N ligand with the hope of generating multinuclear species hopefully containing the chromium metal in lower oxidation states.[17] By using a strongly reducing (*i*-Bu)$_3$Al activator in combination with the particular framework of the above ligand, we anticipated the possibility of forming di- or trimetallic structures, which might help us understand the role of the Cr-Cr interaction in terms or either favoring or disfavoring ethylene oligomerization.

Herein we describe the isolation and characterization of an unprecedented Cr(II) hydride *hexa*-chromium cluster with a diamagnetic tetrahedral core and two peripheral paramagnetic centers. It is worth noting that although there are precedents for Cr-hydrides in the literature,[18] information remains scarce.

5.2 Experimental Section

All reactions were carried out under inert atmosphere using Schlenk techniques or in a purified nitrogen-filled drybox. Solvents were dried using a purification system composed of aluminum oxide. GC-MS analysis of the oligomers was carried out with a Hewlett-Packard HP 5973 gas chromatograph using an Agilent DB1 column and dual FID and MS detector. Elemental analysis was carried out with a PerkinElmer 2400 CHN analyzer. Magnetic susceptibility measurements were performed with a Johnson Matthey balance at room temperature. The samples were powdered and weighed inside a drybox and transferred to sealed and calibrated

tubes for measurements. NMR spectra were recorded on Varian Mercury 400 MHz spectrometer at 300 K. Infrared spectra were recorded on an ABB Bomem FTIR instrument from Nujol mulls prepared in a VAC drybox. All chemical reagents were purchased from commercial sources and used as received. Tri-isobutyl aluminum were purchased from Strem and used as received. Methylaluminoxane (MAO, 20% in toluene) was purchased from Albemarle Corporation. TMA-depleted methylaluminoxane (DMAO) was prepared by removing all the volatiles from MAO *in vacuo* (2 mmHg) and with moderate heating (40 °C) for 6 hours. Ligand 2-[$N(H)CH_2PPh_2$] C_5H_4N[19] and $CrCl_3(THF)_3$[20] were prepared according to literature procedures.

Preparation of [2-(C_5H_4NH)CH_2PPh_2]CrCl3.THF_2 (5.1)

A solution of $CrCl_3(THF)_3$ (0.375g, 1.0 mmol) in THF (15 mL) was added to a solution of Ph_2P CH_2NHPy (0.292g, 1mmol) in THF (5 mL). The color of the solution immediately changed to dark green. Green crystals of **5.1** were obtained by slow evaporation **(**0.26g, 0.50 mmol, 50%). μ_{eff} = 3.81 μ_{MB}. Elemental Analysis % calculated for $C_{26}H_{33}Cl_3CrN_2O_2P$ (found): C 50.64 (50.58), H 4.64 (4.61), N 5.37 (5.32). IR (Nujol): ν_{N-H} 3225 cm^{-1}.

Preparation of $\mu,\kappa^1,\kappa^2,\kappa^3$-N,N,P-{[2-($NCH_2PPh_2$)$C_5H_4N$]Cr($\mu$-H)}$_4$[($\mu$-Cl)Cr($\mu$-Cl)Al(*i*-Bu)$_2$-Cl]$_2$ (5.2)

A Solution of $PyNHCH_2PPh_2$ (0.292 g, 1.0 mmol) in toluene (10 mL) was treated with $CrCl_3(THF)_3$ (0.375g, 1.0 mmol), a blue precipitate formed immediately. The mixture was stirred at room temperature overnight. After the mixture was cooled to -40 ^oC, triisobutylaluminum (0.795, 4.0 mmol) was added dropwise and mixture, dark brown solution formed, stirred for 30 min. After it was warmed to room temperature, the suspension was centrifuged and the supernatant concentrated and then layered with heptanes (3 mL).The resulting dark brown crystal was filtered, washed with cold heptanes (10 mL), dried *in vacuo*, affording **5.2** (0.538, 0.272

mmol, 27.2%). Elemental Analysis % calculated for $C_{94.5}H_{107}Al_{1.5}Cl_{5.5}Cr_6N_8P_4$ (found): C 53.48 (53.12), H 5.30 (5.26), N 5.67 (5.61).

Chemical Degradation of 5.2

Different amounts of hydrogen gas were introduced with a gas-tight volumetric syringe in tightly sealed vials filled with nitrogen gas. Once hydrogen gas was introduced, it was allowed to equilibrate at room temperature for 10 min. after which a 1 μl sample of the gaseous mixture was injected into the GC with TC detector to obtain the calibration curve. Different amounts of the cluster sample were placed in vials under same conditions. Degradation was carried out via addition of acetone/HCl (1/0.1 ml) causing visible gas evolution. The quantification of hydrogen was obtained by determining its concentration in the gas phase via GC analysis relative to the calibration curve.

5.3 X-Ray Data

Table 5.1. Crystal Data and Structure Analysis Results of Complexes **5.1**-**5.2**.

	5.1	**5.2**
Formula	$C_{26}H_{33}C_{l3}CrN_2O_2P$	$C_{94.5}H_{107}Al_{1.5}Cl_{5.5}Cr_6N_8P_4$
FW, gmol^{-1}	594.86	2026.20
Space group	Orthorhombic, Pbca	Monoclinic
***a* (Å)**	15.3487(5)	38.3455(11)
***b* (Å)**	15.4622(5)	11.3143(3)
***c* (Å)**	23.7770(8)	30.4666(14)
α, (deg)	90	90
β, (deg)	90	127.6618(9)
γ, (deg)	90	90
***V* (Å^3)**	5642.9(3)	10463.8(6)
Z	8	4
Radiation	0.71073	0.71073
T (K)	200(2)	200(2)
D_{calcd} (mg/m^3)	1.4	1.286
μ_{calcd} (mm^{-1})	0.772	0.860
***F*$_{000}$**	2472	4188
***R*, *Rw*^{2a}**	0.075, 0.1939	0.0590, 0.1404
GoF	1.132	1.054

[a] $R = \Sigma|F_o| - |F_c|/\Sigma|F_o|$, $Rw = [\Sigma(|F_o| - |F_c|)2/\Sigma wF_o2]^{1/2}$

5.4 Results and Discussion

Treatment of $CrCl_3(THF)_3$ with the amino-phosphine ligand derivative 2-$[N(H)CH_2PPh_2]C_5H_4N$ in THF afforded the corresponding paramagnetic adduct {2-$[N(H)CH_2PPh_2]C_5H_4N$}$CrCl_3$(THF). THF (**5.1**) (Scheme 5.1).

Scheme 5.1

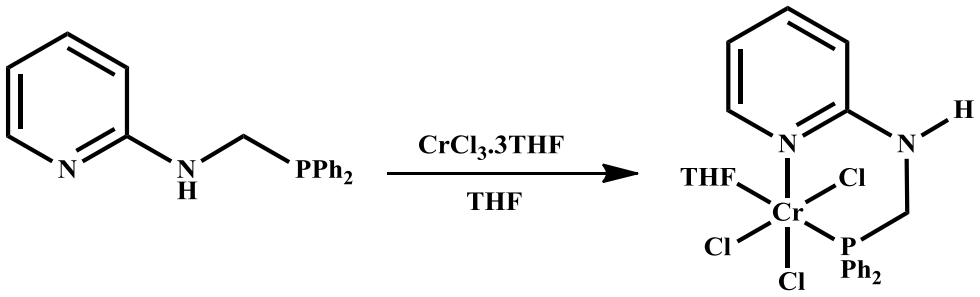

(5.1)

Complex **5.1** features a trivalent chromium atom in a distorted octahedral arrangement surrounded by three chlorine [Cr(1)-Cl(1) = 2.301(2) Å, Cr(1)-Cl(2) = 2.304(2) Å, Cr(1)-Cl(3) = 2.3181(19) Å, N(1)-Cr(1)-Cl(1) = 85.73(16)^o, N(1)-Cr(1)-Cl(2) = 78.29(17)^o, N(1)-Cr(1)-Cl(3) = 86.22(16)^o] and the ligand's phosphorus [Cr(1)-P(1) = 2.422(2) Å, O(1)-Cr(1)-P(1) = 178.18(16) ^{o}] and nitrogen atoms [Cr(1)-N(1) = 2.156(6) Å]. The remaining position is occupied by one THF molecule [Cr(1)-O(1) = 2.083(5) Å, O(1)-Cr(1)-Cl(1) = 91.87(14)^o]. An additional molecule of THF was also found in the lattice.

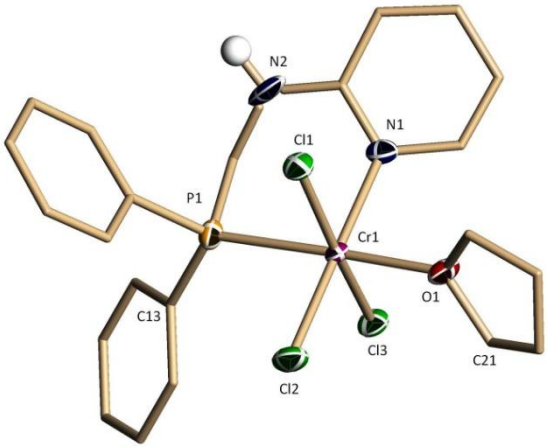

Figure 5.1. Thermal ellipsoid plot of **5.1** with ellipsoids drawn at 50% probability level. Selected bond distances (Å) and angles (deg) for **5.1**: O(1)-Cr(1)-Cl(2) = 87.50(15), Cl(1)-Cr(1)-Cl(2) = 93.13(8), O(1)-Cr(1)-Cl(3) = 92.75(15), Cl(1)-Cr(1)-Cl(3) = 170.80(8), Cl(2)-Cr(1)-Cl(3) = 95.02(8), N(1)-Cr(1)-P(1) = 90.56(17), Cl(1)-Cr(1)-P(1) = 88.39(7), Cl(2)-Cr(1)-P(1) = 0.68(8), Cl(3)-Cr(1)-P(1)= 87.25(7).

Upon activation with MAO in toluene, complex **5.1** displays a good activity as a non-selective oligomerization catalyst with substantial amount of polymer also formed (Table 5.2). No activity was observed when the solvent was switched to methylcyclohexane. The catalytic behavior clearly indicates the occurrence of multiple reaction pathways. The formation of 1-butene for examples rules out a metallacyclic ring expansion mechanism.[21] By contrast, the tail of the distribution with its constant α-factor seems to suggest a S-F distribution, which could be caused by a ring expansion mechanism[22] or by standard alkyl growth. Particularly curious is the *lower* than expected amount of 1-hexene, for which we have no easy explanation. Finally, the non-selective behavior with the presence of substantial amount of heavy olefins is a feature commonly observed for divalent chromium complexes. This suggests that during the activation, the trivalent complex **5.1** mainly undergoes one-electron reduction.

Table 5.2. Ethylene catalyzed oligomerization reactions of **5.1**-**5.2**.[a]

Catalyst	Alkenes (g)	PE (g)	Activity (g/((g of Cr) h))	Linear Alpha Olefins (mol %)								
				C_4	C_6	C_8	C_{10}	C_{12}	C_{14}	C_{16}	C_{18}	α
5.1	36	3.2	55654	11	14	16	15	14	12	10	8	0.76
5.2	22	2.1	43913	4	13	19	18	15	13	10	8	0.78

[a]Conditions: 100mL of toluene, loading 20 μmol of catalyst, 40 bar of ethylene, T = 80 ˚C, (Al:Cr) MAO = 500, reaction time 30 min.

In an attempt to lower the metal oxidation state beyond the divalent state, *in situ* generated complex **5.1** was treated with a stoichiometric amount of the more reducing activator (*i*-Bu)$_3$Al. In the recent past we have successfully used this procedure for the preparation of either a dinuclear divalent hydride[18d] or mixed valence Cr(II)/Cr(I) species.[17b] In the present case, the reaction afforded a remarkable octanuclear and heterometallic hydride cluster $\mu,\kappa^1,\kappa^2,\kappa^3$-N,N,P-{[2-(NCH$_2PPh_2$)C$_5H_4$N]Cr($\mu$-H)}$_4$[($\mu$-Cl)Cr($\mu$-Cl)Al(*i*-Bu)$_2$Cl]$_2$ (**5.2**) (Scheme 5.2). The presence and the number of the hydrides per formula unit was yielded by chemical degradation experiments carried out *in quadruplo* and in sealed vessels. The quantification was obtained by determining via GC the concentration of hydrogen in the gaseous phase relative to a calibration curve.

The crystal structure indicates the presence of a distorted tetrahedral tetrachromium-tetrahydride central core. This unit is mainly in turn assembled by two identical dimetallic units featuring a short Cr-Cr distance [Cr(1)-Cr(2) = 1.9231(11)], bridged by two deprotonated ligands. The first chelates the dimetallic unit using the deprotonated N atom and the pyridine N atoms while the second uses the P and deprotonated amino N atoms. The second dimetallic unit is rotated by approximately ninety deg relative to the first one and the connection is ensured via four edge- bridging hydrides located in the difference Fourier maps. Relevant to this compound is the structure of the weakly paramagnetic cluster [Cp'CrH]$_4$ also containing divalent chromium.

This structure has a more symmetric core with hydrogen atoms capping each face of the coordination tetrahedron.[23]

Scheme 5.2

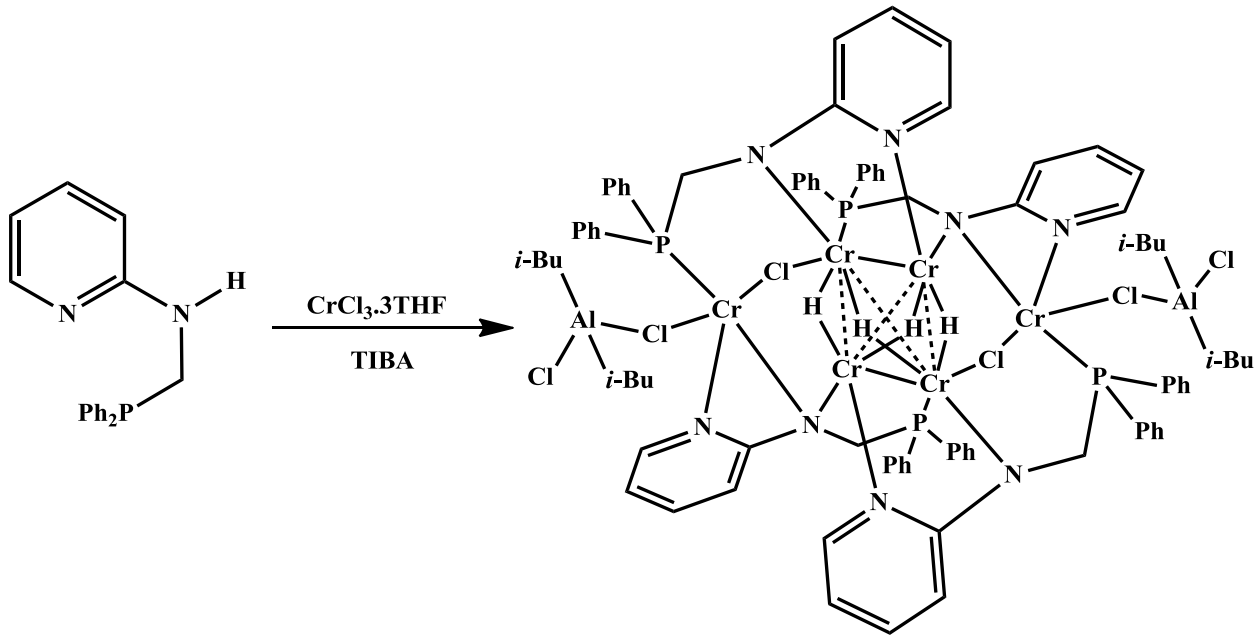

(5.2)

In complex **5.2**, each dimetallic core unit also retains one chlorine atom approximately lying on the metal-metal vector [Cr(2)-Cl(1) = 2.7040(15)Å, Cr(1)-Cr(2)-Cl(1) = 168.17(6)^{o}]. Two of the four deprotonated ligand nitrogen atoms along with the two P atoms and the two pyridine N atoms not connected to the tetrahedral core as well as the two coaxial chlorine atoms, generate two square-pyramidal pockets where two additional chromium atoms are accommodated [Cr(3)-Cl(1) = 2.3691(16)Å, Cr(3)-Cl(2) = 2.5957(19)Å, Cr(3)-P(2) = 2.5490(16), Cr(1)-N(4) = 2.006(4), Cr(2)-N(3) = 2.026(4), Cl(1)-Cr(3)-P(2) = 87.90(5)^{o}, Cr(2)-Cr(1)-N(4) = 95.01(13), Cr(2)-Cr(1)-N(1) = 107.03(13), P(2)-Cr(3)-Cl(2) = 108.55(6)^{o}]. The coordination geometry around these two additional metal centers appears to be square-pyramidal since an additional chlorine atom is located on the apex perpendicular to the plane defined by the donor atoms. In

turn, these chlorine atoms bridge to two aluminate residues. The distance from the square-pyramidal chromium atoms to the nearest Cr center participating in the cluster structure is 3.135 Å, outside direct bonding range.

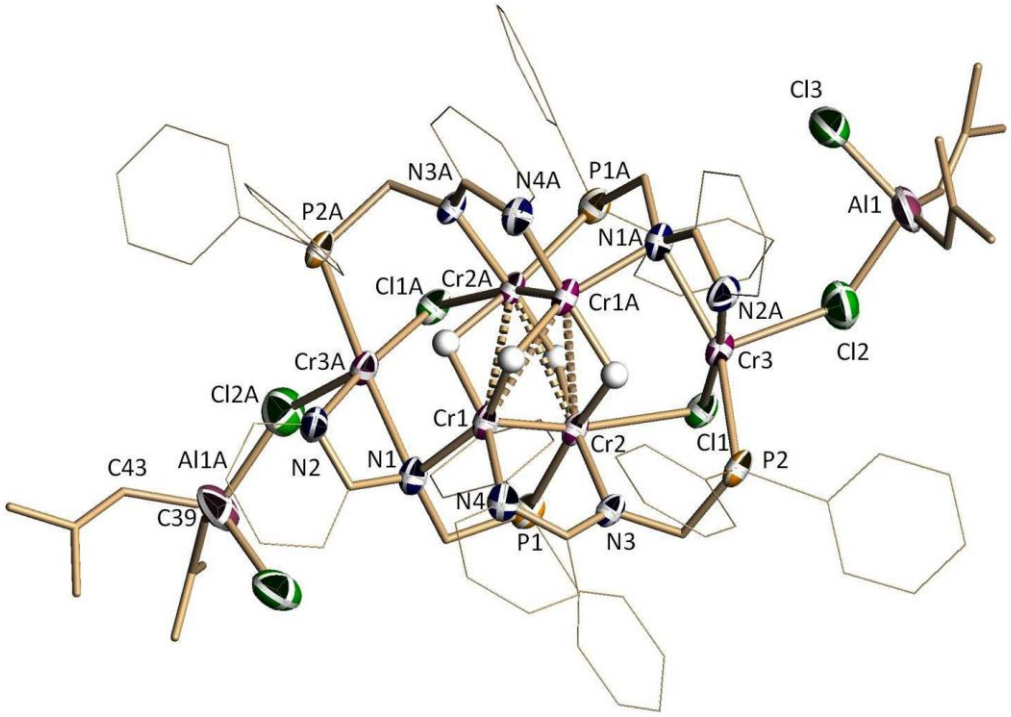

Figure 5.2. Thermal ellipsoid plot of **5.2** with ellipsoids drawn at 50% probability level. Selected bond distances (Å) and angles (deg) for 5.2: Cr(1)-N(1) = 2.091(4), Cr(2)-P(1) = 2.4109(17), Cl(2)-Al(1) = 2.245(3), Cl(3)-Al(1) = 2.177(4), N(4)-Cr(1)-N(1) = 94.00(18), Cr(1)-Cr(2)-N(3) = 95.27(12), Cr(1)-Cr(2)-P(1)91.38(5), N(3)-Cr(2)-P(1) = 89.16(13), N(3)-Cr(2)-Cl(1) = 92.67 (12), P(1)-Cr(2)-Cl(1) = 97.51(5), Cl(1)-Cr(3)-Cl(2) = 89.74(6), Cr(3)-Cl(1)-Cr(2) = 79.57(5), Al(1)-Cl(2)-Cr(3) = 136.17(12), Cl(3)-Al(1)-Cl(2) = 102.61(13).

5.5 Magnetic Measurments

Magnetic analysis was performed on a crushed polycrystalline sample of **5.2**, wrapped in a polyethylene membrane sealed in a glove box to prevent any sample degradation. The direct current (dc) magnetic susceptibility measurements were obtained using a Quantum Design

SQUID magnetometer MPMS-XL7 operating between 1.8 and 300 K for dc-applied fields ranging from −7 to 7 T. Alternating current (ac) susceptibility measurements were carried out under an oscillating ac field of 3 Oe and ac frequencies ranging from 1 to 1500 Hz. The magnetization data was collected at 100 K to check for ferromagnetic impurities which were found to be absent in **5.2**. Diamagnetic corrections were applied for the sample holder and the core diamagnetism from the sample (estimated with Pascal constants).

Charge counting assigns the divalent oxidation state to all six chromium atoms. The square pyramidal geometry of the two peripheral chromium atoms would be compatibale with either high or low-spin configuration. Instead the very short Cr-Cr distance of the central core might be taken as an indication for diamagnetism. The magnetism of **5.2** was probed at variable temperature showing an effective room temperature magnetic moment value of 8.50 μ_B, rapidly dropping to a value of 3.34 μ_B at 1.8K (Figure 5.3). As for the magnetic moment, the room temperature value of μ_{eff} of 8.5 μ_B is slightly lower than the value expected for two non-interacting high-spin square-pyramidal Cr(II) ions (expected value 9.8 μ_B). Moreover, a gradual decrease of the magnetic susceptibility upon decrease of the temperature can be observed. Such behavior can be attributed to antiferromagnetic interaction between the two peripheral Cr(II) ions (assuming a central core composed of diamagnetic $Cr(II)_4$ unit acting as an effective superexchange pathway). However, the large separation between the two Cr(II) ions (7.02 Å) suggest the decrease of the susceptibility can originate from the inherent significant anisotropy as arising from the d^4 high-spin Cr(II) ions.

The *M vs. H* data (Figure 5.4, left) below 8 K shows a rapid increase in the magnetization at low magnetic fields, and a less sharp increase at higher fields reaching 3.59 μ_B under 7K without saturation even at 1.8K. The *M vs. H/T* data (Figure 5.4, right) for **5.2** also displays

similar behavior, where at high fields there is no saturation or overlay onto a single master curve. This confirms the presence of large magnetic anisotropy and/or low-lying excited states. To probe any Single-Molecule Magnet (SMM) behavior, temperature dependence of the out-of-phase (χ'') magnetic susceptibility was investigated. No temperature-dependent signal was observed thus precluding any SMM behavior.

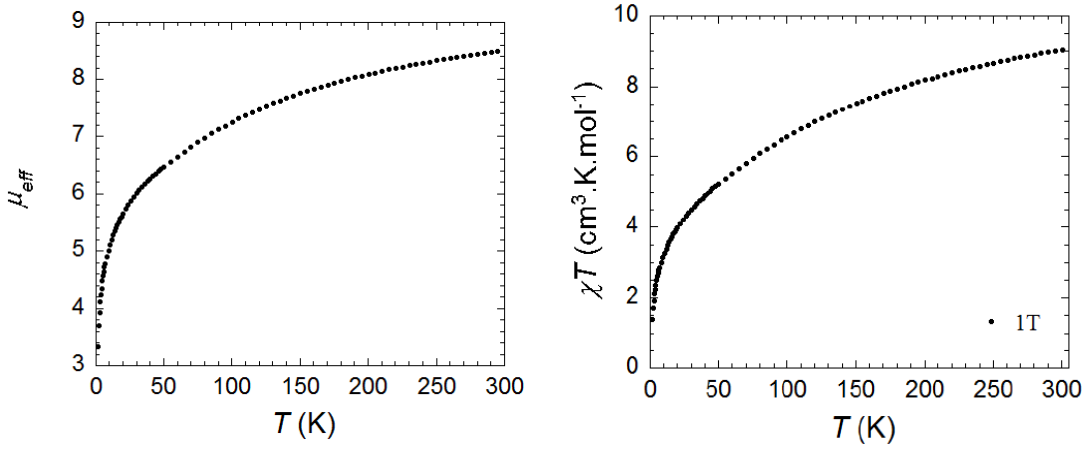

Figure 5.3. Magnetic moment of **5.2** under an applied dc field of 10000 Oe.

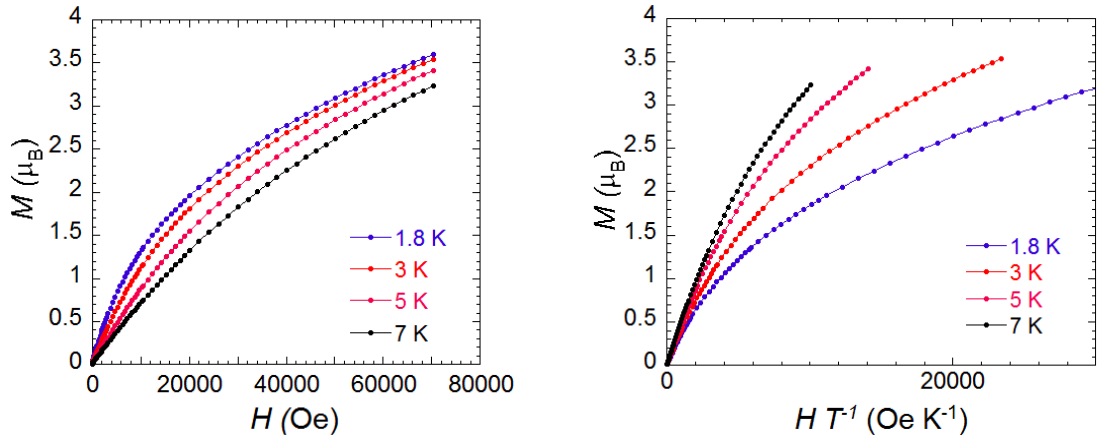

Figure 5.4. Field dependence of the magnetization (left) and reduced magnetization (right) for **5.2** at 1.8, 3, 5, and 7 K.

5.6 Computational Details

All geometries were optimized without constraints - starting from the X-ray structure of **5.2** - at the spin-unrestricted b3-lyp[24]/SV(P)[25] level using the Turbomole program[26]coupled to an external optimizer.[27] Spin density plots were produced using Molden.[28]

DFT calculations were performed to shed some light on the bonding within the Cr_6 cluster of **5.2** and its plausible spin state(s). These calculations should be considered at best qualitative for several reasons. In the first place, ligands had to be strongly simplified (replacing phenyl groups with hydrogens, and omitting the terminal aluminum fragments altogether). Secondly, even with these simplifications we were limited to use a rather modest basis set [SV(P)[23]] for geometry optimization. Finally, the use of a single-determinant unrestricted DFT wavefunction cannot be expected to be a good approximation for the complicated spin state of the real system with its set of six interacting open-shell Cr atoms.

The cluster was built in two stages: initially, only the central Cr_4 core was modeled (cluster **A**), and then the two terminal Cr fragments were added. This was helpful in understanding the interaction between the core and terminal Cr atoms. The dangling η^1-$Cl_2Al^iBu_2$ anions were modeled by chlorides (cluster **B**) or deleted altogether (cluster $\mathbf{C^{2+}}$). For core **A**, we considered the possibility of 0, 8 or 16 unpaired electrons. Coupling to the terminal Cr fragments led us to consider 0, 8, 16 and 24 unpaired electrons for **B** and $\mathbf{C^{2+}}$. All of these possibilities were individually optimized at the b3-lyp level,[24] although in the following we will only discuss the lowest-energy state of each. The lowest-energy spin states (bold in Table 5.3) were then re-optimized using the tpssh[29] and b-p[29d,e,30] functionals.

Table 5.3. Calculated (b3-lyp) relative energies and $<S^2>$ values for spin states of model clusters.

Cluster	# unpaired	E_{rel} (kcal/mol)	$<S^2>$
A	**0**	**0.00**	**7.798**
	8	67.71	23.023
	16	9.79	72.098
B	0	36.98	9.949
	8	**0.00**	**27.394**
	16	64.96	74.541
	24	23.31	156.137
$\mathbf{C^{2+}}$	0	58.93	11.107
	8	**0.00**	**27.349**
	16	98.75	74.318
	24	25.49	156.157
$\mathbf{[CpCrH]_4}$	**0**	**0.00**	**7.663**
	8	48.90	20.414
	16	10.59	72.179

Calculations at the b3-lyp and tpssh level do not reproduce the extreme shortness of the Cr1-Cr2 bond found in **5.2** (for calculated bond lengths, see Table 5.4). On the other hand, b-p predicts even shorter bonds than found in the X-ray strcture. The large differences in calculated Cr-Cr distances obtained with different functionals reflect the "softness" of the Cr-Cr interaction. However, the bonding arrangement is roughly the same in all calculations. The distorted tetrahedral core of the molecule consists of two dimeric units [(Cr1,Cr2) and (Cr1A,Cr2A)]. Within each unit, the Cr atoms are high-spin but AF coupled to each other. The degree of coupling is higher in the b-p structures, with their short Cr-Cr distances, and this is reflected in lower $<S^2>$ values (included in Table 5.4). The two dimeric units are then more weakly F coupled to each other, which still leaves the core unit overall diamagnetic (see Figure 5.5, **A**). Since within the core symmetry-related Cr atoms prefer to have parallel spins, one could expect that when the symmetry-related terminal Cr atoms (Cr3, Cr3A) are added these would also prefer to

have their spins parallel. This is indeed what we find: both **B** and $\mathbf{C}^{2+}$ have a preference for an S_z = 4 "state", and the spins of Cr3 and Cr3A are aligned with those of Cr1 and Cr1A (shown in Figure 5.5 for $\mathbf{C}^{2+}$).

Table 5.4. Comparison of calculated and experimental Cr-Cr distances.

Cluster	Functional	Cr1-Cr1'	Cr1-Cr2(')	Cr2-Cr2'	Cr1-Cr3	Cr2-Cr3	$\langle S^2 \rangle$
5.2	(expt)	2.840	1.923, 2.834	2.935			
A	b3-lyp	2.910	2.881, 2.952	3.959			7.80
	tpssh	2.837	2.575, 2.847	3.122			6.99
	b-p	2.748	1.897, 2.742	2.854			1.69
B	b3-lyp	3.120	2.613, 3.009	3.278	3.233	3.215	23.02
	tpssh	2.987	2.484, 2.899	3.066	3.098	3.135	26.75
	b-p	2.810	1.841, 2.762	2.789	2.920	3.302	20.59
$\mathbf{C}^{2+}$	b3-lyp	3.027	2.598, 3.072	3.154	2.985	3.190	27.35
	tpssh	2.947	2.476, 2.931	2.998	2.893	3.112	26.71
	b-p	2.849	1.850, 2.800	2.823	2.897	3.166	21.34
[Cp'CrH]$_4$	(expt)[18k,21]		2.612-2.681				
[CpCrH]$_4$	b3-lyp		2.846-3.067				7.66
	tpssh		2.784-2.822				7.01
	b-p		2.331-2.780				4.00

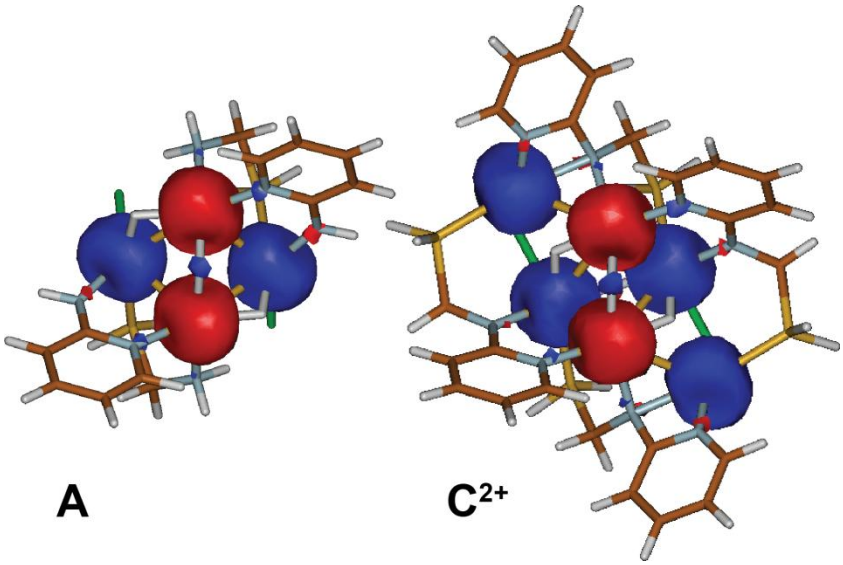

Figure 5.5. Spin density plots for model clusters A and C^{2+}.

Chromium hydride clusters are rather rare. The only example relevant to the present context is the set of $[Cp'CrH]_4$ clusters reported by the group of Theopold.[18k,21] These clusters have a tetrahedral Cr_4 core with hydrides assumed to be located on the faces of the tetrahedron; they are weakly paramagnetic. We have studied simplified model cluster $[CpCrH]_4$ for comparison (see Table 5.2, 5.3), using the same methods as for **A**-**C**. Calculations indicate that an overall low-spin structure is preferred by a modest margin (10.6 kcal/mol, b3-lyp). As for model **A**, the $S_z = 0$ state is heavily spin-contaminated (see Table 5.3) and corresponds to four high-spin Cr^{II} centers coupled ferromagnetically *within* pairs, and antiferromagnetically *between* pairs. Interestingly, optimization at the b3-lyp or tpssh level produces edge-bridging hydrides (approximate cluster symmetry D_2) rather than the symmetrically face-bridging hydrides observed experimentally (approximate cluster symmetry *T*), but all Cr-Cr contacts - whether bridged or unbridged - are rather similar. On the other hand, b-p calculations reproduce the face-bridging hydrides found in the X-ray structure but yield much more variation in the Cr-Cr distances (2.33-2.78 Å) than observed experimentally (2.61-2.68 Å). One could imagine that the

real complexes reported by Theopold have fluxional hydrides and/or dynamic Cr-Cr ditances, but it is equally possible that optimization within a proper spin state (avoiding the UKS artifact of two spin α and two spin β chromium atoms) would lead to symmetric face-bridging hydrides *and* more similar Cr-Cr distances. In any case, it seems reasonable to conclude that the energy difference between edge-bridging and face-bridging hydrides is small for $[Cp'CrH]_4$ and probably also for **5.2**.

Interestingly, complex **5.2** shows a catalytic behavior very similar to **5.1** where a lower amount of 1-butene and more 1-octene is the most noticeable differences (besides a decreased activity). It should also be reiterated that the previously reported divalent and paramagnetic $\{[\mu\text{-}\{(i\text{-Bu})P[N(t\text{-Bu})]_2\}Al(i\text{-Bu})_2]Cr(\mu\text{-H})]_2$ is also a self activating polymerization catalyst of high activity. In contrast, no such behavior was detected with **5.2** and the polymeric material appears to be only heavier oligomers with a Mw centered over 366 g mol^{-1}. It is tempting to suggest at this stage that only the two peripheral Cr units of **5.2** are responsible for the catalytic behavior, while the central core, by being multiply bonded, does not produce any interaction with ethylene even under further activation conditions.

5.7 Conclusions

In conclusion, we have herein reported the synthesis and characterization of unprecedented divalent octanuclear and heterometallic polyhydride chromium complex. The complex containing a Cr_4H_4 core *expected* to be diamagnetic and remains coordinated to two additional divalent high-spin Cr(II) atoms via bridging interactions. Polyhydride cluster was found to act as a non-selective ethylene oligomerization catalyst thus confirming that Cr(II) oxidation state was preserved during the catalytic cycle.

References

(1) (a) Shen, J.; Yap, G. P. A.; Theopold, K. H. *Chem. Commun.* **2014**, DOI: 10.1039/C3CC48746F. (b) Noor, A.; Bauer, T.; Todorova, T. K.; Weber, B.; Gagliardi, L.; Kempe, R. *Chem. Eur. J.* **2013**, *19*, 9825. (c) Chen, H.Z.; Liu, S.C.; Yen, C.-H.; Yu, J.-S. K.; Shieh, Y.-J; Kuo, T.-S.; Tsai, Y.-C. *Angew. Chem. Int. Ed.* **2012**, *51*, 10342. (d) Schwarzmaier, C; Noor, A.; Glatz, G.; Zabel, M.; Timoshkin, A. Y.; Cossairt, B. M.; Cummins, C. C.; Kempe, R.; Scheer, M. *Angew. Chem. Int. Ed.*, **2011**, *50*, 7283. (e) Shen, J.; Yap, G. P. A.; Werner, J.-P.; Theopold, K. H. *Chem. Commun.* **2011**, 12191. (f) Noor, A.; Kempe, R. *Chem. record* **2010**, *10*, 413. (g) Wagner, F. R.; Noor, A.; Kempe, R. *Nat. Chem.* **2009**, *1*, 529. (h) Ni, Chengbao, Ellis, B. D.; Long, G. J.; Power, P. P. *Chem. Commun.* **2009**, 2332. (i) Noor, A.; Glatz, G.; Müller, R.; Kaupp, M.; Demeshko, S.; Kempe, R. *Nat. Chem.* **2009**, *1*, 322. (j) Noor, A.; Wagner, F. R.; Kempe, R. *Angew. Chem. Int. Ed.*, **2008**, *47*, 7246. (k) La Macchia, G.; Gagliardi, L.; Power, P. P.; Brynda, M. *J. Am. Chem. Soc.* **2008**, *130*, 5104. (l) Tsai, Y.-C.; Hsu, C.-W.; Yu, J.-S. K.; Lee, G.-H.; Wang, Y.; Kuo, T.-S. *Angew. Chem. Int. Ed.* **2008**, *47*, 7250. (m) Horvath, S.; gorelsky, S. I.; Gambarotta, S.; Korobkov, I. *Angew Chem. Int. Engl.* **2008**, *47*, 9937. (n) Hsu, C.-W.; Yu, J.-S. K.; Yen, C.-H.; Lee, G.-H.; Wang, Y.; Tsai, Y.-C. *Angew. Chem. Int. Ed.* **2008**, *47*, 9933. (o) Sutton, A. D.; Ngyuen, T.; Fettinger, J. C.; Olmstead, M. M.; Long, G. J.; Power, P. P. *Inorg. Chem.* **2007**, *46*, 4809. (p) Wolf, R.; Brynda, M.; Ni, C.; Long, G. J.; Power, P. P. *J. Am. Chem. Soc.* **2007**, *129*, 6076. (r) Kreisel, K. A.; Yap, G. P. A.; Theopold, K. H. *Chem. Commun.* **2007**, 1510. (r) Wolf, R.; Ni, C.; Nguyen, T.; Brynda, M.; Long, G. J.; Sutton, A. D.; Fischer, R. C.; Fettinger, J. C.; Hellman, M.; Pu, L.; Power, P. P. *Inorg. Chem.* **2007**, *46*, 11277. (s) Kreisel, K. A.;

Yap, G. P. A.; Dmitrenko, O.; Landis, C. R.; Theopold, K. H. *J. Am. Chem. Soc.* **2007**, *129*, 14162. (t) Brynda, M.; Gagliardi, L.; Widmark, P.-O.; Power, P. P.; Roos, B. O. *Angew. Chem. Int. Ed.* **2006**, *45*, 3804. (u) Noh, S. K.; Heintz, R. A.; Janiak, C.; Sendlinger, S. C.; Theopold, K. H. *Angew. Chem. Int. Ed.* **1990**, *29*, 775. (v) Noh, S. K.; Sendlinger, S. C.; Janiak, C.; Theopold, K. H. *J. Am. Chem. Soc.* **1989**, *111*, 9127.

(2) (a) Vollhardt, K., Peter, C.; Cammack, J., K.; Matzger, A., J.; Bauer, A.; Capps, K., B.; Hoff, C. D. *Inorg. Chem.* **1999**, *38*, 2624. (b) Cotton, F. A. and Walton, R. A., *Multiple Bonds Between Metal Atoms*, Oxford University Press, Oxford, UK, 2nd ed., **1992**. (c) Cotton, F. A. *Acc Chem. Rev.* **1978**, *11*, 226. (d) Trogler, W. C.; Gray, H. B. *Acc Chem. Rev.* **1978**, *11*, 232.

(3) (a) Manni, G. L.; Dzubak, A. L.; Mulla, A.; brogden, D. W.; Berry, J. F.; Gagliardi, L. *Chem Eur. J.* **2012**, *18*, 1737. (b) Wu, L.-C.; Hsu, C.-W.; Chunag, Y.-C.; Lee, G.-H.; Tsai, Y.-C.; Wang, Y. *J. Phys. Chem. A* **2011**, *115*, 12602. (c) Wang, H.; Sun, Z.; Xie, Y.; King, R. B.; Schaefer, H. F. *Eur. J. Inorg. Chem.* **2010**, 5161. (d) kurokawa, Y., I.; Nakao, Y.; Sakaki, S. *J. Phys. Chem. A* **2009**, *113*, 3202. (e) Dupré, D. *J. Phys. Chem. A* **2009**, *113*, 1559. (f) La Macchia, G.; Aquliante, F.; Veryazov, V.; Roos, B. O. *Inorg. Chem.* **2008**, *47*, 11455.

(4) (a) Hus, C.-W.; Yu, J.-S. K.; Yen, C.-H, Lee, G.-H.; Wang, Y.; Tasi, Y.-C. *Angew. Chem.* **2008**, *120*, 10081. (b) Tsai, Y.-C.; Hsu, C.-W.; Yu, J.-S. K.; Lee, G.-H.; Wang, Y.; Kuo, T.-S. *Angew. Chem. Int. Ed.* **2008**, *47*, 1.

(5) (a) Sadique, A. R.; Heeg, M. J.; Winter, C. H. *J. Am. Chem. Soc.* **2003**, *125*, 7774. (b) Hao, S.; Gambarotta, S.; Bensimon, C. *J. Am. Chem. Soc.* **1992**, *114*, 3556. (c) Hao, S.; Edema, J. J. H.; Gambarotta, S.; Bensimon, C. *Inorg. Chem.* **1992**, *31*, 2676. (d) Cannon,

R. D. *Inorg. Chem.* **1981**, *20*, 2341. (e) Larkworthy, L. F.; Tabatabai, J. M. *Inorg. Nucl. Chem. Lett.* **1980**, *16*, 427. (f) Abbott, E. H.; Mayer. J. M. *J. Coord. Chem.* **1977**, *6*, 135. (g) Sneeden, R., P.; Zeiss, H. H. *J. Organomet. Chem.* **1973**, *47*, 125.

(6) (a) Noor, A.; Glatz, G.; Müller, R.; Kaupp, M.; Demeshko, S.; Kempe, R. *Z. Anorg. Allg. Chem.* **2009**, *8*, 1149. (b) Halpin, Y.; Cleary, L.; Cassidy, L.; Horne, S.; Dini, D.; Browne, W. R.; Vos, J. G. *Dalton. Trans.* **2009**, 4146. (c) Lazarides, T.; Sykes, D.; Faulkner, S.; Barbieri, A.; Ward, M. D. *Chem. Eur. J.* **2008**, *14*, 9389. (d) Prushan, M. J.; Tomezsko, D. M.; Lofland, S.; Zeller, M.; Hunter, A. D. *Inorg. Chim. Acta.* **2007**, *360*, 2245. (e) Gu, W.; Bian, H.-D.; Xu, J.-Y.; Liu, Z.-Q.; Cheng, P.; Yan, S.-P.; Liao, D.-Z.; Jiang, Z.-H. *Inorg. Chem. Commun* **2003**, *7*, 966. (f) Udugala-Ganehenege, M. Y.; Heeg, M. J.; Hryhorczuk, L. M. *Inorg. Chem.* **2001**, *40*, 1614. (g) Mosher, P. J.; Yap, G. P. A.; Crutchley, R. J. *Inorg. Chem.* **2001**, *40*, 1189. (h) Hao, S.; Gambarotta, S.; Bensimon, C.; Edema, J. J. H. *Inorg. Chim. Acta.* **1993**, *213*, 65.

(7) Nguyen, T.; Sutton, A. D.; Brynda, M.; Fettinger, J. C.; Long, J. G.; Power, P. P. *Science* **2005**, *310*, 844.

(8) (a) Cotton, F. A.; Koch, S. A.; Millar, M. *Inorg. Chem.* **1978**, *17*, 2084. (b) Cotton, F. A.; Koch, S. A. *Inorg. Chem.* **1978**, *17*, 2021. (c) Hein, F.; Tille, D. *Z. Anorg. Allg. Chem.* **1964**, *329*, 72.

(9) (a) Merino, G.; Donald, K., J.; D'Acchioli, J., S.; Hoffmann, R. *J. Am. Chem. Soc.* **2007**, *129*, 15295. (b) Macchia, G. L.; Brynda, M.; Gagliardi, L. *Angew. Chem. Int. Ed.*, **2006**, *45*, 6210.

(10) (a) Licciulli, S.; Thapa, I.; Albahily, K.; Korobkov,I.; Gambarotta, S.; Duchateau, R.; Chevalier, R.; Schuhen, K. *Angew. Chem. Int. Ed.* **2010**, *49*, 9225. (b) Kim, S. K.;

Kim, T. J.; Chung, J. H.; Hahn,T. K.; Chae, S. S.; Lee, H. S.; Cheong, M.; Kang, S. O. *Organometallics* **2010**, *29*, 5805. (c) Bhaduri, S.; Mukhopadhyay, S.; Kulkarni, S. A. *J. Organomet. Chem.* **2009**, *694*, 1297. (d) Budzelaar, P. H. M. *Can. J. Chem.* **2009**, *87*, 832. (e) Jabri, A.; Mason, C. B.; Sim, Y.; Gambarotta, S.; Burchell, T. J.; Duchateau, R. *Angew. Chem. Int. Ed.* **2008**, *47*, 9717. (f) Han, T. K.; Ok, M. A.; Chae, S. S.; S. O. Kang (SK Energy Corporation), WO 2008/088178, **2008**. (g) Agapie, T.; Labinger, J. A.; Brecaw, J. E. *J. Am. Chem. Soc.* **2007**, *129*, 14281. (h) van Rensburg, W. J.; Berg, J.-A.; Steynberg, P. J. *Organometallics* **2007**, *26*, 1000. (i) Kuhlmann, S.; Blann, K.; Bollmann, A.; Dixon, J. T.; Killian, E.; Maumela, M. C.; Maumela, H.; Morgan, D. H.; Pretorius, M.; Taccardi, N.; Wasserscheid, P. *J. Catal.* **2007**, *245*, 279. (j) Killian, E.; Blann, K.; Bollmann, A.; Dixon, J. T.; Kuhlmann, S.; Maumela, M. C.; Maumela, H.; Morgan, D. H.; Nongodlwana, P.; Overett, M. J.; Pretorius, M.; Höfener, K.; Wasserscheid, P. *J. Mol. Catal. A: Chem.* **2007**, *270*, 214. (k) Elowe, P. R.; McCann, C.; Pringle, P. G.; Spitzmesser, S. K.; Bercaw, J. E. *Organomeallics* **2006**, *25*, 5255. (l) Temple, C.; Jabri, A.; Crewdson, P.; Gambarotta, S.; Korobkov, I.; Duchateau, R. *Angew. Chem. Intl. Ed.* **2006**, *45*, 7050. (m) Jabri, A.; Temple, C.; Crewdson, P.; Gambarotta, S.; Korobkov, I.; Duchateau, R. *J. Am. Chem. Soc.* **2006**, *128*, 9238. (n) Schofer, S. J.; Day, M. W.; Henling, L. M.; Labinger, J. A.; Bercaw, J. E. *Organometallics* **2006**, *25*, 2743. (o) van Rensburg, W. J.; Grove, C.; Steynberg, J. P.; Stark, K. B.; Huyser, J. J.; Steynberg, P. J. *Organometallics* **2004**, *23*, 1207. (p) Dixon, J. T.; Green, M. J.; Hess, F. M.; Morgan, D. H. *J. Organomet. Chem.* **2004**, *689*, 3641. (q) Agapie, T.; Schofer, S. J.; Labinger, J. A.; Bercaw, J. E. *J. Am. Chem. Soc.* **2004**, *126*, 1304. (r) Briggs, J. R. *Chem. Commun.* **1989**, 674.

(11) Peitz , S.; Aluri B. R.; Peulecke, N.; Müller, B. H.; Wöhl, A.; Müller, W.; Al-Hazmi M. H.; Mosa, F. M.; Rosenthal, U. C*hem. Eur. J.* **2010**, *16*, 7670.

(12) (a) Shaikh, Y.; Albahily, K.; Sutcliffe, M.; Fomitcheva, V.; Gambarotta, S.; Korobkov, I.; Duchateau, R. *Angew. Chem. Int. Ed.* **2012**, *51*, 1366. (b) Shaikh, Y.; Gurnham, J.; Albahily, K.; Gambarotta, S.; Korobkov, I. *Organometallics* **2012**, *31*, 7427. (c) Schuhen, K.; Chevalier, R.; Gambarotta, S.; Licciulli, S.; Thapa, I.; Duchateau, R. PCT Int. Appl. Patent WO 2011085951A1, 2011.

(13) (a) Overett, M. J.; Blann, K.; Bollmann, A.; Villiers, R. de; Dixon, J. T.; Killian, E.; Maumela, M. C.; Maumela, H.; McGuinness, D. S.; Morgan, D. H. *J. Mol. Catal. A* **2008**, *283*, 114. (b) McGuinness, D. S.; Overett, M.; Tooze, R. P.; Blann, K.; Dixon, J. T.; Slawin, A. M. Z. *Organometallics* **2007**, *26*, 1108. (c) McGuinness, D. S.; Brown, D. B.; Tooze, R. P.; Hess, F. M.; Dixon, J. T.; Slawin, A. M. Z. *Organometallics* **2006**, *25*, 3605. (d) Overett, M. J.; Blann, K.; Bollmann, A.; Dixon, J. T.; Haasbroek, D.; Killian, E.; Maumela, H.; McGuinness, D. S.; Morgan, D. H. *J. Am. Chem. Soc.* **2005**, *127*, 10723. (e) McGuinness, D. S.; Wasserscheid, P.; Morgan, D. H.; Dixon, J. T. *Organometallics* **2005**, *24*, 552. (f) Bollmann, A.; Blann, K.; Dixon, J. T.; Hess, F. M.; Killian, E.; Maumela, H.; McGuinness, D. S.; Morgan, D. H.; Neveling, A.; Otto, S.; Overett, M.; Slawin, A. M. Z.; Wasserscheid, P.; Kuhlmann, S. *J. Am. Chem. Soc.* **2004**, *126*, 14712.

(14) (a) Dulai, A.; McMullin, C. L.; Tenza, K.; Wass, D. F. *Organometallics* **2011**, *30*, 935. (b) Wass, D. *Dalton Trans.* **2007**, 816. and references therein. (c) Bowen, L. E.; Haddow, M. F.; Orpen, A. G.; Wass, D. *Dalton Trans.* **2007**, 1160.

(15) (a) Peitz, S.; Peulecke, N.; Müller, B. H.; , A.; Drexler, H.-J.; Rosenthal, U.; Al-Hazmi, M. H.; Al-Eidan, K. E.; Wöhl, A.; Müller, W. *Organometallics* **2011**, *30*, 2364. (b) Peitz, S.; Peulecke, N.; Aluri, B. P.; Hansen, S.; Muller, B. H.; Spannenberg, A.; Rosenthal, U.; Al-Hazmi, M. H.; Mosa, F. M.; Wohl, A.; Muller, W. *Eur. J. Inorg. Chem.* **2010**, 1167. (c) Wöhl, A.; Müller, W.; Peitz, S.; Peulecke, N.; Aluri, B. P.; Müller, B. H.; Heller, D.; Rosenthal, U.; Al-Hazmi, M. H.; Mosa, F. M. *Chem. Eur. J.* **2010**, *16*, 7833. (d) Peitz, S.; Peulecke, N.; Aluri, B. R.; Müller, B. H.; Spannenberg, A.; Rosenthal, U.; Al-Hazmi, M. H.; Mosa, F. M.; Wöhl, A.; Müller, W. *Chem. Eur. J.* **2010**, *16*, 12127. (e) Peitz, S.; Peulecke, N.; Aluri, B. R.; Müller, B. H.; Spannenberg, A.; Rosenthal, U.; Al-Hazmi, M. H.; Mosa, F. M.; Wöhl, A.; Müller, W. *Organometallics* **2010**, *29*, 5263. (f) Aluri, B. R.; Peulecke, N.; Peitz S.; Spannenberg A.; Müller, B. H.; Schulz, S.; Heller, D.; Al- Hazmi, M. H.; Mosa, F. M.; Wöhl, A.; Müller, W.; Rosenthal, U. *Dalton Trans.* **2010**, 7911.

(16) (a) Alzamly, A.; Gambarotta, S.; Korobkov, I. *Organometallics* **2013**, *32*, 7107. (b) Alzamly, A.; Gambarotta, S.; Korobkov, I. *Organometallics* **2013**, *32*, 7204.

(17) (a) Huang, Y.-L.; Lu, D.-Y.; Yu, H.-C.; Yu, J.-S.; Hsu, C.-W.; Kuo, T.-S.; Lee, G.-H.; Wang, Y.; Tsai, Y.-C. *Angew. Chem. Int. Ed.* **2012**, *51*, 7781. (b) Thapa, I.; Gambarotta, S.; Korobkov, I.; Murugesu, M.; Budzelaar, P. H. M. *Organometallics* **2012**, *31*, 486. (c) Albahily, K.; Fomitcheva, V.; Gambarotta, S.; Korobkov, I.; Murugesu, M.; Gorelsky, S. *J. Am. Chem. Soc.* **2011**, *133*, 6380. (d) Albahily, A.; Shaikh, Y.; Sebastiao, E.; Gambarotta, S.; Korobkov, I.; Gorelsky, S. *J. Am. Chem. Soc.* **2011**, *133*, 6388.

(18) (a) Fischer, P. J.; Neary, M. C.; Avena, L.; Sullivan, K. P.; Hackbarth, K. C. *Organometallics* **2012**, *31*, 2437. (b) Rozenel, S. S.; Chomitz, W. A.; Arnold, J. *Organometallics* **2009**, *28*, 6243. (c) Monillas, W. H.; Yap. G. P. A.; Theopold, K. H.

Angew. Chem. Int. Ed. **2007**, *46*, 6692. (d) Albahily, K.; Al-Baldawi, D.; Gambarotta, S.; Koç, E.; Duchateau, R. *Organometallics* **2008**, *27*, 5943. (e) Addamo, M.; Bombieri, G.; Foresti, Grillone, M. D.; Volpe, M. *Inorg. Chem.* **2004**, *43*, 1603. (f) Filippou, A. C.; Schneider, S.; Schnakenburg, G. *Angew. Chem. Int. Ed.* **2003**, *42*, 4486. (g) MacAdams, L. A.; Buffone, G. P.; Incarvito, C. D.; Golen, J. A.; Rheingold, A. L.; Theopold, K. H. *Chem. Commun.* **2003**, 1164. (h) Sekar, P.; Scheer, M.; Voigt, A.; Kirmse, R. *Organometallics* **1999**, *18*, 2833. (i) Grillone, M. D.; Benetollo, F.; Bombieri, G.; DelPre, A. *J. Organomet. Chem.* **1999**, *575*, 193. (j) Heintz, R. A.; Koetzle, T. F.; Ostrander, R. L.; Rheingold, A. L.; Theopold, K. H.; Wu, P. *Nature* **1995**, *378*, 359. (k) Fryzuk, M. D.; Leznoff, D. B.; Rettig, S. J.; Thompson, R. C. *Inorg. Chem.***1994**, *33*, 5528. (l) Heintz, R. A; Haggerty, B. S.; Wan, H.; Rheingold, A. L.; Theopold, K. H. *Angew. Chem. Int. Ed.* **1992**, *31*, 1077. (m) Roziere, J.; Teulon, P.; Grillone, M. D. *Inorg. Chem.* **1983**, *22*, 557.

(19) Zhang, J.-F; Xin, G.; Fu, W.-F.; Xu, H.; Li, L. *Inorg. Chem. Acta.* **2010**, *363*, 338.

(20) Collman, J. P.; Kittleman, E. T. *Inorg. Synth.* **1966**, *8*, 149.

(21) Kissin, Y. V.; Brandolini, A. J. *J. Polym. Sci. Part A: polym. Chem.* **2008**, 46, 5330.

(22) Tomov, A. T.; Chirinos, J. J.; Jones, D. J.; Long, R. J.; Gibson, V. C. *J. Am. Chem. Soc.* **2005**, *127*, 10166.

(23) Heintz, R. A.; Ostrander, R. L.; Rheingold, A. L.; Theopold, K. H. *J. Am. Chem. Soc.* **1994**, *116*, 11387.

(24) (a) Becke, A. D. *J. Chem. Phys.* **1993**, *98*, 5648. (b) Becke, A. D. *J. Chem. Phys.* **1993**, *98*, 1372. (c) Lee, C. T.; Yang, W. T.; Parr, R. G., *Phys. Rev. B* **1988**, *37*, 785.

(25) Schafer, A.; Horn, H.; Ahlrichs, R. *J. Chem. Phys.* **1992**, 97, 2571.

(26) *TURBOMOLE V6.3*, TURBOMOLE GmbH, since 2007: Karlsruhe, 2011.

(27) (a) Baker, J. *PQS*, 2.4; Parallel Quantum Solutions: Fayetteville, AR, 2001. (b) Baker. J. *J. Comput. Chem.* **1986**, *7*, 385.

(28) Schaftenaar, G.; Noordik, J. H. *J. Comput.-Aided Mol. Des.* **2000**, *14*, 123.

(29) (a) Staroverov, V. N.; Scuseria, G. E.; Tao, J.; Perdew, J. P. *J. Chem. Phys.* **2003**, *119*, 12129. (b) Tao, J.; Perdew, J. P.; Staroverov, V. N.; Scuseria, G. E. *Phys. Rev. Lett.* **2003**, *91*, 146401. (c) Perdew, J. P.; Wang, Y. *Phys. Rev. B* **1992**, *45*, 13244. (d) Slater, J. C. *Phys. Rev.* **1951**, *81*, 385. (e) Dirac, P. A. M. *Proc. Royal Soc. (London) A* **1929**, *123*, 714.

(30) (a) Becke, A. D. *Phys. Rev. A* **1988**, *38*, 3098. (b) Perdew, J. P. *Phys. Rev. B* **1986**, *33*, 8822. (c) Vosko, S. H.; Wilk, L.; Nusair, M. *Can. J. Phys.* **1980**, *58*, 1200.

CHAPTER 6

Chromium-Chromium Double Bond in Binuclear Mixed Valent Chromium Cr(I)-Cr(II) Complex

Manuscript in preparation

6.1 Introduction

The monovalent state of chromium is particularly intriguing not only because of its ability to generate the shortest ever found intermetallic contacts[1] (thought to be the results of direct metal to metal quintuple bonds)[2] but also for its involvement in selective ethylene tri[3]- and tetramerization.[4]

The formation of short Cr-Cr distances in multinuclear complexes,[1,5] whether or not it diagnoses the presence of an attractive intermetallic force,[6] certainly introduces a sufficient stabilization to obliterate the metal catalytic behavior.[7] Therefore, of particular interest are binucleating ligands capable of rigidly holding two monovalent chromium atoms at distances where no direct Cr-Cr interaction may occur but cooperative interactions of the two metals on the same target substrate might still be possible.[8]

A second issue to control the catalytic behavior of monovalent chromium is the facial versus equatorial arrangement of the three donor atoms of a tridentate chelating ligands.[9] It is in fact worth noting that facial ligands have provided the highest performing selective trimerization catalysts.[3b-k]

Last but not least, monovalent chromium might be easily accessible via controlled oxidation of zerovalent complexes stabilized by carbonyls and/or phosphines.[10] In that event, no catalytic behavior has ever been observed. Thus, it is important to generate such species via reduction of di- or trivalent complexes where suitable ligands have been previously coordinated to the metal.[11] This is precisely part of the catalyst activation process, normally carried out with alkyl aluminate reagents under Z-N conditions.[3,12] What remains unclear is whether the monovalent state is reached via a simultaneous two-electron reduction of a trivalent precursor[9,13] (e.g. from reductive elimination of a doubly alkylated metal center) or via transient formation of

divalent intermediates.[14] In fact, divalent species have been shown to oxidize to the trivalent state in the presence of aluminates, most likely via a disproportionation reaction.[15]

Given this scenario, we were interested in studying the ability of the N,N,-dibenzyl-P,P-diphenyl-1,5-diaza-3,7-diphosphacyclooctane, $[(Ph)PCH_2NCH_2(CH_2Ph)]_2$ ligand $[P^{Ph}{}_2N^{Bn}{}_2]$ to afford monovalent species under Z-N activation type of conditions. It should be mentioned that this ligand was successfully used by Bullock for the preparation of rare examples of terminally bonded *cis*- and *trans*-dinitrogen complexes of zerovalent chromium.[16] This in turn reiterated the ability of this cyclic amino-diphospine ligand to trap chromium in its lower valent state.

By treating either a di- or trivalent catalyst precursor of this ligand generated *in situ* with a non-particularly reducing aluminate, Me_3Al, we have now obtained an intriguing Cr(I)-Cr(II) mix-valence complex containing a relatively long Cr-Cr contact. Herein we describe the full characterization and its electronic structure.

6.2 Experimental Section

All reactions were carried out under inert atmosphere using Schlenk techniques or in a purified nitrogen-filled drybox. Solvents were dried using a purification system composed of aluminum oxide. Elemental analysis was carried out with a PerkinElmer 2400 CHN analyzer. NMR spectra were recorded on Varian Mercury 400 MHz spectrometer at 300 K. All chemical reagents were purchased from commercial sources and used as received. Trimethyl aluminium was purchased from Strem and used as received. Ligand $P^{Ph}{}_2N^{Bn}{}_2$,[16] $CrCl_3(THF)_3$[17] and $CrCl_2(THF)_2$[18] were prepared according to literature procedures.

Preparation of $\kappa^1,\kappa^2,\kappa^3$-N,P,P-cyclo[(Ph)PCH$_2$N(CH$_2$Ph)CH$_2$Cr]$_2$(μ-Cl)[AlClMe$_2$] (6.1)

Method A: From $CrCl_3(THF)_3$ precursor

A Solution of the cyclic PNPN ligand (0.64g, 1.0 mmol) in toluene (10 mL) was treated with $CrCl_3(THF)_3$ (0.37g, 1.0 mmol), a dark blue precipitate formed. After twelve hours of stirring at room temperature, the mixture was cooled to -40 ^oC and trimethylaluminum (0.360g, 5.0 mmol) was added dropwise. Stirring was continued for 30 min. While reaching room temperature. The suspension was then centrifuged and the supernatant concentrated, layered with hexanes (3 mL) and stored in the freezer at -40 ^oC for 3 days. The resulting brown crystals of 6.1 were filtered, washed with cold hexanes (10 mL) and dried *in vacuo* (0.355 g, 0.28 mmol, 28%). Elemental Analysis % calculated for $C_{137.5}H_{161}Al_3Cl_8Cr_4N_8P_8$ (found): C 58.73(58.01), H 5.56(5.47), N 4.42(4.40).

Method B: From $CrCl_2(THF)_2$ precursor

A Solution of the cyclic PNPN ligand (0.64g , 1.0 mmol) in toluene (10 mL) was treated with $CrCl_2(THF)_2$ (0.267g, 1.0 mmol), a dark green precipitate formed. After twelve hours of stirring at room temperature, the mixture was cooled to -40 ^oC and trimethylaluminum (0.22g, 3.0 mmol) was added dropwise. Stirring was continued for 30 min. While reaching room temperature. The suspension was then centrifuged and the supernatant concentrated, layered with hexanes (3 mL) and stored in the freezer at -40 ^oC for 3 days. The resulting brown crystals of 6.1 were filtered, washed with cold hexanes (10 mL) and dried *in vacuo* (0.456 g, 0.36 mmol, 36%). Elemental Analysis % calculated for $C_{90}H_{102}AlCl_4Cr_2N_4P_4$ (found): C 58.73(57.85), H 5.56(5.49), N 4.42(4.37).

6.3 X-Ray Data

Table 6.1. Crystal Data and Structure Analysis Results of Complex **6.1**.

	6.1
Formula	$C_{90}\ H_{102}\ Al\ Cl_4Cr_2\ N_4P_4$
FW, gmol^{-1}	1636.42
Space group	Triclinic, P-1
***a* (Å)**	12.0580(14)
***b* (Å)**	18.146(2)
***c* (Å)**	20.810(2)
α, (deg)	70.236(6)
β, (deg)	85.941(6)
γ, (deg)	79.001(6)
***V* (Å^3)**	4206.4(8)
Z	2
Radiation	0.71073
T (K)	200(2)
D_{calcd} (mg/m^3)	1.292
μ_{calcd} (mm^{-1})	0.519
***F*$_{000}$**	1718
***R*, *Rw*^{2a}**	0.0750, 0.1733
GoF	1.021

[a] $R = \Sigma|Fo| - |Fc|/\Sigma|Fj|$, $Rw = [\Sigma(|Fo| - |Fc|)2/\Sigma wFo2]^{1/2}$

6.4 Results and Discussion

The Ligand $P^{Ph}{}_2N^{Bn}{}_2$ was prepared according to a literature procedure.[16] Treatment of chromium (III) chloride complex of the $P^{Ph}{}_2N^{Bn}{}_2$ ligand with 5 equiv of Me_3Al (TMA) or Cr (II) chloride precursor with 3 equiv of TMA afforded in both cases brown crystals of complex $[P^{Ph}{}_2N^{Bn}{}_2CrCl_2P^{Ph}{}_2N^{Bn}{}_2Cr(\mu\text{-}Cl)][AlClMe_2]$ (**6.1)** (Scheme 6.1). Complex **6.1** has a room temperature magnetic moment of 3.36 μ_B indicative of a configuration somewhat intermediate between two and three unpaired electrons.

Scheme 6.1

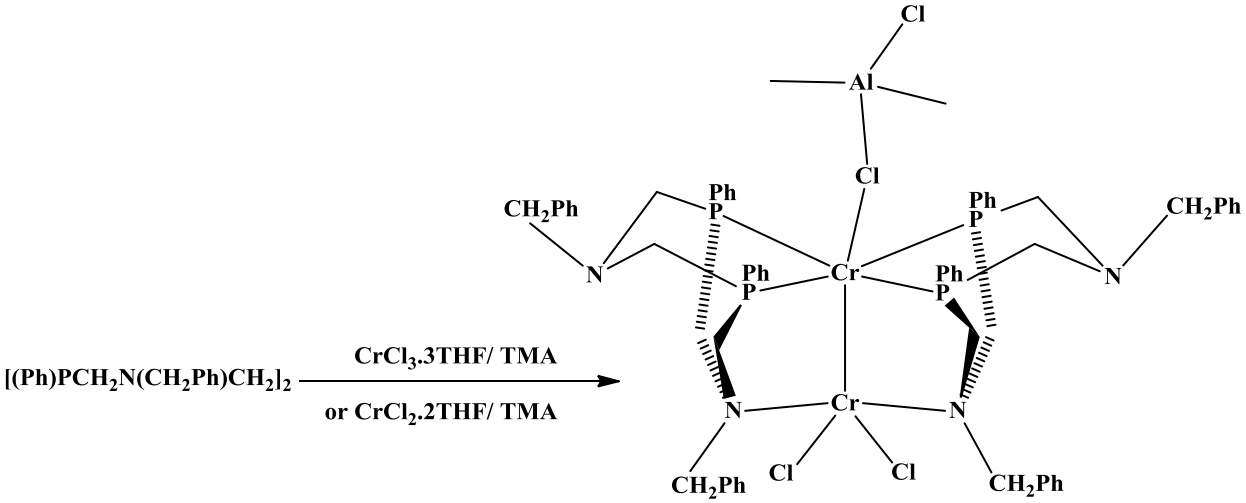

(6.1)

Complex **6.1** exhibits a short Cr(1)-Cr(2) bond distance of 2.0387(8) Å (Figure 6.1), one of the chromium atoms Cr(2) is in distorted square pyramidal geometry, where two chlorine atoms [(Cr(2)-Cl(2) = 2.3289(10)Å, Cr(2)-Cl(3) = 2.3152(10)Å, Cl(3)-Cr(2)-Cl(2) = 123.81(4)^{o}] and two nitrogen donor atoms from two different ligands (Cr(2)-N(2) = 2.234(3)Å, Cr(2)-N(4) = 2.210(3)Å, N(4)-Cr(2)-N(2) = 172.04(10)^{o}] occupy the basal plane and the other Cr(1) occupy the axial plane [Cr(1)-Cr(2) = 2.0387(8)Å]. The geometry around the other chromium atom is distorted octahedral with the four phosphorus atoms occupy the periphery of the complex [(Cr(1)-P(3) = 2.3696(10)Å, Cr(1)- P(4) = 2.3497(10)Å, P(4)-Cr(1)-P(3) = 79.73(3)^{o}, P(3)-Cr(1)-P(2) = 178.48(4)^{o}, Cr(1)-P(1) = 2.3505(10)Å, Cr(1)-P(2) = 2.3754(10)Å, P(4)-Cr(1)-P(1) = 175.79(4)^{o}, P(1)-Cr(1)-P(2) = 80.51(3)^{o}] and the Cr(2) and chlorine atom [Cr(1)-Cl(1) = 2.6766(11)Å, Al(1)-Cl(1)-Cr(1) = 155.71(6)^{o}] on the axial position.

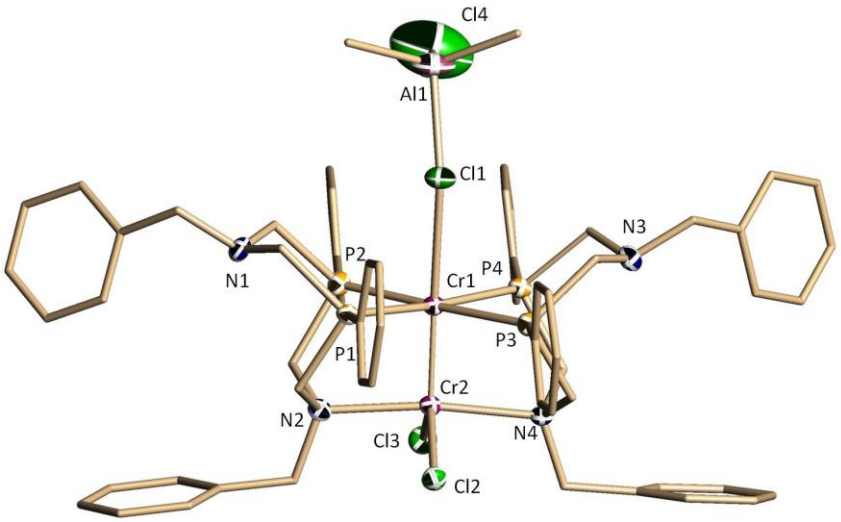

Figure 6.1. Thermal ellipsoid plot of **6.1** with ellipsoids drawn at 50% probability level. Selected bond distances (Å) and angles (deg) for **6.1**: Al(1)-C(62) = 1.956(6), Al(1)-C(61) = 1.981(7), Al(1)-Cl(4) = 2.075(3), Al(1)-Cl(1) = 2.279(16), Cr(2)-Cr(1)-P(4) = 92.46(3), Cr(2)-Cr(1)-P(1) = 91.74(3), Cr(2)-Cr(1)-P(3) = 91.58(3), P(1)-Cr(1)-P(3) = 99.87(4), Cr(2)-Cr(1)-P(2) = 89.88(3), P(4)-Cr(1)-P(2) = 99.79(4), Cr(2)-Cr(1)-Cl(1) = 173.82 (4), P(4)-Cr(1)-Cl(1) = 83.93(4), P(1)-Cr(1)-Cl(1) = 91.91(4), P(3)-Cr(1)-Cl(1) = 92.70(4), P(2)-Cr(1)-Cl(1) = 85.81(4), Cr(1)-Cr(2)-N(4) = 93.52(8), Cr(1)-Cr(2)-N(2) = 94.44(7), Cr(1)-Cr(2)-Cl(3) = 116.84(3), N(4)-Cr(2)-Cl(3) = 87.62(8), N(2)-Cr(2)-Cl(3) = 88.96(8), Cr(1)-Cr(2)-Cl(2) = 119.35(4), N(4)-Cr(2)-Cl(2) = 88.99(8), N(2)-Cr(2)-Cl(2) = 86.95(7), Cl(4)-Al(1)-Cl(1) = 103.10(11).

6.5 Computational Details

DFT calculations were performed using the Gaussian 09 package[19] using the PBE[20] exchange-correlation functional and the TZVP[21] basis set. Tight SCF convergence criteria were used for all calculations. The converged wave functions were tested to confirm that they correspond to the ground-state surface. All calculations for the analysis of the electronic structure, including the generation of initial open-shell wave functions, Mulliken population

analysis[22] and the calculation of Mayer bond order indices[23], orbital occupancy-perturbed bond orders[24] were performed using the AOMix software package.[25]

The asymmetric structure of **6.1** indicates a Class I mixed valence species composed by two non-equivalent chromium atoms in the formal mono- and divalent oxidation states. The particular arrangement of the ligand donor atoms may suggest that the monovalent metal is probably the one surrounded by the soft P atoms. The coordination geometries predict in the absence of direct Cr-Cr interaction a medium spin configuration with three unpaired electron for the monovalent species in square pyramidal field and a high spin with four unpaired electron for the divalent unit in a distorted square planar environment. Given the value of the Cr-Cr distance [2.0387(8) Å] and the room temperature magnetic moment, indicative of the presence of somewhat between two and three unpaired electrons per dimeric unit, both the doublet and quartet spin states were used as input for the calculation. DFT calculations at the spin-unrestricted PBE/TZVP level were carried out using nuclear positions of the heavy atoms from the X-ray crystal structure. To reduce the cost of the computational treatment, four phenyl groups on the periphery of the complex were replaced by hydrogen atoms. All hydrogen positions in the structure were optimized. The quartet spin state gave a substantially higher value of the total energy (37.1 kcal mol^{-1}) indicating the doublet spin state as the ground state. In the ground state, the Cr(1) and Cr(2) atoms have unpaired electron spin densities of -1.19 au and +2.09 au respectively. These atomic spin densities indicate that the unpaired *d* electrons of the two Cr atoms are antiferromagnetically coupled. The analysis of the electronic structure descriptors revealed the nature of the Cr-Cr interaction. As expected, the frontier molecular orbitals are mainly Cr-centered with high 3*d*-character. However, the Cr atom contributions to these MOs are not identical. In fact, the α-,β-LUMO, the α-,β-HOMO and α-HOMO-1 are localized on only

one Cr atom and, as a result, these MOs contribute very little to the Cr-Cr bond as can be established from orbital occupancy-perturbed bond orders (OOPBOs). Such spin localization well accounts for a relatively small value (2.22) of the calculated Mayer bond order for the Cr-Cr interaction. The contributions to the total value of the bond order from the occupied α- and β-spin molecular orbitals are nearly equal (1.12 and 1.10, respectively). In the lowest-energy quartet spin state, the Mayer bond order for the Cr-Cr interaction becomes, as expected, slightly lower (1.96). The antiferromagnetic coupling between the electron spins of the two Cr atoms is expected to be relatively weak and thus can explain the observed magnetic susceptibility data for the complex.

6.6 Conclusions

To conclude, we have isolated an interesting Cr_2 unit with a relatively long dimetallic distance, even though the first intention was to investigate the catalytic behavior of the interesting facial PNP ligand system. As anticipated from the structure, complex **6.1** was found to be inactive toward ethylene oligomerization in toluene by using MAO as an activator. This is in line with the lack of meaningful activity commonly observed for both mono- and divalent multinuclear chromium complexes in the presence of a direct Cr-Cr interaction.

References

(1) (a) Shen, J.; Yap, G. P. A.; Theopold, K. H. *Chem. Commun.* **2014**, DOI: 10.1039/C3CC48746F. (b) Noor, A.; Bauer, T.; Todorova, T. K.; Weber, B.; Gagliardi, L.; Kempe, R. *Chem. Eur. J.* **2013**, *19*, 9825. (c) Chen, H.Z.; Liu, S.C.; Yen, C.-H.; Yu, J.-S. K.; Shieh, Y.-J; Kuo, T.-S.; Tsai, Y.-C. *Angew. Chem. Int. Ed.* **2012**, *51*, 10342. (d) Shen, J.; Yap, G. P. A.; Werner, J.-P.; Theopold, K. H. *Chem Commun.* **2011**, 12191. (e) Noor, A.; Kempe, R. *Chem. record* **2010**, *10*, 413. (f) Wagner, F. R.; Noor, A.; Kempe, R. *Nat. Chem.* **2009**, *1*, 529. (g) Ni, Chengbao, Ellis, B. D.; Long, G. J.; Power, P. P. *Chem Commun.* **2009**, 2332. (h) Tsai, Y.-C.; Hsu, C.- W.; Yu, J.-S. K.; Lee, G.-H.; Wang, Y.; Kuo, T.-S. *Angew. Chem. Int. Ed.* **2008**, *47*, 7250. (i) Horvath, S.; Gorelsky, S. I.; Gambarotta, S.; Korobkov, I. *Angew. Chem.* **2008**, *120*, 10085. (j) Horvath, S.;gorelsky, S. I.; Gambarotta, S.; Korobkov, I. Angew Chem. Int. Engl. 2008, 47, 9937. (k) Hsu, C.-W.; Yu, J.-S. K.; Yen, C.-H.; Lee, G.-H.; Wang, Y.; Tsai, Y.-C. *Angew. Chem. Int. Ed.* **2008**, *47*, 9933. (l) Sutton, A. D.; Ngyuen, T.; Fettinger, J. C.; Olmstead, M. M.; Long, G. J.; Power, P. P. *Inorg. Chem.* **2007**, *46*, 4809. (m) Wolf, R.; Brynda, M.; Ni, C.; Long, G. J.; Power, P. P. *J. Am. Chem. Soc.* **2007**, *129*, 6076. (n) Kreisel, K. A.; Yap, G. P. A.; Theopold, K. H. *Chem Commun.* **2007**, 1510. (o) Wolf, R.; Ni, C.; Nguyen, T.; Brynda, M.; Long, G. J.; Sutton, A. D.; Fischer, R. C.; Fettinger, J. C.; Hellman, M.; Pu, L.; Power, P. P. *Inorg. Chem.* **2007**, *46*, 11277. (p) Kreisel, K. A.; Yap, G. P. A.; Dmitrenko, O.; Landis, C. R.; Theopold, K. H. *J. Am. Chem. Soc.* **2007**, *129*, 14162. (q) Noh, S. K.; heintz, R. A.; Janiak, C.; Sendlinger, S. C.; Theopold, K. H. *Angew. Chem. Int. Ed.* **1990**, *29*, 775. (r) Noh, S. K.; Sendlinger, S. C.; Janiak, C.; Theopold, K. H. *J. Am. Chem. Soc.* **1989**, *111*, 9127.

(2) (a) Schwarzmaier, C; Noor, A.; Glatz, G.; Zabel, M.; Timoshkin, A. Y.; Cossairt, B. M.; Cummins, C. C.; Kempe, R.; Scheer, M. *Angew. Chem. Int. Ed.*, **2011**, *50*, 7283. (b) Noor, A.; Glatz, G.; Müller, R.; Kaupp, M.; Demeshko, S.; Kempe, R. *Nature Chemistry* **2009**, *1*, 322. (c) Noor, A.; Wagner, F. R.; Kempe, R. *Angew. Chem. Int. Ed.*, **2008**, *47*, 7246. (d) La Macchia, G.; Gagliardi, L.; Power, P. P.; Brynda, M. *J. Am. Chem. Soc.* **2008**, *130*, 5104. (d) (e) Brynda, M.; Gagliardi, LF.; Widmark, P.-O.; Power, P. P.; Roos, B. O. *Angew. Chem. Int. Ed.* **2006**, *45*, 3804.

(3) (a) Licciulli, S.; Thapa, I.; Albahily, K.; Korobkov,I.; Gambarotta, S.; Duchateau, R.; Chevalier, R.; Schuhen, K. *Angew. Chem. Int. Ed.* **2010**, *49*, 9225. (b) Bhaduri, S.; Mukhopadhyay, S.; Kulkarni, S. A. *J. Organomet. Chem.* **2009**, *694*, 1297. (c) Jabri, A.; Mason, C. B.; Sim, Y.; Gambarotta, S.; Burchell, T. J.; Duchateau, R. *Angew. Chem. Int. Ed.* **2008**, *47*, 9717. (d) Han, T. K.; Ok, M. A.; Chae, S. S.; S. O. Kang (SK Energy Corporation), WO 2008/088178, **2008**. (e) van Rensburg, W. J.; Berg, J.-A.; Steynberg, P. J. *Organometallics* **2007**, *26*, 1000. (f) Killian, E.; Blann, K.; Bollmann, A.; Dixon, J. T.; Kuhlmann, S.; Maumela, M. C.; Maumela, H.; Morgan, D. H.; Nongodlwana, P.; Overett, M. J.; Pretorius, M.; Höfener, K.; Wasserscheid, P. *J. Mol. Catal. A: Chem.* **2007**, *270*, 214. (g) Jabri, A.; Temple, C.; Crewdson, P.; Gambarotta, S.; Korobkov, I.; Duchateau, R. *J. Am. Chem. Soc.* **2006**, *128*, 9238. (h) Schofer, S. J.; Day, M. W.; Henling, L. M.; Labinger, J. A.; Bercaw, J. E. *Organometallics* **2006**, *25*, 2743. (i) van Rensburg, W. J.; Grove, C.; Steynberg, J. P.; Stark, K. B.; Huyser, J. J.; Steynberg, P. J. *Organometallics* **2004**, *23*, 1207. (j) Agapie, T.; Schofer, S. J.; Labinger, J. A.; Bercaw, J. E. *J. Am. Chem. Soc.* **2004**, *126*, 1304. (k) Briggs, J. R. *Chem. Commun.* **1989**, 674.

(4) (a) Shaikh, Y.; Albahily, K.; Sutcliffe, M.; Fomitcheva, V.; Gambarotta, S.; Korobkov, I.; Duchateau, R. *Angew. Chem. Int. Ed.* **2012**, *51*, 1366. (b) Shaikh, Y.; Gurnham, J.; Albahily, K.; Gambarotta, S.; Korobkov, I. *Organometallics* **2012**, *31*, 7427. (c) Schuhen, K.; Chevalier, R.; Gambarotta, S.; Licciulli, S.; Thapa, I.; Duchateau, R. PCT Int. Appl. Patent WO 2011085951A1, 2011. (d) Kim, S. K.; Kim, T. J.; Chung, J. H.; Hahn,T. K.; Chae, S. S.; Lee, H. S.; Cheong, M.; Kang, S. O. *Organometallics* **2010**, *29*, 5805. (e) Kuhlmann, S.; Blann, K.; Bollmann, A.; Dixon, J. T.; Killian, E.; Maumela, M. C.; Maumela, H.; Morgan, D. H.; Pretorius, M.; Taccardi, N.; Wasserscheid, P. *J. Catal.* **2007**, *245*, 279. (f) Elowe, P. R.; McCann, C.; Pringle, P. G.; Spitzmesser, S. K.; Bercaw, J. E. *Organomeallics* **2006**, *25*, 5255.

(5) Cotton, F. A. and Walton, R. A., *Multiple Bonds Between Metal Atoms*, Oxford University Press, Oxford, UK, 2nd ed., 1992.

(6) (a) Vollhardt, K., Peter, C.; Cammack, J., K.; Matzger, A., J.; Bauer, A.; Capps, K., B.; Hoff, C. D. *Inorg. Chem.* **1999**, *38*, 2624. (b) Cotton, F. A. *Acc Chem. Rev.* **1978**, *11*, 226. (d) Trogler, W. C.; Gray, H. B. *Acc Chem. Rev.* **1978**, *11*, 232.

(7) (a) Sadique, A. R.; Heeg, M. J.; Winter, C. H. *J. Am. Chem. Soc.* **2003**, *125*, 7774. (b) Hao, S.; Gambarotta, S.; Bensimon, C. *J. Am. Chem. Soc.* **1992**, *114*, 3556. (c) Hao, S.; Edema, J. J. H.; Gambarotta, S.; Bensimon, C. *Inorg. Chem.* **1992**, *31*, 2676. (d) Larkworthy, L. F.; Tabatabai, J. M. *Inorg. Nucl. Chem. Lett.* **1980**, 16, 427. (e) Cannon, R. D. *Inorg. Chem.* **1981**, *20*, 2341. (f) Abbott, E. H.; Mayer. J. M. *J. Coord. Chem.* **1977**, *6*, 135. (g) Sneeden, R., P.; Zeiss, H. H. *J. Organomet. Chem.* **1973**, *47*, 125.

(8) Peitz, S.; Aluri B. R.; Peulecke, N.; Müller, B. H.; Wöhl, A.; Müller, W.; Al-Hazmi M. H.; Mosa, F. M.; Rosenthal, U. C*hem. Eur. J.* **2010**, *16*, 7670.

(9) (a) Agapie, T. *Coord. Chem. Rev.* **2011**, *255*, 861. (b) McGuinness, D. *Chem. rev.* **2011**, *111*, 2321 and references cited therein. (c) Dixon, J. T.; Green, M. J.; Hess, F. M.; Morgan, D. H. *J. Organomet. Chem.* **2004**, 689, 3641.

(10) (a) Rucklidge, A. J.; McGuinness, D. S.; Tooze, R. P.; Slawin, A. M. Z.; Pelletier, J. D. A.; Hanton, M. J.; Webb, P. B. *Organometallics* **2007**, *26*, 2782. (b) Bowen, L. E.; Haddow, M. F.; Orpen, A. G.; Wass, D. F. *Dalton Trans.* **2007**, 1160.

(11) (a) Peitz, S.; Peulecke, N.; Bernd, H.; Müller, H.; Spannenberg, A.; Drexler, H.-J.; Rosenthal, U.; Al-Hazmi, M. H.; Al-Eidan, K. E.; Wöhl, A.; Müller, W. *Organometallics* **2011**, *30*, 2364. (b) Licciulli, S.; Albahily, K.; Fomitcheva, V.; Korobkov, I.; Gambarotta, S.; Duchateau, R. *Angew. Chem. Int. Ed.* **2011**, *50*, 2346. (c) Mohamed, H.; Bollmann, A.; Dixon, J.; Gokul, V.; Griesel, L.; Grove, C.; Hess, F.; Maumela, H.; Pepler, L. *Appl. Catal., A* **2003**, *255*, 355. (d) Grove, J. J. C.; Mohamed, H. A.; Griesel, L. (Sasol Technology (Pty) Ltd) WO 03/ 004158, 2002. (f) Wass, D. F. (BP Chemicals Ltd) WO 02/04119, 2002. (h) Dixon, J. T.; Wasserscheid, P.; McGuinness, D. S.; Hess, F. M.; Maumela, H.; Morgan, D. H.; Bollmann, A. (Sasol Technology (Pty) Ltd) WO 03053890, 2001. (i) Köhn, R. D.; Haufe, M.; Kociok-Köhn, G.; Grimm, S.; Wasserscheid, P.; Keim, W. *Angew. Chem. Int. Ed.* **2000**, *39*, 4337.

(12) Manyik, R. M.; Walker, W. E.; Wilson, T. P. (Union Carbide Corporation) US 3300458, 1967.

(13) (a) van Leeuwen, Piet W. N. M; Clément, N. D.; Tschan, M. J.-L. *Coord. Chem. Rev.* **2011**, *255*, 1499. (b) Agapie, T.; Labinger, J. A.; Brecaw, J. E. *J. Am. Chem. Soc.* **2007**, *129*, 14281. (c) Overett, M. J.; Blann, K.; Bollmann, A.; Dixon, J. T.; Haasbroek, D.;

Killian, E.; Maumela, H.; McGuinness, D. S.; Morgan, D. H. *J. Am. Chem. Soc.* **2005**, *127*, 10723.

(14) (a) MacAdams, L. A.; Buffone, G. P.; Incarvito, C. D.; Golen, J. A.; Rheingold, A. L.; Theopold, K. H. *Chem. Commun.* **2003**, 1164. (b) Sugiyama, H.; Aharonian, G.; Gambarotta, S.; Yap, G. P. A.; Budzelaar, P. H. J. *Am. Chem. Soc.* **2002**, *124*, 12268. (c) Schulzke, C.; Enright, D.; Sugiyama, H.; LeBlanc, G.; Gambarotta, S.; Yap, G. P. A.; Thompson, K. K.; Wilson, D. R.; Duchateau, R. *Organometallics* **2002**, *21*, 3810. (d) Bhandari, G.; Kim, Y.; McFarland, J. M.; Rheingold, A. L.; Theopold, K. H. *Organometallics* **1995**, *14*, 738. (e) Winter, M. J. Comprehensive Organometallic Chemistry, 2nd ed.; Wilkinson, G., Ed.; Pergamon Press: Oxford, 1995. (f) Kirtley, S. W. Comprehensive Organometallic Chemistry; Wilkinson, G., Ed.; Pergamon Press: Oxford, 1978. (g) Skupińska, Chem. Rev. 1991, 91, 613.

(15) (a) Temple, C.; Jabri, A.; Crewdson, P.; Gambarotta, S.; Korobkov, I.; Duchateau, R. *Angew. Chem. Int. Ed.* **2006**, *45*, 7050. (b) Jabri, A.; Crewdson, P.; Gambarotta, S.; Korobkov, I.; Duchateau, R. *Organometallics* **2006**, *25*, 715.

(16) Mock, M. T.; Chen, S.; Rousseau, R.; O`Hagen, M. J.; Dougherty, W. G.; Kassel, W. S.; DuBois, D. L.; Bullock, R. M. *Chem. Commun.* **2011**, *47*, 12212.

(17) Collman, J. P.; Kittleman, E. T. *Inorg. Synth.* **1966**, *8*, 149.

(18) Kohler, F. H; rossdorf, W. *Z. Natureforsch. Teil B*, **1977**, *32*, 1026.

(19) Frisch, M. J.; et al. *Gaussian 09*, Revision A.02.

(20) Perdew, J. P.; Burke, K.; Ernzerhof, M. *Phys. Rev. Lett.* **1997**, *78*, 1396.

(21) Schafer, A.; Huber, C.; Ahlrichs, R. *J. Chem. Phys.* **1994**, *100*, 5829.

(22) Mulliken, R. S. *J. Chem. Phys.* **1955**, *23*, 1833.

(23) Mayer, I. *Int. J. Quantum Chem.* **1986**, *29*, 73.

(24) Gorelsky, S. I. *J. Chem. Theory Comput.* **2012**, *8*, 908.

(25) (a) Gorelsky, S. I., AOMix-Software for Electronic Structure Analysis; Centre for Catalysis Research and Innovation, Department of Chemistry, University of Ottawa, ON, 2011; http://www.sg-chem.net; (b) Gorelsky, S. I.; Lever, A. B. P. *J. Organomet. Chem.* **2001**, *635*, 187.

CHAPTER 7
Conclusions

With the aim of addressing the role of the chromium oxidation states on olefins oligomerization (selective versus nonselective), this research work was aiming at designing and preparing various modified PN ligands and their corresponding organoaluminate intermediates generated by the interaction of chromium catalyst precursors and aluminates activators. The isolation of these catalytically active intermediates reiterates the variety of roles played by alkyl aluminum activators, especially for the reduction of the precatalyst.

By using dianaionic PN(pyridine) ligand, we further confirmed that divalent chromium is responsible for the nonselective ethylene oligomerization through chain growth (Cossee-Arlman) mechanism. Moreover, it became also clear that the pyridine donor ring enhances the stability of the divalent oxidation state since it prevents further reduction to the monovalent state. It was also confirmed the existence of the chromium redox dynamism through which the three oxidation states readily interconvert through reductions and disproportionations. On the other hand, when a neutral PN(pyridine) ligand was used to attempt the isolation of a catalytically active species, a Cr(I) species was isolated and fully characterized. Furthermore, modification of the neutral ligand by introducing two PNP motifs *ortho* to the pyridine donor ring, led to unprecedented fragmentation of the ligand system preserving the Cr(II) oxidation states, and producing nonselective ethylene oligomerization catalysts.

Once more, when pyridine was introduced into anionic NNP framework, the activation by alkylaluminium cocatalysts resulted in ligand deprotonation and formation of a highly active Schulz-Flory polyhydride Cr(II) cluster catalyst. All the above work suggest that the pyridine

donor ring enhances the stabilization of the chromium (II) oxidation state formed during the activation step, preventing further reduction to the monovalent state required for selectivity.

Finally, when pyridine donor ligand was replaced by an N-donor aliphatic amine as in the case of PNPN cyclic ligand used, a Cr(I)-Cr(II) binuclear complex was isolated and tested as a potential catalyst for ethylene oligomerization. However, its activity was inferior which may attributed to the constrained geometry around the bimetallic core of the formed complex.

Nonetheless, this thesis work further confirms the central role of the chromium oxidation state in determining the type of catalytic activity and which in turn may be tuned by applying various ancillary ligands and alkyl aluminums. This will encourage researcher to find effective strategies to design catalysts for specific purposes and to make effort to rationalize the catalytic activity by isolation of catalytically active species.

Appendices

Appendix A

Ethylene Oligomerization: General Procedure

Oligomerizations were carried out in a 200 mL high-pressure Büchi reactor containing a heating/cooling jacket. A preweighted amount of catalyst was dissolved in toluene (10 mL) under nitrogen and injected into the preheated reactor already charged with co-catalyst and toluene (total volume 100 mL). Solutions were heated using a thermostatic bath and charged with ethylene, maintaining the pressure throughout the run. Oligomerizations were quenched by cooling to 0°C, releasing the pressure, and adding MeOH/HCl (80% MeOH solution). The total yield of oligomers was determined by ^{1}H NMR by integrating the intensity of the olefinic multiplets against the solvent resonance. The composition of the mixture of oligomers was determined by GC/MS with single oligomer quantification by GC using an FID detector. The alpha value was measured with the C(n+2)/Cn ratio for the range C6-C20. The insoluble polymeric solid was isolated by filtration and dried prior to measuring its mass.

Appendix B

X-ray Crystallography: General Procedure

Crystals were mounted on thin glass fibers using paraffin oil. Prior to data collection crystals were cooled to 200.15 °K. Data were collected on a Bruker AXS SMART single crystal diffractometer equipped with a sealed Mo tube source (wavelength 0.71073 Å) APEX II CCD detector. Raw data collection and processing were performed with APEX II software package from BRUKER AXS.[1] Diffraction data were collected with a sequence of 0.5° ω scans at 0, 120, and 240° in φ. Initial unit cell parameters were determined from 60 data frames with 0.3° ω scan each, collected at the different sections of the Ewald sphere. Semiempirical absorption corrections based on equivalent reflections were applied.[2] The structures were solved by direct methods, completed with difference Fourier synthesis, and refined with full-matrix least-squares procedures based on F^2. For all of the compounds all hydrogen atom positions were calculated on the basis of the geometry of related non-hydrogen atoms. All hydrogen atoms were treated as idealized contributions during the refinement. All scattering factors are contained in several versions of the SHELXTL program library, with the latest version used being v.6.12.[3]

References

(1) APEX Software Suite v.2010; Bruker AXS: Madison, WI, **2005**.

(2) Blessing, R. *Acta Crystallogr.* **1995**, A*51*, 33.

(3) Sheldrick, G. M. *Acta Crystallogr.* **2008**, *A64*, 112.

B. 1. X-ray Data Collection for Complexes 2.1-2.6

Data collection results for compounds **2.1**–**2.6** represent the best data sets obtained in several trials for each sample. The crystals were mounted on thin glass fibers using paraffin oil. Prior to data collection, crystals were cooled to 200.15 K. Data were collected on a Bruker AXS KAPPA single-crystal diffractometer equipped with a sealed Mo tube source (wavelength 0.71073 Å) APEX II CCD detector. Raw data collection and processing were performed with the APEX II software package from BRUKER AXS.[1] Diffraction data for samples of **2.3** and **2.4** were collected with a sequence of 0.5° ω scans at 0, 120, and 240° in φ. Because of the lower unit cell symmetry in order to ensure adequate data redundancy, diffraction data for **2.1**, **2.2**, **2.5**, and **2.6** were collected with a sequence of 0.5° ω scans at 0, 90, 180, and 270° in φ. Initial unit cell parameters were determined from 60 data frames with 0.3° ω scan each, collected at the different sections of the Ewald sphere. Semiempirical absorption corrections based on equivalent reflections were applied.[2]Systematic absences in the diffraction data set and unit-cell parameters were consistent with triclinic $P\bar{1}$ (No. 2) for compounds **2.1**, **2.2**, **2.5**, and **2.6**, monoclinic $P2_1/n$ (No. 14, alternative settings) for compound **2.3**, and monoclinic $P2_1/c$ (No. 14) for **2.4**. Solutions in the centrosymmetric space groups for all compounds yielded chemically reasonable and computationally stable results of refinement. The structures were solved by direct methods, completed with difference Fourier synthesis, and refined with full-matrix least-squares procedures based on F^2.

Diffraction data for **2.1** were collected to 0.75 Å resolution; however, due to the small crystal size and weak diffraction it was discovered that both R(int) and R(σ) exceeded 35% for the data below 1.10 Å resolution. On the basis of the R(σ) value, data were truncated to 0.95 Å resolution for refinement. Refinement of the structural model for **2.1** revealed that all of the

molecules of the compound are located in general positions. In addition to the target complex molecule the asymmetric unit also contains two molecules of THF crystallization solvent with full occupancy.

Similarly to the data for **2.1**, diffraction data for the crystal of complex **2.2** were collected to 0.75 Å resolutions. The small crystal size and weak diffraction contributed to the growth of both R(int) and $R(\sigma)$ to over 35% for the data below 1.05 Å resolution. On the basis of the $R(\sigma)$ value, data were truncated to 0.95 Å resolution for refinement. The structural model of **2.2** displays two independent molecules per one asymmetric unit, where both molecules are located in general positions. In addition to two molecules of the target compound, three partially occupied molecules of toluene solvent were discovered in the lattice. Two of the molecules appear to be positionally disordered, where disorder is not related to the unit cell symmetry elements. Originally atomic position occupancies were refined to obtain reasonable thermal parameter values. However, the occupancy was fixed at 50% for all three molecular positions of the solvent units. All carbon atoms for toluene solvent molecules were refined in isotropic approximations to avoid introducing an excessive amount of constraints/restraints as well as to preserve an acceptable data to parameter ratio. In addition to that, sets of thermal parameter constraints (EADP), geometry (FLAT, DFIX) and rigid body restraints (AFIX 66), and geometry constraints (SADI) were used to maintain reasonable molecular geometry and thermal motion values for solvent molecules. A close examination of the locations of the strongest residual electron density peaks revealed the presence of several peaks with values of 1.23–0.72 electrons in close proximity to the nondisordered toluene molecule. Several other electron density peaks were discovered in the VOID space of the unit cell. The values of the latter peaks did not exceed 1.14 electrons (one-fifth of a carbon atom). All of the attempts to model these electron density

peaks into molecules of acceptable geometry were unsuccessful without an excessive amount of geometrical and rigid body restraints.

All structural fragments are situated in general positions in the asymmetric unit of structural model for compound **2.3**. Together with the target compound molecules, two partially occupied molecules of toluene crystallization solvent were discovered in the crystalline lattice. Occupancy factors of the carbon atoms were initially refined to obtain acceptable thermal motion parameter values; however, occupancy was fixed at 50% for each molecular position at the final stages of the refinement. Sets of constraints (SIMU, DELU) and rigid body restraints (AFIX 66) were used to maintain reasonable molecular geometry and thermal motion values for solvent molecules.

The structural model for the compound **2.4** includes two molecules of the target complex per asymmetric unit as well as one fully occupied molecule of toluene, all located in general positions. In the final refinement stages for the model of **2.4** it was noticed that the thermal parameters for several structural fragments suggested the presence of disorder. Positional disorder not related to symmetry elements was introduced for the *i*-Pr moieties based at C(30), C(42), C(75), and C(83). Occupation factors for these fragment were successfully refined to the following values: 50:50 for the fragments C(30)–C(33) and C(75)–C(78); 60:40 for the fragment C(83)–C(86), and finally 65:35 for the fragment C(42)–C(45). Several sets of geometry constraints (SADI) were introduced to ensure acceptable molecular geometry for these fragments. To obtain acceptable values of thermal motion parameters and avoid further splitting of atomic positions, sets of thermal parameter constraints (SIMU, RIGU for for the fragment C(42)–C(45), EADP for all other fragments) were introduced into the refinement routine. For the

same reasons all carbon atoms of the toluene solvent molecule were refined with isotropic thermal motion approximations.

The structure of compound **2.5** contains a cationic metal moiety and an $AlCl_3(C_2H_5)$ fragment located in general positions. One molecule of hexane crystallization solvent is located at the inversion center. The occupancy of the carbon atoms of this hexane molecule was initially refined to obtain acceptable thermal parameter values. In the final stages of refinement, the occupancy value was preset to 50%, resulting in reasonable thermal motion parameter values and stable computational results. A set of geometry restraints (DFIX, DANG) was used to maintain an acceptable molecular geometry during the refinement.

The asymmetric unit of **2.6** reveals two molecules of the target complex and two partially occupied molecules of toluene, all located in general positions. In the final refinement stages unusually large thermal parameters for several carbon atoms in the model of **2.6** indicated the presence of disorder. Positional disorder not related to symmetry elements was introduced for the Et moieties based at C(65), C(67), and C(69). Occupational factors for all these fragment were refined to 50:50, demonstrating reasonable isotropic thermal motion parameter values and stable refinement results. Several sets of geometry restraints (DFIX) were introduced to ensure an acceptable molecular geometry for these fragments. To obtain acceptable values of anisotropic thermal motion parameters, conserve an adequate data to parameter ratio, and avoid further splitting of atomic positions, sets of thermal parameter constraints (EADP) were introduced into the refinement routine for all these disordered moieties. For the same reasons all carbon atoms of the toluene solvent molecule were refined as rigid body models (AFIX 66) with isotropic thermal motion approximations. A close examination of the strongest residual electron density peaks revealed the presence of several peak with values of 1.17–0.68 electrons in close proximity to the

toluene molecules. Several other electron density peaks were discovered in the VOID space of the unit cell. The values of the latter peaks did not exceed 1.12 electrons (one-fifth of a carbon atom). All of the attempts to model these electron density peaks into molecules of acceptable geometry were unsuccessful without an excessive amount of geometrical and rigid body restraints.

For all of the compounds all hydrogen atom positions were calculated on the basis of the geometry of related non-hydrogen atoms. All hydrogen atoms were treated as idealized contributions during the refinement. All scattering factors are contained in several versions of the SHELXTL program library, with the latest version used being v.6.12.[3]

References

(1) *APEX Software Suite v.2010*; Bruker AXS, Madison, WI, 2005.

(2) Blessing, R. *Acta Crystallogr.* **1995**, A*51*, 33.

(3) Sheldrick, G. M. *Acta Crystallogr.* **2008**, *A64*, 112.

B. 2. X-ray Data Collection for Complexes 3.1-3.7

Data collection results for compounds **3.1-3.7** represent the best data sets obtained in several trials for each sample. The crystals were mounted on thin glass fibers using paraffin oil. Prior to data collection crystals were cooled to 200.15 °K. Data were collected on a Bruker AXS KAPPA single crystal diffractometer equipped with a sealed Mo tube source (wavelength 0.71073 Å) and an APEX II CCD detector. Raw data collection and processing were performed with APEX II software package from BRUKER AXS.[1]Diffraction data for **3.2, 3.3, 3.6** and **3.7** samples were collected with a sequence of 0.5° ω scans at 0, 120, and 240° in φ. Due to lower unit cell symmetry and in order to ensure adequate data redundancy, diffraction data for **3.1, 3.4** and **3.5** were collected with a sequence of 0.5° ω scans at 0, 90, 180 and 270° inφ. Initial unit cell parameters were determined from 60 data frames with 0.3° ω scan each, collected at different sections of the Ewald sphere. Semi-empirical absorption corrections based on equivalent reflections were applied.[2] Systematic absences in the diffraction data-set and unit-cell parameters were consistent with triclinic **P**$\bar{1}$ (№2) for compounds **3.1, 3.4** and **3.5,** monoclinic **P**$2_1/n$ (№14, alternative settings) for **3.2,** monoclinic **P**2_1 (№4) for **3.3**, monoclinic **C***c* (№9) for **3.6** and orthorhombic **P**$2_12_12_1$ (№19) for **3.7**. Solutions in the centrosymmetric space groups for **3.1, 3.2** and **3.4** yielded chemically reasonable and computationally stable results of refinement. However, data for the complexes **3.3**, **3.6** and **3.7** suggested non-centrosymmetric space groups for the model refinement. The structures were solved by direct methods, completed with difference Fourier synthesis, and refined with full-matrix least-squares procedures based on F^2.

Diffraction data for **3.1** were collected to 0.75Å resolution. However due to small crystal size and weak diffraction, both R(int) and R(sigma) exceeded 35% for the data below 1.00Å resolution. Based on R(sigma) value, data were truncated to 0.95Å resolution for refinement.

Asymmetric unit for this crystallographic model of **1** consists of one target molecule with all the atoms located in general position.

Refinement of the structural model for **3.2** revealed that all the molecules are located in general positions. In addition to the target molecule, the asymmetric unit also contains one molecule of THF with full occupancy.

The asymmetric unit of **3.3** contains one chiral molecule located in general position. Refinement results suggested the presence of two non-merohedrally twinned domains. Careful examination of the original data frames and reciprocal space diffraction pictures confirmed the initial twining assumption. In order to find independent orientation matrices, 1347 reflections were collected from 4 sets of 40 frames each in different sections of the Ewald sphere. Collected data were processed with CELL_NOW software[3] and produced two independent orientation matrices. Data set was re-integrated with two obtained matrices and treated for twinning absorption corrections. Consecutive model refinement was performed using HKLF5 reflection data file. Twinning domain ratio coefficient (BASF) was refined to 0.3770. Final Flack parameter value, due to chiral space group, was refined to 0.09(2).

The molecule of **3.4** is situated in a general position of the asymmetric unit. Together with the target compound, one molecule of toluene was located at the inversion center. Due to the special position, this solvent molecule is disordered over two inversion related positions with occupancy factors of the carbon atoms fixed at 50%. A set of thermal parameters constrains (SIMU, DELU) and rigid body restrains (AFIX 66) were used to maintain reasonable molecular geometry and thermal motion values for the toluene molecule.

The structural model of **3.5** consists of two oppositely charged ligand-Cr and alkyl-Al-Cl units located in general positions of the asymmetric unit. In the final refinement stages, unusually

large thermal parameters for several carbon atoms suggested the presence of disorder. Positional disorder non related to symmetry elements was introduced for three Et fragments based at C(34), C(36), and C(38). Carbon atom positions for these moieties were split in two positions with equal occupancy. Attempt to introduce anisotropic thermal motion parameters resulted in stable refinement results. However to avoid further splitting of atomic positions, a set of anisotropic parameter constrains (SIMU, DELU) was used to maintain acceptable anisotropic displacement values. Several sets of geometry constrains (SADI) were also introduced to ensure acceptable molecular geometry for these three disordered ethyl groups.

Diffraction data for **3.6** were collected to 0.75Å resolution, however due to small crystal size and weak diffraction, both R(int) and R(sigma) exceed 35% for the data below 0.85Å resolution. Based on R(sigma) value, data were truncated to 0.80Å resolution for refinement. Structural model of **3.6** displays one independent molecule of target compound and three partially occupied toluene molecules per asymmetric unit with all four molecules located in general positions. Initially, atomic positions occupancy factors for toluene were refined to obtain reasonable thermal parameters values. However, the occupancy was fixed at 50% for all atoms of those three solvent. All carbon atoms for toluene were refined with isotropic approximation to avoid introducing excessive amount of constrains/restrains as well as to preserve acceptable data to parameters ratio. In addition, geometry (DFIX) and rigid body restrains (AFIX 66) and geometry constrains (SADI) were used to maintain reasonable molecular geometry and thermal motion values for all the three toluene molecules.

Diffraction data for **3.7** were collected to 0.75Å resolution. However due to small crystal size and weak diffraction, both R(int) and R(sigma) exceed 35% for the data below 0.89Å resolution. Based on R(sigma), the value data were truncated to 0.85Å resolution for refinement.

The structural model of **3.7** consists of two oppositely charged Cr and Al-Cl fragments located in general positions of the asymmetric unit. On the final refinement stages, unusually large thermal parameters for several carbon atoms indicated the presence of disorder. Positional disorder non related to symmetry elements was introduced for the Cl(1) atomic position as well as *i*-Pr moieties based at C(71), C(75), and C(83). These units were refined with 50% : 50% occupancy, obtaining reasonable isotropic thermal motion parameters values and stable refinement results. Several sets of geometry constrains (SADI) were introduced to ensure acceptable molecular geometry for these fragments. However, to conserve adequate data to parameters ratio and avoid further splitting of atomic positions the disordered moieties were all refined with isotropic thermal motion approximation.

For all the compounds the hydrogen atoms positions were calculated based on the geometry of related non-hydrogen atoms. All hydrogen atoms were treated as idealized contributions during the refinement. All scattering factors were contained in several versions of the SHELXTL program library, with the latest version used being v.6.12.[4]

References

(1) APEX Software Suite v.2012; Bruker AXS: Madison, WI, **2005**.

(2) Blessing, R. *Acta Cryst.* **1995**, *A51*, 33.

(3) G. Sheldrick, Cell_Now, Bruker-AXS: Madison, WI, **2004.**

(4) Sheldrick, G.M. *Acta Cryst.* **2008**, *A64*, 112.

B. 3. X-ray Data Collection for Complexes 4.1-4.3

Data collection results for compounds **4.1, 4.2** and **4.3** represent the best data sets obtained in several trials for each sample. The crystals were mounted on thin glass fibers using paraffin oil. Prior to data collection crystals were cooled to 200.15 °K. Data were collected on a Bruker AXS SMART single crystal diffractometer equipped with a sealed Mo tube source (wavelength 0.71073 Å) APEX II CCD detector. Raw data collection and processing were performed with APEX II software package from BRUKER AXS.[1] Diffraction data for **4.3** sample were collected with a sequence of 0.5° ω scans at 0, 120, and 240° in φ. Due to lower unit cell symmetry in order to ensure adequate data redundancy, diffraction data for **4.1** and **4.2** were collected with a sequence of 0.5° ω scans at 0, 90, 180 and 270° in φ. Initial unit cell parameters were determined from 60 data frames with 0.3° ω scan each collected at the different sections of the Ewald sphere. Semi-empirical absorption corrections based on equivalent reflections were applied.[2] Systematic absences in the diffraction data-set and unit-cell parameters were consistent with triclinic $\mathbf{P\bar{1}}$ (№2) for compounds **4.1** and **4.2**, monoclinic $\mathbf{P}2_1/c$ (№14) for compounds **4.3**. Solutions in the centrosymmetric space groups for all compound yielded chemically reasonable and computationally stable results of refinement. The structures were solved by direct methods, completed with difference Fourier synthesis, and refined with full-matrix least-squares procedures based on F^2.

Refinement of the structural model for **4.1** revealed that all the molecules in the structure are located in general positions. In addition to the target complex molecule asymmetric unit also contains three fully occupied molecules of THF crystallization solvent in the lattice.

Diffraction data for the crystal of **4.2** complex were collected to 0.75Å resolution, however due to small crystal size and weak diffraction it was discovered that both R(int) and

R(sigma) exceed 35% for the data below 1.00Å resolution. Based on R(sigma) value data were truncated to 0.95Å resolution for refinement. Structural model of **4.2** displays one independent molecule of target compound in general position. Anisotropic refinement of the target compound model discovered slightly enlarged thermal motion parameters for carbon atoms of one phenyl ring substituents. It appeared that phenyl ring experience minor rotational disorder, however the values of the thermal motion parameters were not large enough to split the positions of the constituting carbon atoms. Instead, set of thermal motion constrains (SIMU, RIGU) were used for these six carbon atoms in order to achieve reasonable values of the thermal motion parameters. Refinement also suggested that asymmetric unit also contained and one partially occupied toluene crystallization solvent molecule located on the inversion center and disordered over two positions by inversion symmetry operation. Originally, atomic positions occupancy factors for toluene solvent molecule were refined to obtain reasonable thermal parameters values. However, on later stages of refinement carbon atoms occupancies were fixed at 25%. All carbon atoms for toluene solvent molecules were refined with isotropic approximation to avoid introducing excessive amount of constrains/restrains as well as to preserve acceptable data to parameters ratio. In order to avoid unreasonably large isotropic displacement values, all atomic isotropic displacement parameters for toluene solvent molecule were constraint to the same value (EADP). In addition to that, geometry (DFIX, FLAT) and rigid body restrains (AFIX 66) and geometry constrains (SADI) were used to maintain reasonable molecular geometry of toluene molecule.

Diffraction data for the crystal of the complex **4.3** were collected to 0.75Å resolution, however due to small crystal size and weak diffraction it was discovered that both R(int) and R(sigma) exceed 35% for the data below 1.00Å resolution. Based on R(sigma) value data were

truncated to 0.95Å resolution for refinement. Structural model of **4.3** consists of one independent molecule of target compound and one partially occupied toluene crystallization solvent molecule per asymmetric unit, where both fragments are located in the general positions. Originally atomic positions occupancy factors for toluene solvent molecule were refined to obtain reasonable thermal parameters values. However, occupancy was fixed at 35% for all the atoms of the solvent. All carbon atoms for toluene solvent molecule were refined with isotropic approximation to avoid introducing excessive amount of constrains/restrains as well as to preserve acceptable data to parameters ratio. In addition to that, geometry (DFIX, FLAT) and rigid body restrains (AFIX 66) and geometry constrains (SADI) were used to maintain reasonable molecular geometry and thermal motion values for all three of toluene molecules.

For all the compounds all hydrogen atoms positions were calculated based on the geometry of the related non-hydrogen atoms. All hydrogen atoms were treated as idealized contributions during the refinement. All scattering factors are contained in several versions of the SHELXTL program library, with the latest version used being v.6.12.[3]

References

(1) APEX Software Suite v.2010; Bruker AXS: Madison, WI, **2005**.

(2) Blessing, R. *Acta Cryst.* **1995**, *A51*, 33.

(3) Sheldrick, G.M. *Acta Cryst.* **2008**, *A64*, 112.

B. 4. X-ray Data Collection for Complexes 5.1-5.2

Data collection results for compounds **5.1** and **5.2** represent the best data sets obtained in several trials for each sample. The crystals were mounted on thin glass fibers using paraffin oil. Prior to data collection crystals were cooled to 200 °K. Data were collected on a Bruker AXS KAPPA single crystal diffractometer equipped with a sealed Mo tube source (wavelength 0.71073 Å) APEX II CCD detector. Raw data collection and processing were performed with APEX II software package from BRUKER AXS.[1] Diffraction data for both **5.1** and **5.2** were collected with a sequence of 0.5° ω scans at 0, 120, and 240° in φ. Initial unit cell parameters were determined from 60 data frames with 0.3° ω scan each, collected at different sections of the Ewald sphere. Semi-empirical absorption corrections based on equivalent reflections were applied.[2] Systematic absences in the diffraction data-set and unit-cell parameters were consistent with orthorhombic **P***bca* (№61) for **5.1** and monoclinic **C**-centered **C***2/c* (№15) for **5.2**. Solutions in the centrosymmetric space groups for both compounds yielded chemically reasonable and computationally stable refinement results. The structures were solved by direct methods, completed with difference Fourier synthesis, and refined with full-matrix least-squares procedures based on F^2.

Refinement of the structural model for **5.1** revealed that all the molecules in the structure are located in general positions. In addition to the target complex molecule, the asymmetric unit also contains one molecule of crystallization THF in the lattice. All the atoms in the structural model were refined with full set of anisotropic displacement parameters. Thermal motion parameters for C(13) based aromatic ring and for C(21) carbon atom of coordinated THF molecule suggested the presence of positional disorder non-related to symmetry elements of the crystal space group. Positional disorder was treated for the all disordered positions of phenyl

substituent and one carbon atom of the THF fragment. Initially, occupational factors for all disordered atoms were allowed to refine. However, on the final stages of structure refinement occupational factors were restrained to 50%: 50% values for phenyl fragment and to 65%: 35% for the carbon atom in THF molecule. Several sets of geometry constrains (SADI) were introduced to ensure acceptable molecular geometry for these fragments. To obtain acceptable values of thermal motion parameters and avoid further splitting of atomic positions sets of thermal parameters constrains (SIMU, DELU) were introduced into the refinement routine. Introduction of thermal motion restrains allowed successful anisotropic refinement for all disordered atomic positions.

The structural model of **5.2** displays one molecule of the target compound located at the inversion center of the space group. The compound structure appears to be dimeric with an asymmetric unit containing only half of the molecule. All the atoms in the structural model were refined with full set of anisotropic displacement parameters. The Cr-Cr core fragment bridging hydrogen atoms were localized as the strongest residual density peaks at the latter refinement stages. After assigning these hydrogen atoms positions refinement parameters there were restrained to the "riding" type with the possibility of refining Cr-H distances (AFIX 4). However, to ensure the compliance with non-x-ray related data, all H-Cr distances were restrained to refine to the same value with the set of positional restrains (SADI). On the final refinement stages for the model of **5.2,** the thermal parameters suggested partial occupancy for the Al(1) based fragment as well as the presence of disorder for i-Bu substituents on Al moiety. Positional disorder non related to symmetry elements was introduced for the *i*-Bu moieties based at C(39) and C(43). Occupational factors for these fragment were successfully refined to the following values: 37.5% : 37.5% for both fragments. Several sets of geometry constrains (SADI) were

introduced to ensure acceptable molecular geometry. To obtain acceptable values of thermal motion parameters and avoid further splitting of atomic positions sets of thermal parameters, constrains (SIMU, RIGU) were introduced into the refinement routine. In addition to the target compound, one disordered molecule of toluene solvent was discovered in the lattice. This molecule appears to have positional disorder not related to the unit cell symmetry elements. Originally, atomic positions occupancies were refined to obtain reasonable thermal parameters values. However, occupancy was fixed at 50% for both disordered molecular positions of the solvent unit. All carbon atoms for toluene solvent molecules were refined with isotropic approximation to avoid introducing excessive amount of constrains/restrains as well as to preserve acceptable data to parameters ratio. In addition, the set of thermal parameters constrains (EADP), geometry (FLAT, DFIX) and rigid body restrains (AFIX 66) and geometry constrains (SADI) were used to maintain reasonable molecular geometry and thermal motion values for solvent molecules.

For all the compounds, all hydrogen atom positions were calculated based on the geometry of the related non-hydrogen atoms. All hydrogen atoms were treated as idealized contributions during the refinement. All scattering factors are contained in several versions of the SHELXTL 2013 program library.[3]

References

(1) APEX Software Suite v.2010; Bruker AXS: Madison, WI, **2005**.

(2) Blessing, R. *Acta Cryst.* **1995**, *A51*, 33.

(3) Sheldrick, G.M. *Acta Cryst.* **2008**, *A64*, 112.